



Implementation of Texas Mechanistic-Empirical Flexible Pavement Design System (TxME)

Implementation Report 5-6622-01-R1

Cooperative Research Program

TEXAS A&M TRANSPORTATION INSTITUTE
COLLEGE STATION, TEXAS

in cooperation with the
Federal Highway Administration and the
Texas Department of Transportation
<http://tti.tamu.edu/documents/5-6622-01-R1.pdf>

1. Report No. FHWA/TX-18/5-6622-01-R1		2. Government Accession No.		3. Recipient's Catalog No.	
4. Title and Subtitle IMPLEMENTATION OF TEXAS MECHANISTIC-EMPIRICAL FLEXIBLE PAVEMENT DESIGN SYSTEM (TxME)				5. Report Date Published: February 2019	
				6. Performing Organization Code	
7. Author(s) Sheng Hu, Asif Rahman, Jun Zhang, Fujie Zhou, and Tom Scullion				8. Performing Organization Report No. Report 5-6622-01-R1	
9. Performing Organization Name and Address Texas A&M Transportation Institute College Station, Texas 77843-3135				10. Work Unit No. (TRAIS)	
				11. Contract or Grant No. Project 5-6622-01	
12. Sponsoring Agency Name and Address Texas Department of Transportation Research and Technology Implementation Office 125 E. 11 th Street Austin, Texas 78701-2483				13. Type of Report and Period Covered Technical Report: March 2015–August 2018	
				14. Sponsoring Agency Code	
15. Supplementary Notes Project performed in cooperation with the Texas Department of Transportation and the Federal Highway Administration. Project Title: Field Implementation of the Texas Mechanistic-Empirical Pavement Design Process in Six TxDOT Districts URL: http://tti.tamu.edu/documents/5-6622-01-R1.pdf					
16. Abstract The Texas Mechanistic-Empirical flexible pavement design system (TxME) allows Texas pavement designers to take full advantage of new or premium materials, with a full consideration of the influential factors including pavement structure, traffic volume, and environmental condition. To further enhance and implement the software, extensive lab testing was conducted to develop default material properties. These properties include the default dynamic modulus, rutting and cracking properties of asphalt concrete (AC) mixtures, and moduli of other layer materials. Specifically, the relationships between reclaimed asphalt pavement/reclaimed asphalt shingles contents and the AC material properties were established and incorporated into the TxME. In addition, default load spectra and initial construction cost analysis were integrated into the TxME. All these features greatly enhanced the practicality and ease of using TxME when conducting pavement design. The Texas Flexible Pavement Database was used to calibrate the TxME performance models. The calibrated TxME was then employed to predict performance of 11 identified test sections located in six different districts. The comparison between the TxME predictions and the field performance survey results further confirmed the validation of the calibrated performance models. Overall, the current TxME is practical, user-friendly, and ready for statewide implementation.					
17. Key Words: TxME, Mechanistic Empirical, Flexible Pavement Design, RAP, RAS, Load Spectra, Rutting, Cracking, Implementation			18. Distribution Statement No restrictions. This document is available to the public through NTIS: National Technical Information Service Alexandria, Virginia, 22312 http://www.ntis.gov		
19. Security Classif. (of this report) Unclassified		20. Security Classif. (of this page) Unclassified		21. No. of Pages 158	22. Price

**IMPLEMENTATION OF TEXAS MECHANISTIC-EMPIRICAL
FLEXIBLE PAVEMENT DESIGN SYSTEM (TxME)**

by

Sheng Hu, Ph.D., P.E.
Associate Research Engineer
Texas A&M Transportation Institute

Asif Rahman, Ph.D.
Research Specialist
Texas A&M Transportation Institute

Jun Zhang, Ph.D.
Research Specialist
Texas A&M Transportation Institute

Fujie Zhou, Ph.D., P.E.
Research Engineer
Texas A&M Transportation Institute

and

Tom Scullion, P.E.
Senior Research Engineer
Texas A&M Transportation Institute

Report 5-6622-01-R1
Project 5-6622-01

Project Title: Field Implementation of the Texas Mechanistic-Empirical Pavement Design
Process in Six TxDOT Districts

Performed in cooperation with the
Texas Department of Transportation
and the
Federal Highway Administration

Published: February 2019

TEXAS A&M TRANSPORTATION INSTITUTE
College Station, Texas 77843-3135

DISCLAIMER

The contents of this report reflect the views of the authors, who are responsible for the facts and the accuracy of the data presented here. The contents do not necessarily reflect the official view or policies of the Federal Highway Administration (FHWA) or the Texas Department of Transportation (TxDOT). This report does not constitute a standard, specification, or regulation, nor is it intended for construction, bidding, or permit purposes.

The United States Government and the State of Texas do not endorse products or manufacturers. Trade or manufacturers' names appear here solely because they are considered essential to the object of this report.

The researcher in charge was Dr. Sheng Hu, P.E. (Texas, #103577).

ACKNOWLEDGMENTS

This project was made possible by the Texas Department of Transportation (TxDOT) in cooperation with the Federal Highway Administration (FHWA). In particular, the guidance and technical assistance provided by the project manager Kevin Pete, Joe Adams (former project manager), the project advisors Enad Mahmoud, Gisel Carrasco, and Joe Leidy (former project advisor) proved invaluable. The following project advisors also provided valuable input throughout the course of the project, and their guidance is duly acknowledged: Hua Chen, Soojun Ha, and Miguel Arellano.

Special thanks are also extended to the following TTI research group and UTEP staff for their assistance with the flexible pavement database project: Sang-Ick Lee (TTI), Lubinda Walubita (TTI), Imad Abdallah (UTEP), and Daniel Rodriguez (UTEP).

TABLE OF CONTENTS

	Page
List of Figures	ix
List of Tables	xii
List of Acronyms	xiv
Chapter 1. Introduction	1
Background and Objectives	1
Report Organization.....	2
Chapter 2. TxME Description and Training Workshop	3
Pavement Structure and Associated Material Properties	3
Traffic Loading	7
Climate.....	10
Reliability Related Input	12
Output	12
Connection with FPS 21	13
Help File.....	15
Workshop.....	16
Chapter 3. Develop Default Material Properties for TXME	19
Develop Default Moduli for Pavement Materials.....	19
Develop Default Rutting Properties for Pavement Materials	27
Develop Default Cracking Properties for Pavement Materials.....	33
Incorporate Default Values into TxME	36
Chapter 4. Develop Default Axle Load Spectra for TXME	39
Methodology	39
Sources of Traffic Data.....	40
Development of Default Load Spectra Inputs for IH.....	41
Development of Default Load Spectra Inputs for US/IH	52
Development of Default Load Spectra Inputs for FM Roads	58
Development of Default Load Spectra Inputs for Roads in Energy Sectors	63
Incorporate Default Values into TxME	66
Chapter 5. Develop Default Initial Construction Cost	67
Initial Construction Costs of AC Mixtures with No RAP/RAS	67
Initial Construction Costs of AC Mixtures with RAP/RAS	72
Cost of Other Layer Materials	74
Incorporate Initial Construction Cost into TxME.....	75
Chapter 6. TxME Performance Model Calibration	77
Calibration of Base/Subgrade Rutting Model.....	77
Calibration of Asphalt Layer Rutting Model	81
Calibration of Fatigue Cracking Model	85
Chapter 7. Demonstration and Verification of TxME with Independent Field Test	
Sections	89
Identify Projects and Test Sections.....	89
Visit Test Sections and Conduct Field Survey	97
Assemble Samples and Run Lab Test.....	108
Assemble Traffic Information.....	112
Use TxME to Simulate Test Sections and Predict Performance.....	117

Compare TxME Predicted Performance with Field Survey	124
Chapter 8. Conclusions and Recommendations.....	127
Summary and Conclusions	127
Recommendations.....	128
References	131
Appendix: TxME Prediction Results for 11 Test Sections.....	133

LIST OF FIGURES

	Page
Figure 1. Main Screen of User Interface.....	4
Figure 2. Pavement Structure Information Screen.....	5
Figure 3. AC Layer Dynamic Modulus Input Screen.....	6
Figure 4. AC Layer Fracture Properties Input Screen.....	6
Figure 5. AC Layer Rutting Properties Input Screen.....	7
Figure 6. Traffic ESALs (Level 2) Input Screen.....	8
Figure 7. Traffic Load Spectrum (Level 1) Input Screen.....	9
Figure 8. Traffic Monthly Adjustment Input Screen.....	9
Figure 9. Traffic Axle Load Distribution Input Screen.....	10
Figure 10. Climate for a Specific Weather Station Input Screen.....	11
Figure 11. Climatic Data Interpolation Input Screen.....	11
Figure 12. Reliability Related Input Screen for a Three-Layer Conventional Pavement.....	12
Figure 13. Output of TxME in Excel File Format.....	13
Figure 14. Connection Concept between FPS 21 and TxME.....	14
Figure 15. An Example of TxME Pavement Structure Imported from FPS 21.....	15
Figure 16. TxME Help File.....	15
Figure 17. Dynamic Modulus Master Curve and Equations.....	20
Figure 18. Comparison between Default (Predicted) $ E^* $ from Master Curve and Measured $ E^* $ Values for HMA Mixture (a) Type C, PG 64-22, (b) Type D, PG 64-22, (c) Superpave C, PG 70-22, and (d) Superpave C, PG 76-22.....	22
Figure 19. Test Matrices of RAP/RAS Mixture Characterization for (a) Type D and (b) SMA C.....	23
Figure 20. Comparison between Default (Predicted) $ E^* $ from Master Curve and Measured $ E^* $ Values for RAP/RAS Mixes.....	26
Figure 21. Repeated Load Permanent Deformation Test Result and Rutting Parameters: μ and α	28
Figure 22. Comparison of Default and Measured Rutting Parameters (a) Considering All Available α -Data and (b) Considering All Available μ -Data.....	30
Figure 23. Comparison between the Predicted and Observed (Measured) RAP/RAS Mixes Rutting Properties (a) Alpha and (b) μ	32
Figure 24. OT Result and Determination of Fracture Properties: A and n	33
Figure 25. Overall Comparison of Virgin Asphalt Mixtures Default and Measured Fracture Properties: (a) A Values and (b) n Values.....	35
Figure 26. Comparison between the Predicted and Observed (Measured) RAP/RAS Mixes Fracture Properties (a) A and (b) n	36
Figure 27. TxME Screen of Incorporating Default Material Properties.....	37
Figure 28. VCDs for IH WIM Stations.....	42
Figure 29. Examples of TxME Predicted Results: (a) C8 Ranged from 0.9 Percent to 5.1 Percent, (b) C9 Ranged from 30.4 Percent to 80.2 Percent, and (c) C12 Ranged from 0.4 Percent to 2.3 Percent.....	44
Figure 30. Comparison of the Number of APT for Tandem Axle.....	45
Figure 31. Sensitivity Analysis Results: (a) Rutting and (b) Cracking.....	46
Figure 32. Examples of MAF for (a) C5 and (b) C9.....	48

Figure 33. Sensitivity Analysis Results for MAF: (a) Rutting and (b) Cracking.	49
Figure 34. Sensitivity Analysis Results of ALD: (a) Rutting, (b) Cracking, and (c) ALDs of Heavy, Medium and Light Default Input for Tandem Axle.....	52
Figure 35. VCDs for US/SH.	53
Figure 36. Sensitivity Analysis Results: (a) C8, (b) C9, and (c) C11.....	54
Figure 37. Sensitivity Analysis Results of ALD for US/SH: (a) Rutting, (b) Cracking, and (c) ALDs of Heavy, Medium, and Light Default Input for Tandem Axle.....	58
Figure 38. Comparison of Cumulative Tandem ALDs of C9 for Three Default ALD Inputs.....	61
Figure 39. Three Default ALDs for FM: (a) Rutting and (b) Cracking.....	62
Figure 40. (a) Comparison of Predicted Cracking Performances with Use of Different ALDs for IH, US/SH, FM, and Roads in Energy Sectors, and (b) Comparison of ALDs.....	65
Figure 41. TxME Screen of Incorporating Default Load Spectra.	66
Figure 42. Twelve-Month Average Low Bid Prices of (a) Dense Graded, (b) Superpave, and (c) SMA Mixtures.	69
Figure 43. Comparison between the Actual CF and Predicted CF.....	74
Figure 44. TxME Initial Construction Cost Analysis (a) Input and (b) Output.....	76
Figure 45. Observed versus TxME Predicted Rut Depths for Surface Treated Pavement Sections when (a) TxME Defaults Are Used and (b) Database Parameters Are Used.	80
Figure 46. Observed versus TxME Predicted Rut Depths when (a) Database Material Parameter Values Used and (b) TxME Default Material Parameter Values Used.....	84
Figure 47. Observed versus TxME Predicted Rut Depths.....	85
Figure 48. Observed versus TxME Predicted Fatigue Cracking Area when (a) Database Material Parameters Are Used and (b) TxME Default Parameters Are Used.....	87
Figure 49. TxME Simulation Results and the Observed Fatigue Cracking Area for UTEP-1, UTEP-2, and UTEP-3 Test Sections.	88
Figure 50. Projects and Test Section Location.	90
Figure 51. US 259 Test Sections (a) Map Location and (b) Pavement Structure.....	92
Figure 52. SH 6 Test Section (a) Map Location and (b) Pavement Structure.	93
Figure 53. SH 7 Test Sections (a) Map Location and (b) Pavement Structure.....	94
Figure 54. FM 3549 Test Section (a) Map Location and (b) Pavement Structure.....	95
Figure 55. US 87 Test Section (a) Map Location and (b) Pavement Structure.	96
Figure 56. FM 1463 Test Sections (a) Map Location and (b) Pavement Structure.....	97
Figure 57. US 259 Field Visiting Photos (a) 2015-02-20, Identifying Test Section and (b) 2016-01-22, Sampling Subgrade and Base Material.	99
Figure 58. SH 6 Field Visiting Photos (a) 2016-11-09, Field Survey and (b) 2018-07-21, Field Survey.	100
Figure 59. SH 7_S1 Field Visiting Photos (a) 2015-08-27, HMA Sampling during Surface Layer Construction and (b) 2018-07-18, Field Survey.....	101
Figure 60. SH 7_S2 Field Visiting Photos (a) 2016-04-04, Base Material Sampling during Base Layer Construction and (b) 2018-07-18, Field Survey.	102
Figure 61. FM 3549 Field Visiting Photos (a) 2015-09-23, Subbase Material Sampling during Construction and (b) 2018-07-17, Field Survey.....	103

Figure 62. US 87 Field Visiting Photos (a) 2016-11-18, HMA Material Sampling during Surface Layer Construction and (b) 2018-07-20, Field Survey.....	104
Figure 63. FM 1463 Field Visiting Photos (a) 2016-06-15, HMA Material Sampling during Surface Layer Construction and (b) 2018-07-22, Field Survey.	105
Figure 64. Transverse Crack and Longitudinal Crack on FM 3549 Test Section.	106
Figure 65. Longitudinal Crack on FM 1463_S4 Test Section.....	107
Figure 66. TxDOT Statewide Planning Map.	113
Figure 67. ESAL Calculation Using ACPA Web Application.	114
Figure 68. Portable WIM Station on SH 6.....	115
Figure 69. TxME Pavement Structure Input for Test Section FM 3549.	118
Figure 70. TxME HMA Material Property Input for Test Section FM 3549.	119
Figure 71. TxME Climate Input for Test Section FM 3549.	120
Figure 72. TxME Traffic Input for Test Section FM 3549.....	121
Figure 73. TxME Reliability/Performance Criteria Input for Test Section FM 3549.	122
Figure 74. TxME Predicted Rut Depth for Test Section FM 3549.....	122
Figure 75. TxME Predicted AC Fatigue Cracking for Test Section FM 3549.	123
Figure 76. TxME Predicted Thermal Cracking for Test Section FM 3549.	123
Figure 77. SH 6 Rut Depth Comparison between TxME Prediction and Field Survey.	125
Figure 78. SH 7_S1 Rut Depth Comparison between TxME Prediction and Field Survey.	125
Figure 79. FM 3549 Thermal Cracking Comparison between TxME Prediction and Field Survey.	126
Figure 80. US 259_S1 TxME Prediction of (a) Rut Depth, (b) Fatigue Cracking, and (c) Thermal Cracking.	134
Figure 81. US 259_S1 TxME Prediction of (a) Rut Depth, (b) Fatigue Cracking, and (c) Thermal Cracking.	135
Figure 82. SH 6 TxME Prediction of Total Rut Depth when Traffic Input Is (a) Level 2 – ESALs and (b) Level 1 – Load Spectra.	136
Figure 83. SH 7_S1 TxME Prediction of (a) AC Rut Depth, (b) Fatigue Cracking, and (c) Thermal Cracking.	137
Figure 84. SH 7_S2 TxME Prediction of Total Rut Depth.....	138
Figure 85. FM 3549 TxME Prediction of (a) Total Rut Depth, (b) Fatigue Cracking, and (c) Thermal Cracking.....	139
Figure 86. US 87 TxME Prediction of (a) AC Rut Depth, (b) Fatigue Cracking, and (c) Thermal Cracking.	140
Figure 87. FM 1463_S1 TxME Prediction of (a) AC Rut Depth, (b) Fatigue Cracking, and (c) Thermal Cracking.	141
Figure 88. FM 1463_S2 TxME Prediction of (a) AC Rut Depth, (b) Fatigue Cracking, and (c) Thermal Cracking.	142
Figure 89. FM 1463_S1 TxME Prediction of (a) AC Rut Depth, (b) Fatigue Cracking, and (c) Thermal Cracking.	143
Figure 90. FM 1463_S1 TxME Prediction of (a) AC Rut Depth, (b) Fatigue Cracking, and (c) Thermal Cracking.	144

LIST OF TABLES

	Page
Table 1. Default Values for Dynamic Modulus of Typical Virgin Asphalt Mixes Used in Texas.	21
Table 2. Average $ E^* $ of Type D RAP/RAS Mixtures.	24
Table 3. Average $ E^* $ of SMA C RAP/RAS Mixtures.	25
Table 4. $ E^* $ Adjustment Factors for RAP/RAS Mixes.	26
Table 5. Default Modulus Values for Other Pavement Materials.	27
Table 6. Default Rutting Properties for Typical Virgin Asphalt Mixes Often Used in Texas.	29
Table 7. Rutting Properties of RAP/RAS Mixtures.	31
Table 8. Optimized RAP/RAS Adjustment Factors for Rutting Properties.	32
Table 9. Default Rutting Parameters for Other Pavement Materials.	33
Table 10. Default Fracture Properties for Typical Virgin Asphalt Mixes Often Used in Texas.	34
Table 11. RAP/RAS Adjustment Factors for Fracture Properties.	36
Table 12. WIM Stations Used for Data Analysis.	41
Table 13. Percentage Ranges for Each Truck Class Based on All WIM Stations.	43
Table 14. Default Inputs of VCD for IH.	45
Table 15. Default Input of APT for IH.	47
Table 16. Average Values of MAF.	50
Table 17. Location Information for Three Default ALDs.	52
Table 18. Percentage Ranges for Each Truck Class Based on All the WIM Stations.	53
Table 19. Default Inputs of VCD for US/SH.	55
Table 20. Average Value of APT.	55
Table 21. Average Values of MAF.	56
Table 22. Location Information for Three Default ALDs.	58
Table 23. Default Input of VCD for FM.	59
Table 24. Average Value of APT.	59
Table 25. Average Values of MAF.	60
Table 26. Default Input of VCD for FM.	63
Table 27. Average Value of APT.	64
Table 28. Costs for Binder-Specific Dense-Graded Type C AC Mixtures.	70
Table 29. TxME Default Initial Construction Cost of AC Mixtures.	71
Table 30. Cost Factors for Various AC Mixtures with Recycled Materials.	73
Table 31. Costs of Base/Subbase/Subgrade Layer Materials.	75
Table 32. Surface Treated Sections with Measured Rut Performance Data.	78
Table 33. Tests Sections and Their Rut Parameters from TxDOT Database.	79
Table 34. Test Sections Considered for TxME Rutting Calibration.	82
Table 35. Tests Sections and Their Fatigue Performance Data.	86
Table 36. GPS Coordinate and Length of Each Test Section.	91
Table 37. SH 6 Rut Depth Survey Result.	107
Table 38. SH 7_S1 Rut Depth Survey Result.	107
Table 39. FM 3549 Cracking Survey Result.	108
Table 40. FM 1463_S4 Cracking Survey Result.	108

Table 41. HMA (Plant Mix) Tests Specification.....	109
Table 42. FB/Subbase Material Tests Specification.....	109
Table 43. Stabilized Base/Subbase Material Tests Specification.....	110
Table 44. Subgrade Soil Tests Specification.....	110
Table 45. HMA Dynamic Modulus of Test Sections.....	111
Table 46. HMA Fracture Property and Rutting Property of Test Sections.....	112
Table 47. Base/Subbase/Subgrade Material Property of Test Sections.....	112
Table 48. ESALs of Test Sections.....	115
Table 49. VCD of SH 6 Test Section.....	116
Table 50. APT of SH 6 Test Section.....	116
Table 51. MAFs of SH 6 Test Section.....	116
Table 52. ALD of SH 6 Test Section (Steering Single Axle, January).....	117
Table 53. TxME Predicted Distress for Each Test Section.....	133

LIST OF ACRONYMS

AADTT	Average Annual Daily Truck Traffic
AASHTO	American Association of State Highway and Transportation Officials
AC	Asphalt Concrete
ACPA	American Concrete Pavement Association
ALD	Axle Load Distribution
APT	Axles Per Truck
CF	Calibration factor
CSJ	Control Section Job
ESAL	Equivalent Single Axle Load
FA	Fly Ash
FB	Flexible base
FM	Farm-to-market
FWD	Falling Weight Deflectometer
FPS	Flexible Pavement Design System
HMA	Hot-Mix Asphalt
IH	Interstate Highway
LFA	Lime Fly Ash
MAF	Monthly Adjustment Factor
OT	Overlay Test (based on Tex-248-F)
PG	Performance grade
RAP	Reclaimed Asphalt Pavements
RAS	Reclaimed Asphalt Shingles
RBL	Rich Bottom Layer
SH	State highway
SMA	Stone Matrix Asphalt
TxDOT	Texas Department of Transportation
TxME	Texas Mechanistic-Empirical Flexible Pavement Design System
US	U.S. highway
VCD	Vehicle Class Distribution
WIM	Weigh-in-motion

CHAPTER 1. INTRODUCTION

BACKGROUND AND OBJECTIVES

The Texas Department of Transportation (TxDOT) has been using the flexible pavement design system (FPS) for several decades. FPS was developed on basis of AASHO road test data. Overall, it serves well but with some limitations (Liu and Scullion 2006). For example, the full benefits of using premium materials (including both asphalt mixes and base materials) cannot be quantified, because no other material property than material modulus is required by FPS. Developments over the last several decades have offered an opportunity for more rational and rigorous pavement design procedures. Substantial work has already been completed in Texas, nationally, and internationally, in all aspects of modeling, materials characterization, and structural design. These and other assets provided the technical infrastructure that made it possible to develop the Texas Mechanistic-Empirical flexible pavement design system (TxME). This new system enables Texas pavement designers to take full advantage of new or premium materials, with a full consideration of the influential factors including pavement structure, traffic volume, and environmental conditions. After the TxME system development was preliminarily completed at the end of 2014 (Hu et al. 2014), TxDOT initiated this implementation project in March 2015 to further calibrate, enhance, and pilot implement this system in selected Texas districts.

The main objectives of this project were to:

- Develop training workshop materials and present the training workshop to the project team and selected districts.
- Familiarize the district engineers with the complete ME design process that entails enhanced inputs.
- Demonstrate the advantages when premium materials, load spectra, and local climate data are used.
- Refine/finalize lab tests for TxME key input parameters and determine default values.
- Enhance the program by further calibration and model fine-tuning based on lab/field performance data from identified test sections.

During this project, extensive lab testing was conducted to develop default material properties for TxME. In addition, the default load spectra information and initial construction cost analysis were integrated into the TxME. After calibrated with Texas Flexible Pavement Database (Walubita et al. 2012, 2015), the calibrated TxME was further verified with independent test sections. The comparison between the TxME predictions and the field performance survey results confirmed the validity of TxME performance models. This report mainly focuses on how the TxME was enhanced by incorporating default material property, default load spectra, and initial construction cost analysis, and how this enhanced system was calibrated using the Texas Flexible Pavement Database and verified by field test sections.

REPORT ORGANIZATION

This report is organized into the following eight chapters:

- Chapter 1: Introduction, providing a brief description of the project background, objectives, and report organization.
- Chapter 2: TxME description, summarizing the overall design, inputs and outputs, user interfaces, and functions of TxME.
- Chapter 3: Develop default material properties for TxME. The default material properties include the pavement material moduli, layer rutting properties, and asphalt layer cracking properties. Especially for asphalt mixture with reclaimed asphalt pavements (RAP) or reclaimed asphalt shingles (RAS) material, the relationships between default dynamic modulus/rutting property/cracking property and RAP/RAS contents are developed.
- Chapter 4: Develop default axle load spectra for TxME. Based on the traffic data of identified weigh-in-motion (WIM) stations, the Texas highways are divided into four categories: Interstate Highway (IH), state highway (SH), U.S. highway (US), farm-to-market road (FM), and energy sector road. For each type of highway, according to their truck volume (high, medium, low) and weight (heavy, medium, and light) features, the corresponding default/typical load spectra information such as vehicle class distribution (VCD), axle load distribution (ALD), monthly adjustment factor (MAF), and axles per truck (APT) information are suggested and incorporated into the TxME.
- Chapter 5: Develop default initial construction cost. This chapter describes how the initial construction costs of pavement layer materials especially the asphalt concrete (AC) mixtures with RAP/RAS were determined and incorporated into the TxME software
- Chapter 6: TxME performance model calibration. In this study, the Texas Flexible Pavement Database were used to calibrate the TxME performance models. The base/subgrade rutting model was calibrated based on the identified surface treatment pavement test sections in the database, and the AC rutting and fatigue cracking model was calibrated based on the identified conventional pavement test sections.
- Chapter 7: TxME verification by field test sections. Eleven test sections were identified in six different districts. Their layer materials were sampled and tested, and their field performances were monitored. The calibrated and enhanced TxME was employed to conduct performance predictions for these identified test sections and was verified by the comparison between the performance predictions and the field survey results.
- Chapter 8: Conclusions and Recommendations.

Additionally, this report includes one appendix, which provides more details on the TxME performance prediction results for identified test sections, titled “TxME Prediction Results for 11 Test Sections.”

CHAPTER 2. TXME DESCRIPTION AND TRAINING WORKSHOP

The TxME design system enables TxDOT designers to take full advantage of new or premium materials and to make more economically reliable designs. Three types of flexible pavement structures can be handled in the TxME, including:

- Surface treated.
- Conventional or thin hot-mix asphalt (HMA).
- Perpetual pavement.

For any type of pavement design and analysis, there are four categories of input:

- Pavement structure and associated material properties.
- Traffic loading.
- Climate.
- Reliability-related input, including performance criteria and variability, etc.

The following describes these four categories of input and then output to provide an overview of TxME.

PAVEMENT STRUCTURE AND ASSOCIATED MATERIAL PROPERTIES

The user interface aspects of the main screen, pavement structure screen, and material properties input screen are briefly illustrated below.

Main Screen

Figure 1 presents the main screen of the TxME. In this screen, four major input categories are listed on the left side of the node tree, such as Structure, Climate, Traffic, and Reliability. Double-clicking each node activates the corresponding input window on the right side.

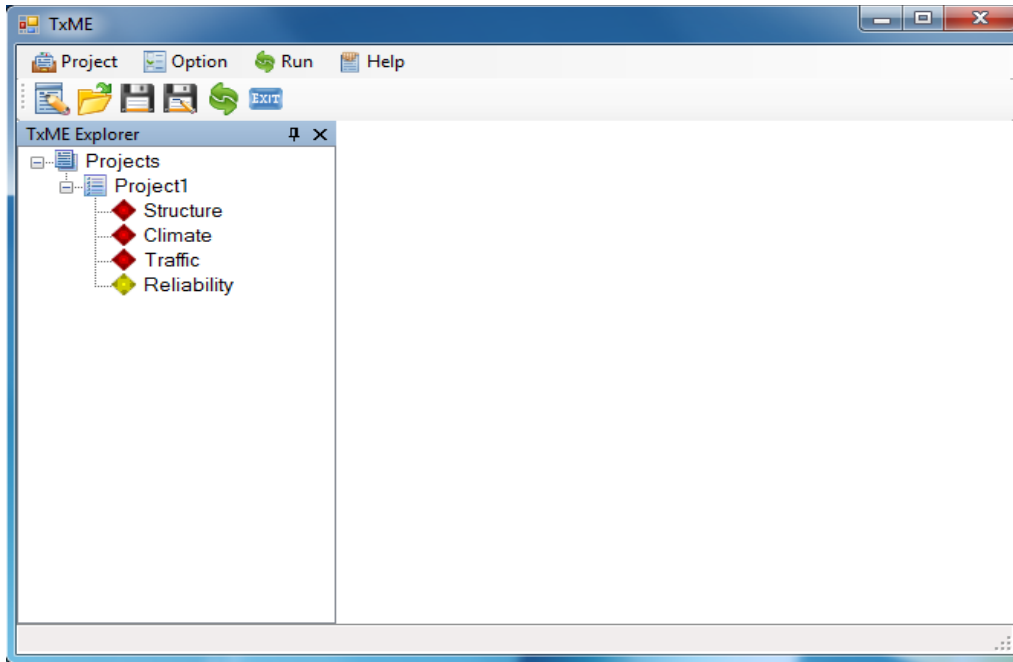


Figure 1. Main Screen of User Interface.

Pavement Structure

Figure 2 presents the pavement structure input screen. On this screen, the upper left window shows the pavement type and location; the upper right window lists available AC layer material, base layer material, and subbase layer material icons; the lower left window shows the pavement structure; and the lower right window shows the layer material properties.

Users can build their own pavement structures by dragging the layer material icons into the pavement structure window. To remove a layer from the pavement structure window, users just need to click the layer and choose “Remove this layer” from the pop-up menu.

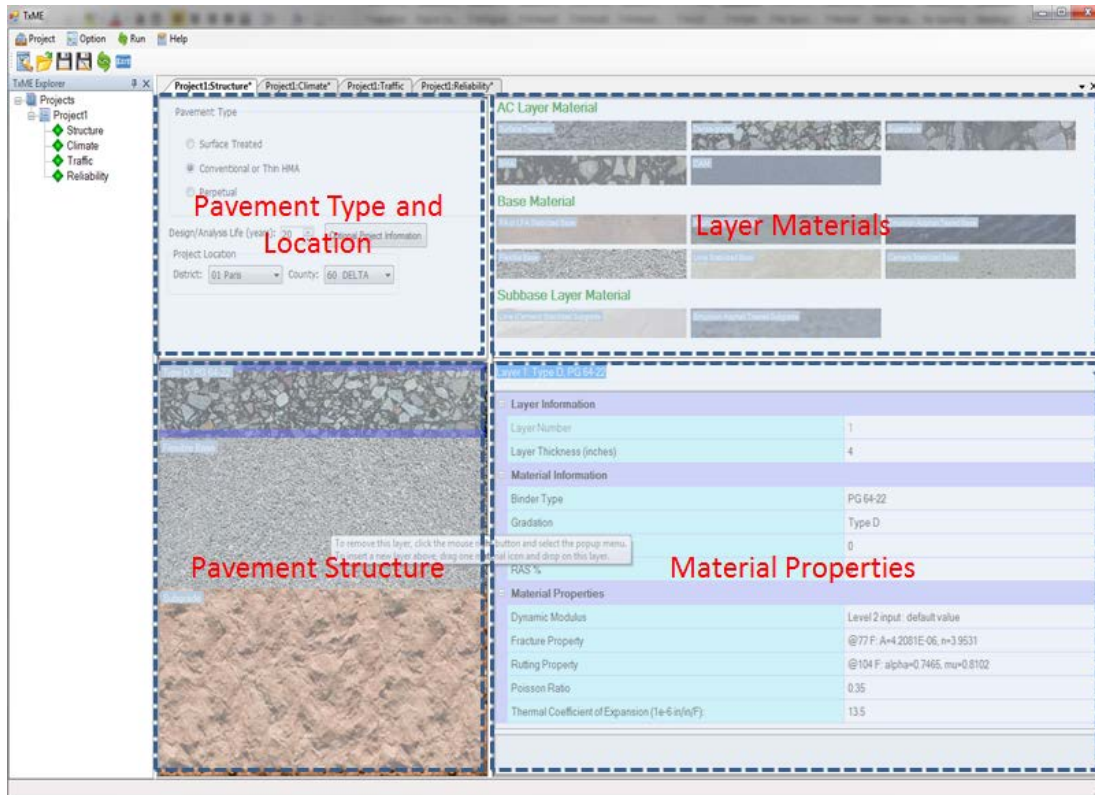


Figure 2. Pavement Structure Information Screen.

Material Properties

As in Figure 2, by clicking each layer in the pavement structure window, users can browse or edit this layer thickness and layer material properties in the material properties window. For some property inputs such as Thickness, Poisson's Ratio, etc., the user only needs to input a single parameter. For more complicated inputs such as dynamic modulus and fracture/rutting properties, the user needs to click on the item drop-down menu, and the expanded input screen will pop up. Several material property input screens are illustrated below, including:

- Figure 3, presenting the dynamic modulus inputs for AC layers.
- Figure 4 and Figure 5, presenting AC layer fracture property and rutting property inputs, respectively.

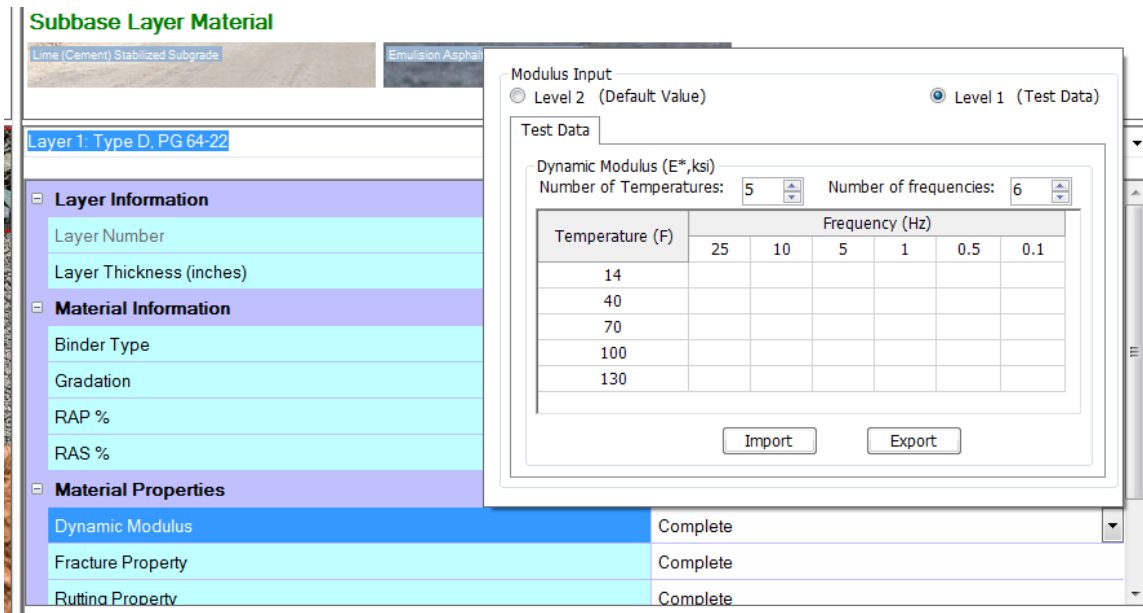


Figure 3. AC Layer Dynamic Modulus Input Screen.

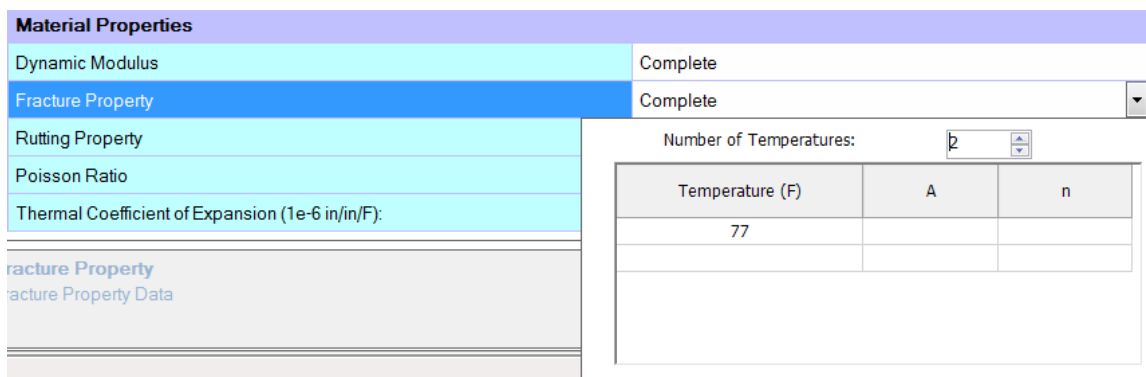


Figure 4. AC Layer Fracture Properties Input Screen.

Layer 1: SurfaceTreat, PG 64-22

Layer Information	
Layer Number	
Layer Thickness (inches)	
Material Information	
Binder Type	
RAP %	
RAS %	
Material Properties	
Dynamic Modulus	
Fracture Property	
Rutting Property	Complete
Poisson Ratio	0.35
Thermal Coefficient of Expansion (1e-6 in/in/F):	13.5

Number of Temperatures:

Temperature (F)	alpha	mu
104		

Figure 5. AC Layer Rutting Properties Input Screen.

TRAFFIC LOADING

There are two levels of traffic inputs in TxME: one is equivalent single axle load (ESAL) input and the other is axle load spectrum input. The following illustrates the difference between these inputs.

Traffic ESALs (Level 2) Input

Figure 6 shows the traffic ESALs (Level 2) input screen. The most important input is the total ESAL number for 20 years (one lane and one direction). The ADT-Beginning and ADT-End represent average daily traffic in the beginning and in the end, respectively. These values are used to determine the vehicle growth rate. The tire pressure is used to determine the tire contact area. The operational speed (could be posted speed limit, or lower in urban traffic) impacts the AC layer modulus since it relates to loading time.

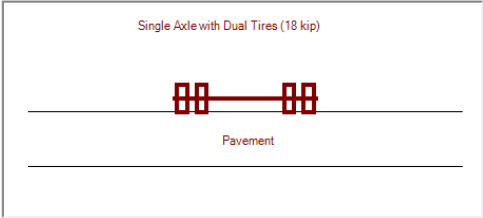
Project1:Structure* Project1:Climate* **Project1:Traffic** Project1:Reliability*

Traffic Input

Level 2: ESALs Level 1: Load Spectra

Level 2: ESALs

Single Axle with Dual Tires (18 kip)



Pavement

Tire Pressure (psi):	<input type="text" value="100"/>	18 kip ESALs 20 YR (1 DIR) (millions):	<input type="text" value="3.0"/>
ADT-Beginning (Veh/Day):	<input type="text" value="2000"/>	Operation Speed (mph):	<input type="text" value="60"/>
ADT-End 20 YR (Veh/Day):	<input type="text" value="3500"/>		

Figure 6. Traffic ESALs (Level 2) Input Screen.

Axle Load Spectra (Level 1) Input

Figure 7 is the traffic (truck classes 4–13) axle load spectra (Level 1) input screen. In this screen, the left window shows the general information and axle configuration information such as average annual daily truck traffic (AADTT) number, operational speed, tire pressure, axle spacing, etc.; the upper right window shows the VCD and growth rate information; and the lower right window shows the axle numbers for each vehicle class. By clicking the Monthly Adjustment or Axle Load Distribution button in Figure 7, screens such as Figure 8 or Figure 9 pop up. These screens let users define the ALDs for each vehicle class and their monthly variations.

Traffic Input

Level 2: ESAs Level 1: Load Spectra

Level 1: Load Spectra

General Traffic Information

Traffic Two-way AADTT: 500

Number of Lanes in Design Direction: 2

Percent of Trucks in Design Lane (%): 95.0

Operation Speed (mph): 60

General Information

Axle Configuration

Axle Tire

Single Tire Pressure (psi): 100

Dual Tire Pressure (psi): 100

Dual Tire Spacing (in): 12

Axle Spacing

Tandem Axle (n): 51.6

Tridem Axle (n): 49.2

Quad Axle (n): 49.2

Axle Configuration

Monthly Adjustment Axle Load Distribution

Vehicle Class Distribution and Growth

Vehicle Class	Pictorial View	Distribution (%)	Growth Rate (%)	Growth Function
Class 4		1.8	4	Compound
Class 5		24.6	4	Compound
Class 6		7.8	4	Compound
Class 7		0.5	4	Compound
Class 8		21.3	4	Compound
Class 9		0.8	4	Compound
Class 10		3.3	4	Compound
Class 11		0.8	4	Compound
Class 12		3.3	4	Compound
Class 13		15.3	4	Compound
Sum of Distribution (%)		100.0		

Vehicle Class Distribution and Growth

Axes Per Truck

Vehicle Class	Steering Axle	Other Single Axles	Tandem Axles	Tridem Axles	Quad Axles
Class 4	0	1.62	0.39	0	0
Class 5	0	2	0	0	0
Class 6	0	1.02	0.99	0	0
Class 7	0	1	0.26	0.83	0
Class 8	0	2.30	0.67	0	0
Class 9	0	1.19	1.09	0.89	0
Class 10	0	4.29	0.26	0.06	0
Class 11	0	3.62	1.14	0.06	0
Class 12	0	2.15	2.13	0.35	0
Class 13	0				

Axes per Truck

Note: Steering Axle -- Single axle, single tire; Other Single Axle -- Single axle, dual tires.

Figure 7. Traffic Load Spectrum (Level 1) Input Screen.

Monthly Adjustment

Load MAF From File Export to MAF File

Monthly Adjustment Factors

Month	Class_4	Class_5	Class_6	Class_7	Class_8	Class_9	Class_10	Class_11	Class_12	Class_13
January	1	1	1	1	1	1	1	1	1	1
February	1	1	1	1	1	1	1	1	1	1
March	1	1	1	1	1	1	1	1	1	1
April	1	1	1	1	1	1	1	1	1	1
May	1	1	1	1	1	1	1	1	1	1
June	1	1	1	1	1	1	1	1	1	1
July	1	1	1	1	1	1	1	1	1	1
August	1	1	1	1	1	1	1	1	1	1
September	1	1	1	1	1	1	1	1	1	1
October	1	1	1	1	1	1	1	1	1	1
November	1	1	1	1	1	1	1	1	1	1
December	1	1	1	1	1	1	1	1	1	1

OK Cancel

Figure 8. Traffic Monthly Adjustment Input Screen.

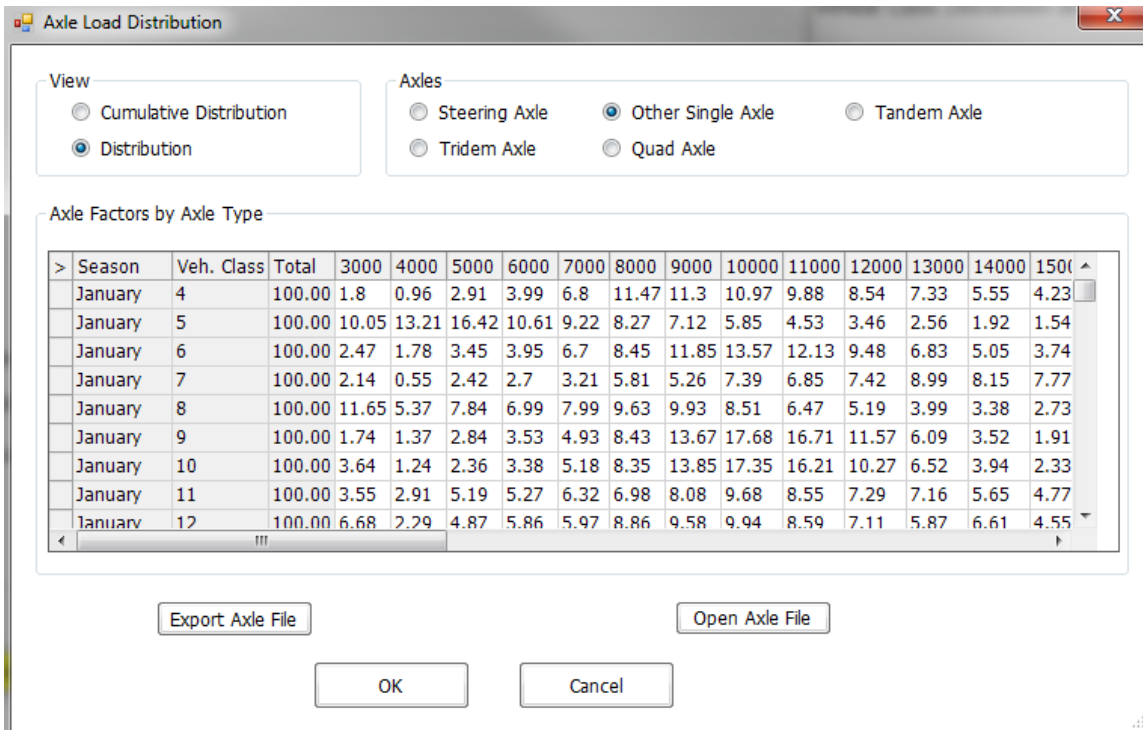


Figure 9. Traffic Axle Load Distribution Input Screen.

CLIMATE

There are two ways to attach the climatic information to a given project location: users can either assign a specific weather station or use interpolated climatic data based on the coordinates of the location.

Figure 10 presents the climate input screen when users choose a specific weather station. Generally, the left part of the screen allows the user to select a weather station, and the right part shows the summary of the weather data, such as average temperature or precipitation. The tables on the right side will not appear until after a station location is selected (OK button activated). The user can find more detailed information like hourly data by clicking the Hourly Data tab on the upper right part of the screen.

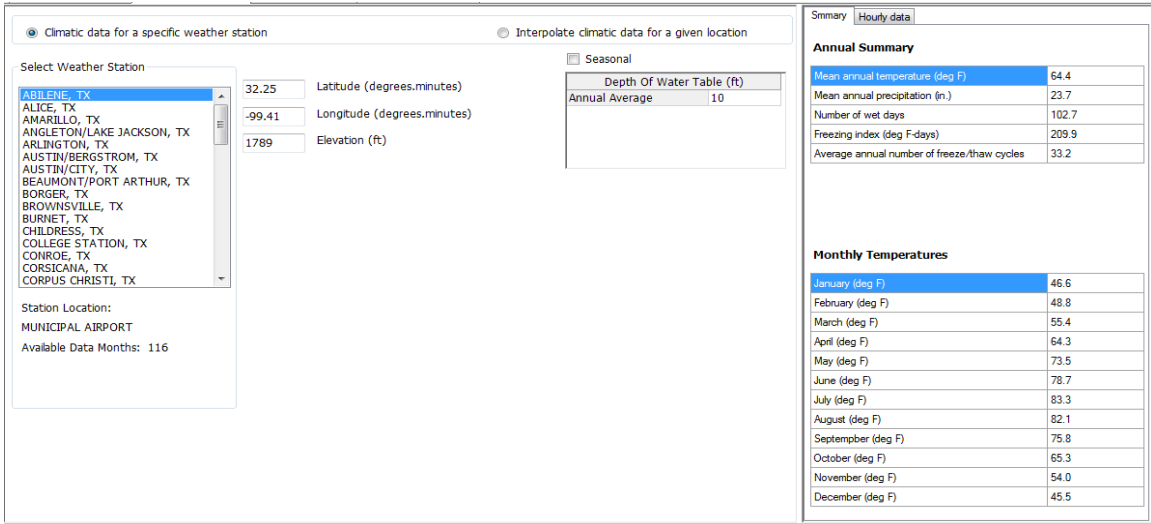


Figure 10. Climate for a Specific Weather Station Input Screen.

For a project location without a pre-listed weather station, users can choose the radio button “Interpolate climatic data for a given location” and the application will provide six weather stations nearby for the user to select for interpolation. Figure 11 presents the user input screen for climate data interpolation. The lines and numbers such as “#1, #2...” in the graph show the relative positions and distances from the location defined by the coordinates. The interpolated hourly data information is listed in the right part of the screen.

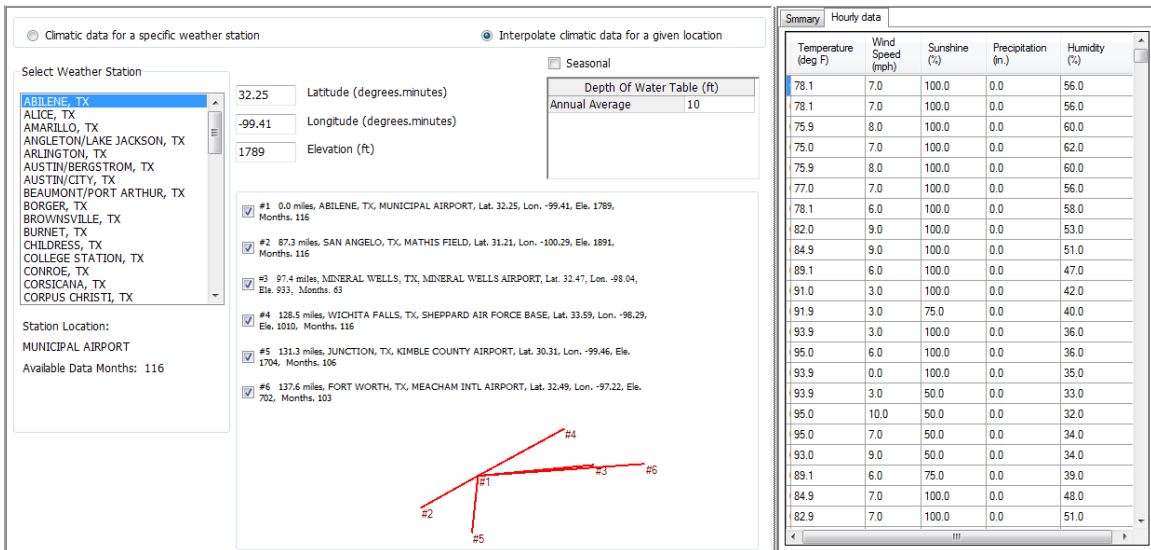


Figure 11. Climatic Data Interpolation Input Screen.

RELIABILITY RELATED INPUT

Figure 12 presents the reliability related input screen for a three-layer conventional pavement. Two input categories are displayed in this screen. On the left side are the performance criteria inputs, and on the right side are the variability inputs. For the performance criteria inputs, the user supplies the analysis stop criteria (performance limit) and reliability level in terms of percentage. For variability inputs, the user checks the applicable checkboxes and modifies the coefficient of variation value.

The screenshot shows a software interface with four tabs at the top: Project1:Structure*, Project1:Climate*, Project1:Traffic*, and Project1:Reliability*. The 'Project1:Reliability*' tab is active. The interface is split into two panels.

Performance Criteria Panel:

Performance	Limit	Reliability (%)
Rutting (inch)	0.5	50
Thermal cracking (ft/mile)	2112	50
Fatigue cracking of AC layer (percent)	50	50

Variability of Input Parameters Panel:

Use	Parameter	Coefficient of Variation (%)
<input checked="" type="checkbox"/>	Layer 1 (AC: DenseGraded) - Thickness	10
<input type="checkbox"/>	Layer 1 (AC: DenseGraded) - Modulus	
<input type="checkbox"/>	Layer 1 (AC: DenseGraded) - Fracture Property A	
<input type="checkbox"/>	Layer 1 (AC: DenseGraded) - Fracture Property n	
<input type="checkbox"/>	Layer 1 (AC: DenseGraded) - Rutting Property Alpha	
<input type="checkbox"/>	Layer 1 (AC: DenseGraded) - Rutting Property Mu	
<input type="checkbox"/>	Layer 2 (Base: FlexibleBase) - Thickness	
<input type="checkbox"/>	Layer 2 (Base: FlexibleBase) - Modulus	
<input type="checkbox"/>	Layer 2 (Base: FlexibleBase) - Rutting Property Alpha	
<input type="checkbox"/>	Layer 2 (Base: FlexibleBase) - Rutting Property Mu	
<input type="checkbox"/>	Layer 3 (Subgrade) - Modulus	
<input type="checkbox"/>	Layer 3 (Subgrade) - Rutting Property Alpha	
<input type="checkbox"/>	Layer 3 (Subgrade) - Rutting Property Mu	
<input checked="" type="checkbox"/>	Traffic - ESALs or AADTT	10

Figure 12. Reliability Related Input Screen for a Three-Layer Conventional Pavement.

Both performance criteria and variability parameters are related to pavement structure and pavement type. Whenever the pavement structure or pavement type changes, these parameters are changed accordingly. Note that in the TxME, Rosenblueth's $2n+1$ (n is number of variables with uncertainty) method is used to perform the reliability analysis, which has high practical benefit in terms of program operating efficiency for mechanistic-empirical flexible pavement designs (Rosenblueth 1975, Hu et al. 2012a).

OUTPUT

The output of TxME is organized into an Excel[®] file, which is mainly composed of three parts: the summary of user's inputs, the analysis result table, and the distress plots. See Figure 13. The predicted distresses are keyed to the pavement structure and pavement type. The following information discusses and illustrates the output for each pavement type.



Figure 13. Output of TxME in Excel File Format.

CONNECTION WITH FPS 21

FPS 21 is the flexible pavement design system currently used by TxDOT. The users' input of FPS 21 includes pavement location, beginning and ending serviceability indices, traffic ESALs, elastic modulus (can be based on falling weight deflectometer [FWD] backcalculation) of each layer, maximum and minimum thickness of each layer, etc. FPS 21 reports combinations of layer thicknesses that fulfill the performance equation as constrained by the inputs. Note that FPS 21 only uses FWD backcalculated/estimated elastic modulus, and Poisson's ratio to represent each layer's properties; it does not use any lab testing data, so it is impossible to determine performance benefits from improved base materials or superior asphalt mixes. To evaluate these benefits, TxME is designed to import pertinent input and output information from FPS 21, then to incorporate additional specific test results such as rutting properties or fracture properties, to conduct the performance check. Figure 14 shows the connection concept.

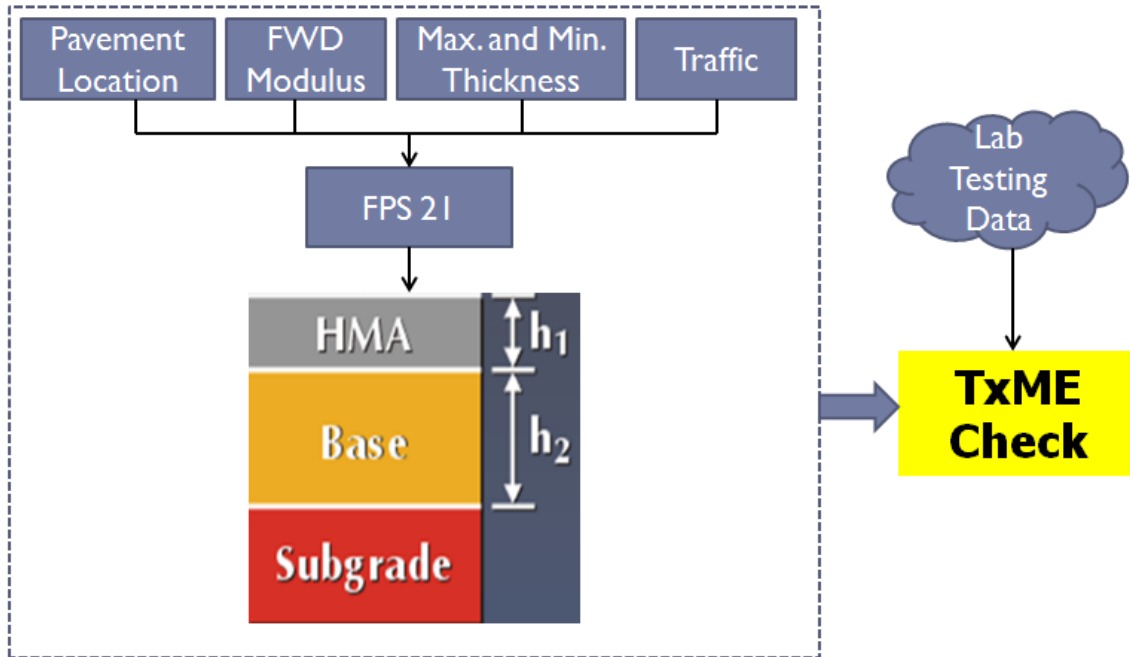


Figure 14. Connection Concept between FPS 21 and TxME.

Figure 15 shows an example of a TxME pavement structure imported from FPS 21 using a specially modified version of the program. By clicking the button TxME Check in the FPS 21 screen, the TxME will be launched and automatically import the related information, such as pavement location, layer type, layer thickness, ESALs, and so on. The left part of Figure 15 is the FPS 21 recommended design option, and the right part is the TxME pavement structure after importation. TxME also searches the embedded database and provides default values for lab testing data. Users can edit these values if specific lab test results are available.

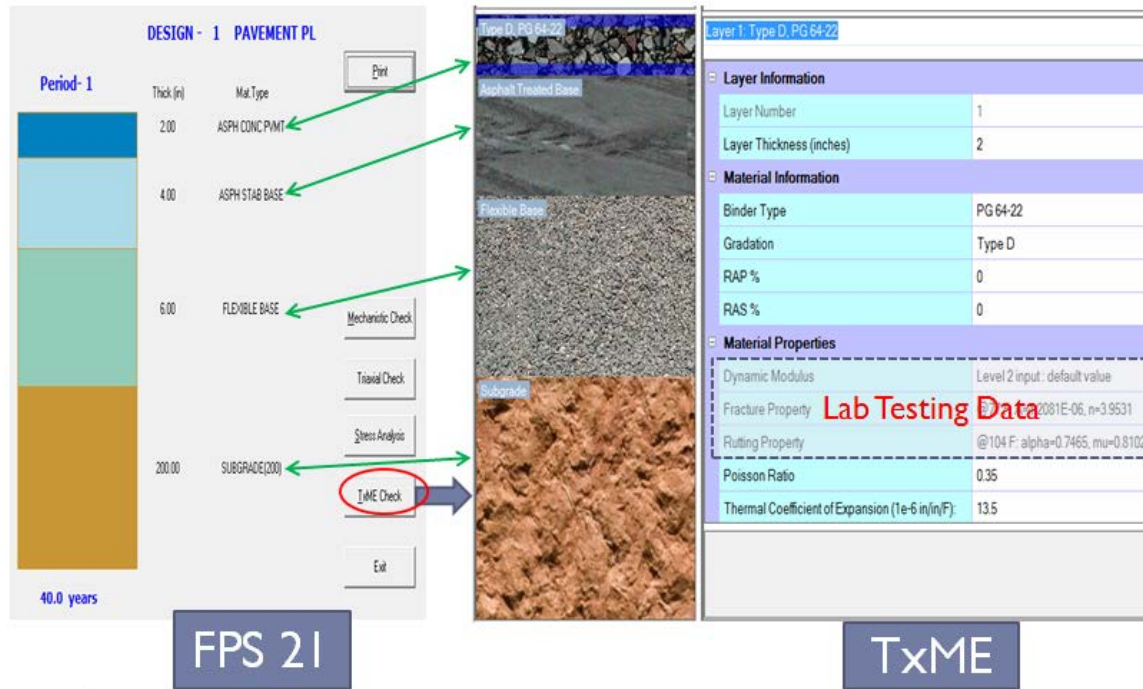


Figure 15. An Example of TxME Pavement Structure Imported from FPS 21.

HELP FILE

Figure 16 shows the TxME Help File. Much more details about input/output instructions and definitions can be found in this file. Users can push F1 anytime to access this help file and browse corresponding page.

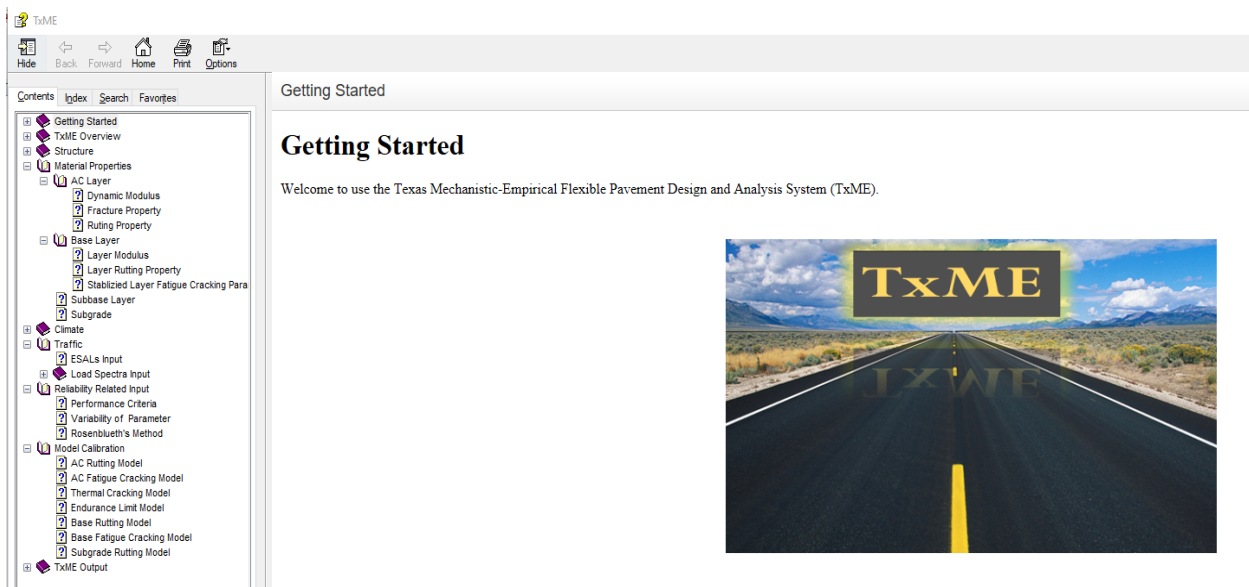


Figure 16. TxME Help File.

WORKSHOP

One important task of the project 5-6622-01 is to conduct workshop for the project monitoring committee and participating districts. The goal of this task was to help TxDOT engineers to get familiar with TxME software and collect their feedback and trial experiences. With the coordination and help of project advisors Enad Mahmoud and Gisel Carrasco, researchers conducted five workshops and trained more than 85 TxDOT engineers on how to use TxME to analyze pavement performance. The following lists the workshop time, location, and number of attendees:

- 09-27-2016, TxDOT Austin Headquarters: A total of 19 TxDOT engineers attended the workshop. They came from Austin, Lufkin, Houston, Laredo, Fort Worth, Lubbock, Yoakum, Waco, Abilene, Corpus Christi, Odessa, Paris, and Bryan Districts.
- 10-05-2016, TxDOT Austin Headquarters: A total of 12 TxDOT engineers attended the workshop. They came from Austin, San Angelo, El Paso, and Atlanta Districts.
- 04-24-2017, Waco District: A total of 21 TxDOT engineers attended the workshop. The engineers came from Waco, Tyler, and Dallas Districts.
- 05-03-2017, Corpus Christi District: 6 TxDOT engineers attended the workshop. The engineers came from Corpus Christi, Pharr, and San Angelo Districts.
- 05-09-2017, Lubbock District: A total of 27 TxDOT engineers attended the workshop. The engineers came from Lubbock, Odessa, Amarillo, Abilene, and San Angelo Districts.

According to the discussions during the workshops and the evaluation forms collected after the training workshop, the attendees believed that TxME is a very helpful and useful software and easy to use. They expressed the workshop was informative, and they liked the examples, exercises, and step by step training through the program. Their specific comments and suggestion of improvements are summarized below.

- **Comments:**
 - Instructors were knowledgeable about the program and the material being taught.
 - Information was useful and beneficial for future pavement design.
 - The software was explained very well for detailed understanding.
 - Like the hands-on experience and the training examples/exercises.
 - Instructors were very accommodating to questions and hardware/software issues.
 - Like that material variations are considered in the TxME. Very good.
 - The hands-on training was very helpful. Also the history of the system was explained very well.
 - The program is simple to use.
 - The developer is available for questions and trouble shooting.
 - Instructors were enthusiastic about subject and encourage questions.
 - The workshop showed the flexibility and ease of use of TxME.

- Like the interface of connecting TxME and FPS 21.
- Like the trainings that allow you to practice and get immediate feedback.
- Very cool software. Enjoy seeing software before it is complete so that we can still make recommendations.
- Hope the TxME can be implemented in Texas pavement design process in the near future.
- **Suggestions and Recommendations:**
 - Measure the impacts of maintenance in the program. Need some cost analysis.
 - Lots of acronyms were used (e.g., WIM); not everyone knows what these acronyms mean.
 - Consider different pavement structures in examples.
 - Revise/Update the program to evaluate other HMA surface mixes (e.g., Tom mix, Novachip).
 - More exercises show how it can be used with a specific design from the districts.
 - Provide guidance for parameter adjusted locally (District).
 - Explain more about the models used in TxME. Were they the same as the Mechanistic-Empirical Pavement Design Guide?
 - A little more guidance on downloading and installing software.
 - Integrate FPS 21 and TxME into one package.
 - Have digital copy of PowerPoints available instead of just printouts.
 - Examples are too basic for some of the experienced pavement designers.
 - Need more traffic load spectra data.
 - During demonstration, show the FPS input page to make sure each parameter value be the same as that in the handout example.
 - Need more lab testing data (default values of material properties) that can be put into TxME.
 - Need default values for the Mixture with Type B gradation.
 - Need help button or F1 short key for each entry like FPS 21.

According to these comments and feedbacks, researchers will add the following updates to the TxME system to increase its versatility and design optimization for specific TxME applications:

- Develop default material properties for more Texas mixtures including RAP/RAS mixes.
- Develop default load spectrums for energy sectors.
- Add help file to TxME.
- Calculate and output initial construction costs.

The workshop training materials have been submitted as 5-6622-01-P1 and 5-6622-01-P2. The copy of attendee sheets and evaluation forms are attached in the 5-6622-1-P3.

CHAPTER 3. DEVELOP DEFAULT MATERIAL PROPERTIES FOR TXME

Pavement structure is composed of different layers and various materials. Material types and associated engineering properties have significant impacts on pavement performance. It is often said garbage in, garbage out. This is very true for any pavement design systems including TxME. Thus, it is crucial to have accurate material properties for each material as inputs to TxME. Meanwhile, it is not practical, if not impossible, to run every test for each pavement material to obtain engineering properties TxME needs for every pavement design. In order to balance the accuracy and practicality of pavement design, researchers made substantial efforts to develop default engineering properties of the most often used pavement materials in Texas. This chapter describes the following efforts:

- Develop default moduli for pavement materials.
- Develop default rutting properties for pavement materials.
- Develop default cracking properties for pavement materials.
- Incorporate default values into TxME.

DEVELOP DEFAULT MODULI FOR PAVEMENT MATERIALS

Researchers performed dynamic modulus tests for asphalt mixes with and without RAP or RAS, resilient modulus tests for granular materials, stabilized materials, and subgrade soils. Asphalt mixes are visco-elastic material under small strain conditions, which is a function of time and temperature. To fully characterize the visco-elastic property of asphalt mixes, a dynamic master curve is often described by a sigmoidal function (Witczak and Solti 2004), as given by Equation 3-1:

$$\log |E^*| = \delta + \frac{\alpha}{1 + e^{\beta + \gamma \log t_r}} \quad (3-1)$$

where

- δ = the minimum value of $\log|E^*|$ in the sigmoid function.
 α = vertical span of the function (i.e., $\delta + \alpha$ indicates the highest value of $\log|E^*|$ possible in the sigmoid function).
 β and γ = the shape parameters for the sigmoid curve.
 t_r = reduced loading time.

Based on the time-temperature superposition principle, $\log t_r$ in Equation 3-1 can be expressed as follows:

$$\log t_r = \log t - \log a_T \quad (3-2)$$

where

t = the actual loading time at a given temperature T .

a_T = the temperature shift factor.

The time-temperature shift factor a_T can be fitted by a second order polynomial given as:

$$\log a_T = aT^2 + bT + c \quad (3-3)$$

where a , b , and c are regression coefficients.

Figure 17 shows an example of dynamic modulus (E^*) master curve and the corresponding equations.

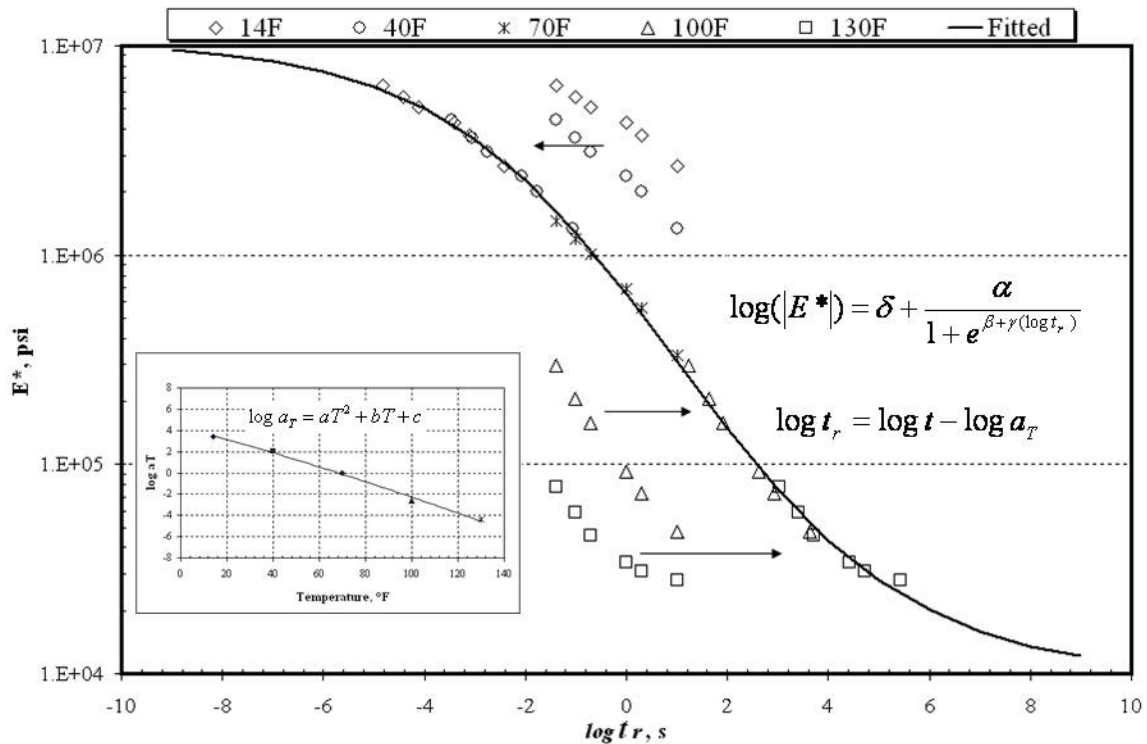


Figure 17. Dynamic Modulus Master Curve and Equations.

Table 1 lists dynamic modulus values for most often used virgin asphalt mixes in Texas.

Table 1. Default Values for Dynamic Modulus of Typical Virgin Asphalt Mixes Used in Texas.

PG	Mix Type	δ	α	β	γ	A	b	c
64-22	Type B	1.51848	2.97297	-0.81390	0.45244	0.00035	-0.12527	7.05293
70-22	Type B	1.74055	2.76990	-0.79098	0.45769	0.00024	-0.10633	6.26014
76-22	Type B	1.83720	2.67805	-0.82916	0.45883	0.00022	-0.10021	5.93963
64-28	Type B	1.40980	3.11887	-0.69857	0.43316	0.00032	-0.11583	6.51862
70-28	Type B	1.61447	2.93839	-0.67169	0.43368	0.00023	-0.10011	5.88021
64-22	Type C	1.51037	2.94191	-0.81681	0.45247	0.00035	-0.12521	7.04985
70-22	Type C	1.73019	2.74069	-0.79394	0.45786	0.00024	-0.10631	6.25924
76-22	Type C	1.82646	2.64910	-0.83216	0.45917	0.00022	-0.10016	5.93751
64-28	Type C	1.40113	3.08811	-0.70145	0.43291	0.00032	-0.11566	6.51138
70-28	Type C	1.60352	2.90952	-0.67490	0.43348	0.00023	-0.09998	5.87436
64-22	Type D	1.52143	2.90579	-0.80740	0.45437	0.00035	-0.12568	7.06576
70-22	Type D	1.74101	2.70536	-0.78165	0.45948	0.00024	-0.10643	6.26374
76-22	Type D	1.83493	2.61634	-0.81923	0.46023	0.00022	-0.10038	5.94666
64-28	Type D	1.42119	3.04079	-0.69150	0.43645	0.00033	-0.11630	6.53531
70-28	Type D	1.62349	2.86281	-0.66223	0.43685	0.00023	-0.10027	5.88716
64-22	Superpave B	1.52366	2.94367	-0.81116	0.45300	0.00035	-0.12533	7.05327
70-22	Superpave B	1.74391	2.74238	-0.78702	0.45816	0.00024	-0.10636	6.26102
76-22	Superpave B	1.83935	2.65178	-0.82495	0.45915	0.00022	-0.10026	5.94192
64-28	Superpave B	1.41828	3.08544	-0.69521	0.43418	0.00033	-0.11593	6.52183
70-28	Superpave B	1.62121	2.90661	-0.66765	0.43466	0.00023	-0.10017	5.88271
64-22	Superpave C	1.52617	2.90797	-0.80930	0.45372	0.00035	-0.12546	7.05795
70-22	Superpave C	1.74469	2.70832	-0.78465	0.45888	0.00024	-0.10639	6.26202
76-22	Superpave C	1.83899	2.61885	-0.82237	0.45978	0.00022	-0.10031	5.94372
64-28	Superpave C	1.42367	3.04585	-0.69351	0.43531	0.00033	-0.11604	6.52564
70-28	Superpave C	1.62492	2.86862	-0.66531	0.43575	0.00023	-0.10018	5.88316
64-22	Superpave D	1.62730	2.77240	-0.74671	0.47817	0.00039	-0.13115	7.25181
70-22	Superpave D	1.71892	2.71701	-0.77798	0.46081	0.00024	-0.10653	6.26777
76-22	Superpave D	1.81294	2.62804	-0.81532	0.46135	0.00022	-0.10051	5.95239
64-28	Superpave D	1.39774	3.05198	-0.69021	0.43871	0.00033	-0.11692	6.55884
70-28	Superpave D	1.60440	2.87056	-0.65845	0.43904	0.00023	-0.10044	5.89480
76-22	SMA-C	1.75309	2.64946	-0.81559	0.47702	0.00027	-0.10759	6.18780
76-22	SMA-D	1.74301	2.61438	-0.79720	0.47997	0.00028	-0.10850	6.22168
76-22	SMA-F	1.74603	2.58684	-0.78233	0.48234	0.00029	-0.10921	6.24835
70-28	SMA-C	1.39767	3.07334	-0.67280	0.41230	0.00030	-0.11013	6.25727
70-28	SMA-D	1.39929	3.02455	-0.65423	0.41613	0.00030	-0.11089	6.28474
70-28	SMA-F	1.41193	2.98570	-0.64022	0.41930	0.00031	-0.11147	6.30451
64-22	RBL	1.54037	2.94191	-0.81681	0.45247	0.00035	-0.12521	7.04985

PG = performance grade; SMA = stone matrix asphalt; RBL = rich bottom layer

Figure 18 shows the comparison between the default (or predicted) $|E^*|$ from master curve and the measured $|E^*|$ from laboratory dynamic modulus testing.

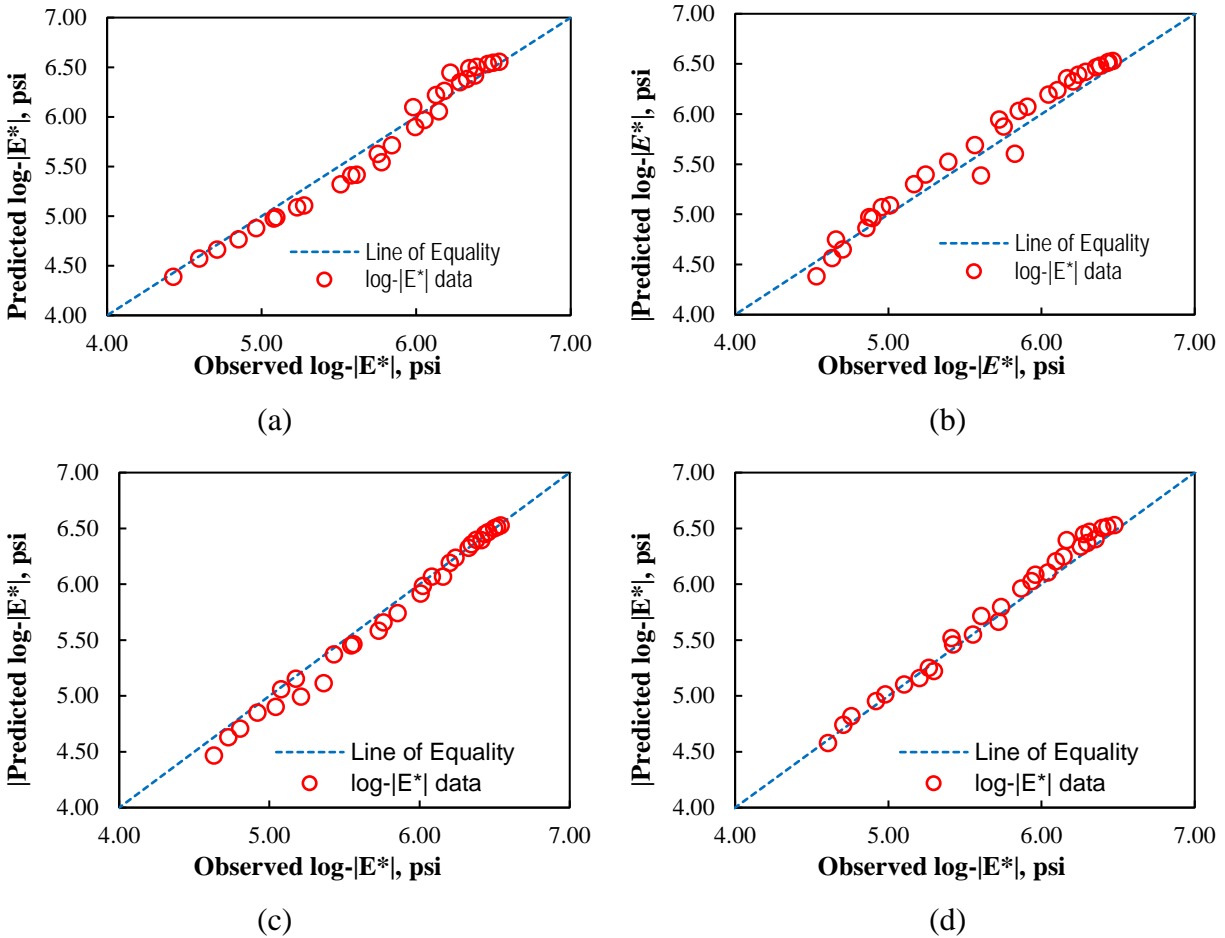
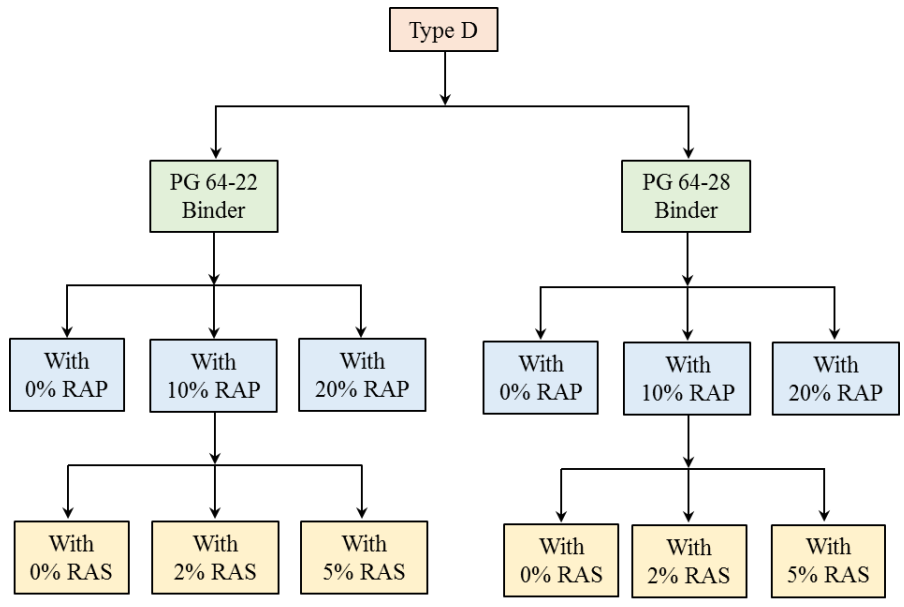
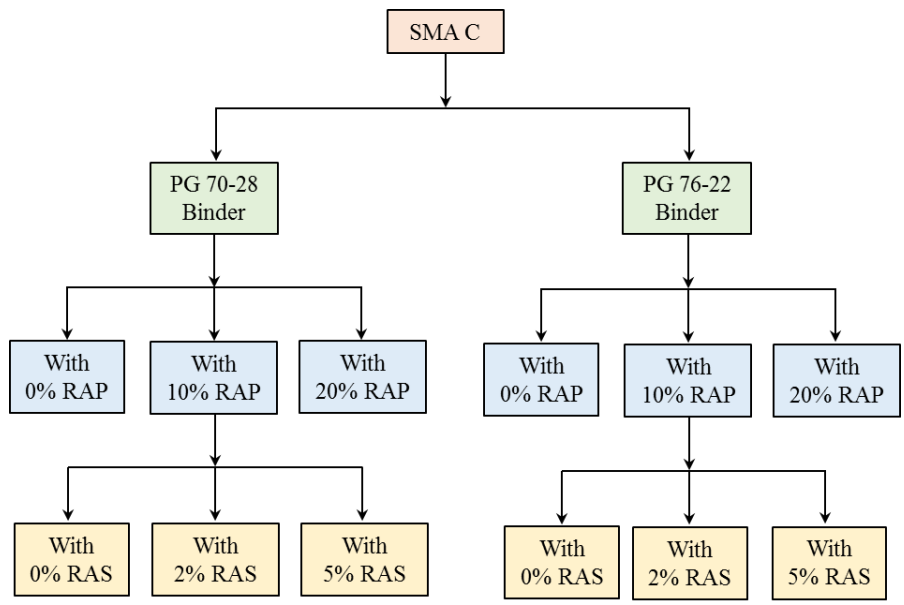


Figure 18. Comparison between Default (Predicted) $|E^*|$ from Master Curve and Measured $|E^*|$ Values for HMA Mixture (a) Type C, PG 64-22, (b) Type D, PG 64-22, (c) Superpave C, PG 70-22, and (d) Superpave C, PG 76-22.

Furthermore, RAP and RAS have been widely used in asphalt mixes in recent years. In most cases, adding RAP and RAS into the mixes make it stiffer. But there are no any quantitative relationships in the literature to describe how RAP and RAS affect dynamic modulus of asphalt mixes. A comprehensive laboratory testing was conducted to address such an issue in this study. Figure 19 shows the RAP/RAS mixtures test matrices for different combinations of AC gradation type, binder type, and RAP/RAS contents. The dynamic modulus tests were conducted following the American Association of State Highway and Transportation Officials (AASHTO) standard (AASHTO 2003). The average dynamic modulus $|E^*|$ values for each mixture are listed in Table 2 and Table 3.



(a)



(b)

Figure 19. Test Matrices of RAP/RAS Mixture Characterization for (a) Type D and (b) SMA C.

Table 2. Average |E*| of Type D RAP/RAS Mixtures.

AC Mix	Binder Grade	RAP %	RAS %	E* Values (ksi)						
				Temp. (°F)	Loading Frequencies (Hz)					
					25	10	5	1	0.5	0.1
Type D	PG64-22	0	0	14	3076.58	2991.91	2916.12	2694.63	2577.37	2250.63
				40	2427.46	2229.63	2064.44	1640.00	1446.87	1005.75
				70	1186.83	943.12	772.89	446.42	339.86	168.04
				100	285.85	190.88	138.36	63.72	45.62	21.74
				130	46.16	30.01	21.98	11.42	8.92	5.48
		10	0	14	3070.29	2982.27	2904.69	2682.85	2567.64	2252.23
				40	2406.47	2214.75	2056.36	1653.69	1471.36	1052.86
				70	1204.06	972.80	809.73	489.58	381.37	199.28
				100	316.20	217.44	161.03	77.21	55.88	26.75
				130	54.82	35.89	26.27	13.36	10.26	5.99
		10	2	14	3128.50	3012.00	2912.66	2642.47	2508.77	2160.64
				40	2364.30	2159.92	1996.03	1595.52	1420.15	1027.23
				70	1210.30	992.59	839.01	533.12	426.62	239.26
				100	381.02	274.17	210.18	108.34	80.29	39.55
				130	83.81	56.07	41.30	20.57	15.42	8.27
		10	5	14	3480.63	3345.89	3232.50	2929.78	2782.51	2404.91
				40	2589.73	2366.70	2189.87	1763.40	1578.44	1165.39
				70	1318.18	1091.80	932.27	612.59	499.65	296.05
				100	431.63	319.40	250.91	138.10	105.58	55.99
				130	104.52	72.88	55.42	29.66	22.88	13.00
		20	0	14	3416.08	3327.48	3248.32	3017.36	2895.10	2553.62
				40	2755.36	2550.60	2378.66	1931.25	1724.23	1239.92
				70	1465.72	1193.26	997.83	606.56	472.29	244.92
				100	414.22	284.92	210.53	99.79	71.73	33.81
	130			74.89	48.53	35.23	17.61	13.45	7.80	
	PG64-28	0	0	14	2656.93	2550.35	2456.73	2192.43	2058.02	1703.27
				40	1949.00	1743.38	1578.17	1180.71	1012.78	659.77
				70	859.40	665.63	536.71	304.52	232.96	121.14
				100	217.52	150.08	112.79	58.64	44.85	25.44
				130	49.20	35.00	27.55	16.93	14.17	10.06
		10	0	14	2661.01	2564.74	2479.36	2234.59	2108.09	1767.81
				40	2030.72	1835.70	1676.21	1281.64	1109.95	738.11
				70	981.76	772.95	630.19	364.03	279.34	144.37
				100	273.44	188.67	141.09	71.40	53.68	29.03
				130	61.90	42.84	32.94	19.14	15.64	10.58
		10	2	14	2395.04	2325.00	2262.75	2082.88	1988.75	1729.99
				40	1903.12	1751.31	1625.16	1302.90	1156.81	822.97
				70	1005.97	818.58	685.63	422.80	333.37	181.60
				100	308.19	218.64	166.41	86.33	65.08	34.75
				130	70.60	48.92	37.46	21.28	17.16	11.18
		10	5	14	2780.99	2681.84	2597.73	2370.51	2258.69	1968.60
				40	2133.97	1963.47	1826.91	1492.63	1345.48	1011.92
				70	1163.16	977.35	844.48	572.54	474.22	292.82
				100	428.58	325.57	261.32	152.12	119.46	67.87
				130	122.82	88.99	69.77	40.24	32.11	19.74
		20	0	14	2580.51	2508.64	2444.38	2257.02	2158.11	1883.62
				40	2068.06	1906.81	1771.95	1424.37	1265.54	900.23
				70	1101.41	895.94	749.71	460.08	361.58	195.13
100				334.17	235.83	178.72	91.80	68.95	36.62	
130	74.94			51.71	39.52	22.43	18.10	11.86		

Table 3. Average |E*| of SMA C RAP/RAS Mixtures.

AC Mix	Binder Grade	RAP %	RAS %	E* Values (ksi)						
				Temp. (°F)	Loading Frequencies (Hz)					
					25	10	5	1	0.5	0.1
SMA C	PG70-28	0	0	14	2152.21	2086.48	2027.25	1853.17	1760.97	1506.20
				40	1683.58	1534.86	1411.40	1099.42	960.95	655.55
				70	829.64	659.76	543.02	323.91	253.54	139.82
				100	237.70	169.47	130.83	72.95	57.68	35.52
				130	62.43	46.50	37.93	25.37	21.99	16.85
		10	0	14	2123.43	2064.89	2012.08	1856.24	1773.16	1540.95
				40	1688.02	1550.21	1434.87	1138.75	1004.68	701.44
				70	854.56	685.95	568.33	342.72	268.65	146.97
				100	242.88	172.31	132.11	71.76	55.89	33.04
				130	58.92	43.04	34.56	22.26	19.00	14.09
		10	2	14	2125.32	2029.06	1948.52	1736.11	1634.40	1379.46
				40	1548.51	1401.52	1286.66	1016.57	902.82	657.01
				70	791.84	655.85	561.50	376.14	311.69	196.14
				100	294.24	226.33	184.45	113.61	92.26	57.78
				130	98.31	74.93	61.35	39.67	33.37	23.26
		10	5	14	2287.18	2191.08	2110.65	1898.08	1795.87	1537.65
				40	1690.73	1540.63	1422.70	1142.34	1022.59	759.20
				70	884.75	739.50	637.57	433.68	361.37	229.28
				100	331.72	256.07	208.93	128.22	103.65	63.73
				130	107.39	81.19	65.95	41.60	34.55	23.30
	20	0	14	2304.45	2220.92	2147.50	1939.69	1833.53	1550.93	
			40	1773.58	1612.14	1480.78	1156.88	1015.72	706.80	
			70	915.51	741.25	620.26	387.28	309.62	178.60	
			100	306.69	224.94	176.81	101.07	80.09	48.59	
			130	90.66	67.15	54.21	34.82	29.52	21.40	
	PG76-22	0	0	14	2219.19	2060.40	1935.65	1636.08	1505.45	1207.57
				40	1379.91	1211.70	1088.74	824.61	722.44	516.86
				70	612.45	503.03	430.26	293.27	246.96	164.27
				100	228.50	181.15	151.80	101.01	85.09	58.07
				130	87.63	70.20	59.69	41.89	36.37	26.95
		10	0	14	2092.88	1951.68	1841.74	1579.84	1465.99	1205.26
				40	1327.48	1180.68	1072.76	837.55	744.63	552.32
				70	621.06	519.63	450.69	316.42	269.25	181.89
				100	240.46	192.13	161.46	106.80	89.18	58.74
				130	88.55	69.78	58.33	38.80	32.73	22.42
		10	2	14	1792.42	1709.11	1641.46	1469.95	1390.59	1196.90
				40	1283.94	1171.68	1085.47	885.83	802.13	619.18
				70	680.51	581.43	511.79	370.41	318.81	220.44
				100	283.90	229.72	194.76	131.37	110.65	74.50
				130	108.81	86.79	73.29	50.13	42.88	30.53
		10	5	14	2094.35	1999.72	1922.74	1727.30	1636.79	1416.00
				40	1474.13	1345.40	1247.11	1021.57	927.93	725.24
				70	755.46	649.37	575.63	427.81	374.37	272.67
				100	320.58	267.39	233.07	170.29	149.40	111.96
				130	140.98	119.58	106.16	82.25	74.41	60.39
		20	0	14	2362.25	2218.61	2104.53	1825.28	1700.76	1409.01
				40	1562.26	1396.30	1272.48	997.77	887.64	657.57
				70	752.40	629.29	545.27	381.33	323.84	217.95
100				294.38	234.84	197.22	130.69	109.44	72.99	
130				110.64	87.69	73.77	50.13	42.80	30.38	

By investigating the values in the Table 2 and Table 3, the parameters in Equations 3-1 and 3-3 (δ , α , a , b , and c) are found to be not significantly affected by the inclusion of RAP or RAS in the AC mixture. However, the shape parameters β and γ of the $|E^*|$ master curve are significantly affected by the inclusion of RAP or RAS in the mixture, and they vary with the RAP and RAS percent contents. The study showed that, if the $|E^*|$ master curve of a virgin AC mixture can be represented by Equation 3-1, then $|E^*|$ master curve of the same AC mixture with RAP and RAS contents can be best approximated by the following expression:

$$\log |E^*| = \delta + \frac{\alpha}{1 + e^{(1 + \beta_R P_{RAP}) * (1 + \beta_S P_{RAS}) * \beta + (1 + \gamma_R P_{RAP}) * (1 + \gamma_S P_{RAS}) * \gamma \log t_r}} \quad (3-4)$$

where

- δ , α , β , and γ = the same $|E^*|$ master curve parameters as those of the virgin AC mix.
- P_{RAP} and P_{RAS} = the percentages of RAP and RAS in the AC mixture.
- β_R and β_S = the factors affecting the β -parameter due to RAP and RAS contents.
- γ_R and γ_S = the factors affecting the γ -parameter due to the RAP and RAS contents.

Laboratory $|E^*|$ data of AC mixture with different RAP and RAS contents can be fitted to obtain the values of β_R , β_S , γ_R and γ_S (see Table 4). Figure 20 shows the goodness of Equation 3-4.

Table 4. $|E^*|$ Adjustment Factors for RAP/RAS Mixes.

β_R	β_S	γ_R	γ_S
0.0111	0.04968	-0.00095	-0.00837

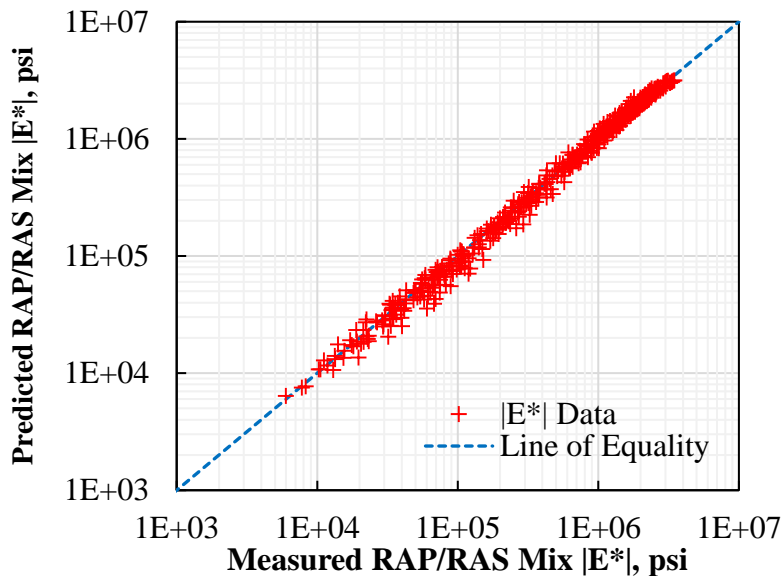


Figure 20. Comparison between Default (Predicted) $|E^*|$ from Master Curve and Measured $|E^*|$ Values for RAP/RAS Mixes.

Different from dynamic modulus of asphalt layer, moduli of other materials are not considered to be sensitive to time or temperature. Typical values consistent with FPS 21 are recommended, as present in Table 5. The subgrade modulus is consistent with FPS 21, which depends on the district county.

Table 5. Default Modulus Values for Other Pavement Materials.

Pavement materials		Typical values (ksi)
Base	Flexible base (FB)	50
	Cement stabilized base	200
	Fly Ash (FA) or Lime Fly Ash (LFA) stabilized base	100
	Asphalt treated base	300
	Emulsion asphalt treated base	75
Subbase	Lime (cement) stabilized subbase	40
	Emulsion asphalt treated subbase	40

DEVELOP DEFAULT RUTTING PROPERTIES FOR PAVEMENT MATERIALS

VESYS layer rutting model was adopted as one of the TxME performance models. As given in Equations 3-5, the permanent strain (or deformation) per loading application is a function of the number of load applications and two rutting parameters: μ and α .

$$\frac{\Delta e_p(N)}{\varepsilon} = \mu N^{-\alpha} \quad (3-5)$$

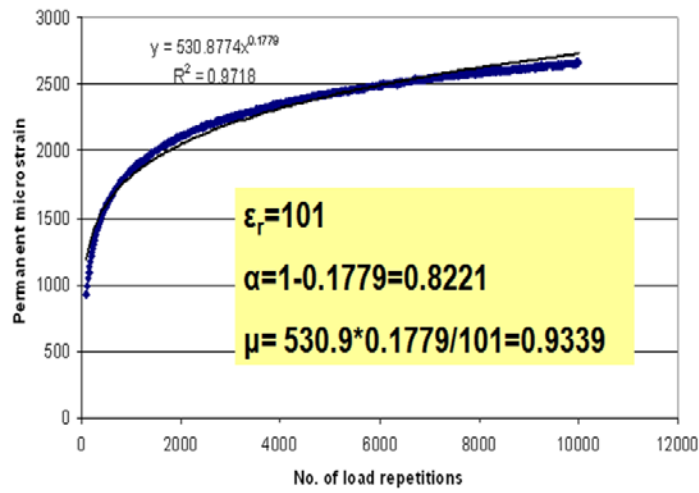
where

$\Delta e_p(N)$ = the vertical permanent strain at load application, N .

ε = the resilient strain.

μ and α = the rutting parameters that depend on the state of stress, temperature, etc., and can be determined from laboratory repeated load permanent deformation test.

Figure 21 shows an example of the laboratory repeated load permanent deformation test and the determination of rutting parameters: μ and α (Zhou and Scullion 2004, Hu et al. 2011).



$$\mu = \frac{ab}{\epsilon_r}$$

$$\alpha = 1 - b$$

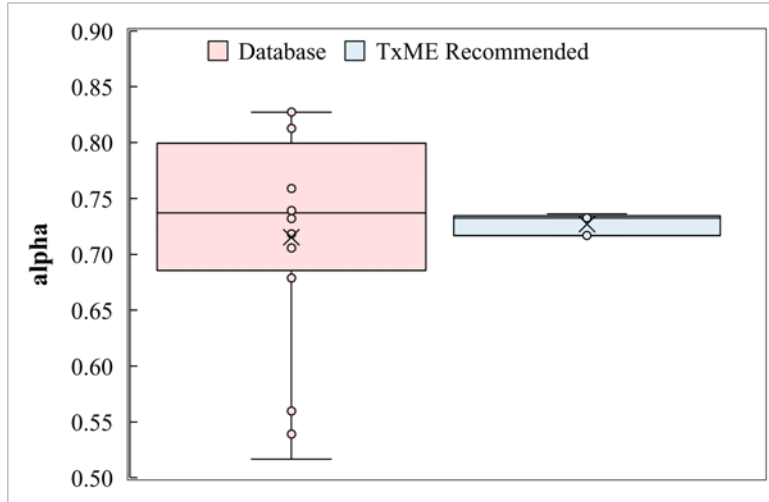
Figure 21. Repeated Load Permanent Deformation Test Result and Rutting Parameters: μ and α .

Table 6 lists the recommended default values of rutting parameters for most often used virgin asphalt mixes in Texas.

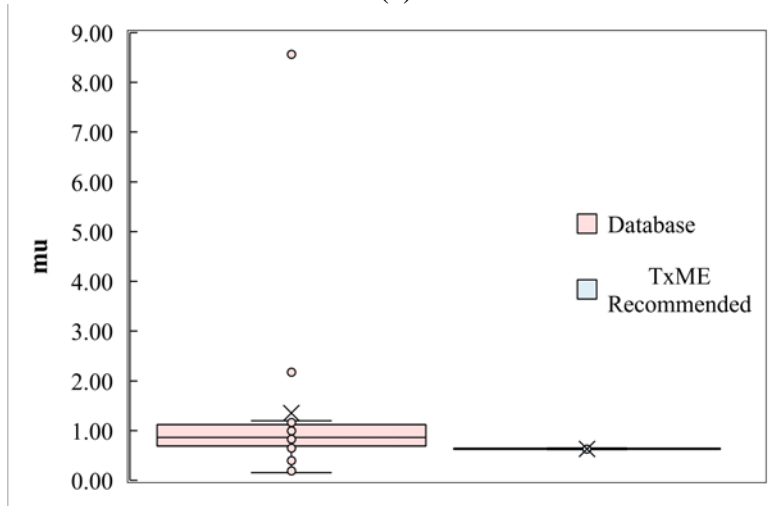
Table 6. Default Rutting Properties for Typical Virgin Asphalt Mixes Often Used in Texas.

PG	Mix Type	δ	α
64-22	Type B	0.7168	0.6459
70-22	Type B	0.7326	0.6314
76-22	Type B	0.7363	0.6283
64-28	Type B	0.7168	0.6508
70-28	Type B	0.7326	0.6184
64-22	Type C	0.7315	0.7234
70-22	Type C	0.7423	0.7014
76-22	Type C	0.7485	0.6756
64-28	Type C	0.7315	0.7306
70-28	Type C	0.7423	0.6986
64-22	Type D	0.7465	0.8102
70-22	Type D	0.7521	0.7792
76-22	Type D	0.7609	0.7265
64-28	Type D	0.7465	0.8202
70-28	Type D	0.7521	0.7892
64-22	Superpave B	0.7168	0.6459
70-22	Superpave B	0.7326	0.6314
76-22	Superpave B	0.7363	0.6283
64-28	Superpave B	0.7168	0.6508
70-28	Superpave B	0.7323	0.6184
64-22	Superpave C	0.7315	0.7234
70-22	Superpave C	0.7423	0.7014
76-22	Superpave C	0.7485	0.6756
64-28	Superpave C	0.7315	0.7306
70-28	Superpave C	0.7423	0.6986
64-22	Superpave D	0.7465	0.8102
70-22	Superpave D	0.7521	0.7792
76-22	Superpave D	0.7609	0.7265
64-28	Superpave D	0.7465	0.8202
70-28	Superpave D	0.7521	0.7892
76-22	SMA-C	0.7106	0.7761
76-22	SMA-D	0.7106	0.7856
76-22	SMA-F	0.7106	0.8004
70-28	SMA-C	0.7106	0.7761
70-28	SMA-D	0.7106	0.7856
70-28	SMA-F	0.7106	0.8004
64-22	RBL	0.7315	0.7234

Figure 22 shows the comparison between the default (TxME recommended) and the measured rutting parameters in the Texas Flexible Pavement Database.



(a)



(b)

Figure 22. Comparison of Default and Measured Rutting Parameters (a) Considering All Available α -Data and (b) Considering All Available μ -Data.

Furthermore, this study also evaluated the impact of RAP/RAS on rutting parameters of asphalt mixes. The repeated load tests for RAP/RAS mixtures were conducted following the same test matrices in Figure 19. Table 7 lists the measured rutting properties of RAP/RAS mixtures.

Table 7. Rutting Properties of RAP/RAS Mixtures.

Sample ID NO.	Mix Type	Binder Grade	RAP%	RAS%	α	μ	ε (at N = 200)
1	SMA C	PG70-28	0	0	0.729835	0.287527	174.4
2	SMA C	PG70-28	0	0	0.71149	0.490467	140.2333
3	SMA C	PG70-28	10	0	0.728801	0.387486	122.0333
4	SMA C	PG70-28	10	0	0.716865	0.443129	109.5667
5	SMA C	PG70-28	10	2	0.726809	0.386488	120.9673
6	SMA C	PG70-28	10	2	0.728659	0.423698	117.7328
7	SMA C	PG70-28	10	5	0.730954	0.410298	113.9667
8	SMA C	PG70-28	10	5	0.734775	0.2761	89.76667
9	SMA C	PG70-28	20	0	0.730954	0.410298	113.9667
10	SMA C	PG70-28	20	0	0.734775	0.2761	89.76667
11	SMA C	PG76-22	0	0	0.70709	0.281499	141.8333
12	SMA C	PG76-22	0	0	0.703057	0.347021	123.1667
13	SMA C	PG76-22	10	0	0.689476	0.175873	89.63333
14	SMA C	PG76-22	10	0	0.676643	0.23886	93.5
15	SMA C	PG76-22	10	2	0.724341	0.218932	121.5
16	SMA C	PG76-22	10	2	0.744341	0.198329	118.9
17	SMA C	PG76-22	10	5	0.737448	0.158698	107.3
18	SMA C	PG76-22	10	5	0.691463	0.128755	131.0667
19	SMA C	PG76-22	20	0	0.674606	0.293473	97.16667
20	SMA C	PG76-22	20	0	0.649908	0.224778	82.46667
21	Type D	PG64-22	0	0	0.741648	0.68672	202.3
22	Type D	PG64-22	0	0	0.711472	0.652098	202
23	Type D	PG64-22	10	0	0.720433	0.6295	120.1
24	Type D	PG64-22	10	0	0.71463	0.581515	137.4667
25	Type D	PG64-22	10	2	0.770921	0.655936	101.1333
26	Type D	PG64-22	10	2	0.849085	0.770921	97.53333
27	Type D	PG64-22	10	5	0.753887	0.479623	78.4
28	Type D	PG64-22	10	5	0.830485	0.349006	83.6
29	Type D	PG64-22	20	0	0.81333	0.856822	112.7
30	Type D	PG64-22	20	0	0.766107	0.66112	100.7
31	Type D	PG64-28	0	0	0.670374	0.419483	224.6667
32	Type D	PG64-28	0	0	0.798315	0.333427	208.3667
33	Type D	PG64-28	10	0	0.758898	0.237179	153.4667
34	Type D	PG64-28	10	0	0.74976	0.400782	157.3667
35	Type D	PG64-28	10	2	0.770921	0.655936	101.1333
36	Type D	PG64-28	10	2	0.849085	0.770921	97.53333
37	Type D	PG64-28	10	5	0.753887	0.479623	78.4
38	Type D	PG64-28	10	5	0.830485	0.349006	83.6
39	Type D	PG64-28	20	0	0.823591	0.457532	120.3667
40	Type D	PG64-28	20	0	0.750469	0.376501	137.0333

Based on this observation, the following equations are recommended for RAP/RAS mixes:

$$\alpha = (1 + P_{RAP} * k_R) * (1 + P_{RAS} * k_S) * \alpha_{virgin} \quad (3-6)$$

$$\mu = (1 + P_{RAS} * l_S) * \mu_{virgin} \quad (3-7)$$

where

α_{virgin} and μ_{virgin} = the rutting parameters for the virgin (zero-RAP and zero-RAS contents) asphalt mixes (see Table 7).

P_{RAP} and P_{RAS} = the percentages of RAP and RAS in the AC mixture.

k_R and k_S = the adjustment factors for the α -parameter due to RAP and RAS contents.

l_S = the adjustment factors affecting the μ -parameter due to RAS contents.

Least-square method were used to determine k_R , k_S , and l_S , and Figure 23 shows the comparison between the predicted from Equations 3-6 and 3-7 and the observed (measured) rutting properties.

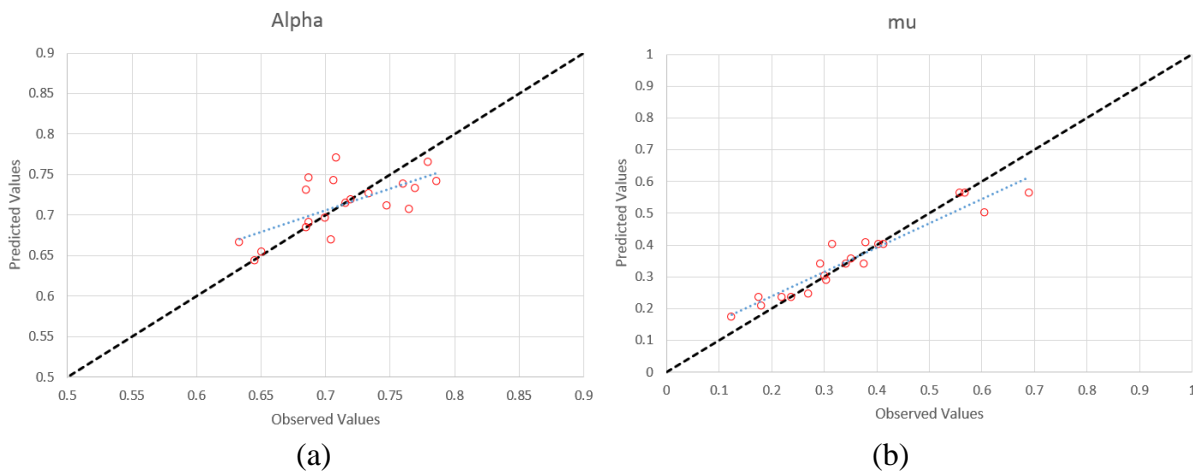


Figure 23. Comparison between the Predicted and Observed (Measured) RAP/RAS Mixes Rutting Properties (a) Alpha and (b) mu.

Table 8 lists the optimized k_R , k_S , and l_S values.

Table 8. Optimized RAP/RAS Adjustment Factors for Rutting Properties.

k_R	k_S	l_S
0.001709	0.010745	-0.054942

Additionally, default rutting parameters for other materials are also developed based on laboratory test results, as described in Table 9.

Table 9. Default Rutting Parameters for Other Pavement Materials.

Pavement materials		μ	α
Base	FB	0.8706	0.0981
	Asphalt treated base	0.8710	0.0909
	Emulsion asphalt treated base	0.8710	0.0909
Subbase	Emulsion asphalt treated subbase	0.8710	0.0909
Subgrade		0.8507	0.0836

DEVELOP DEFAULT CRACKING PROPERTIES FOR PAVEMENT MATERIALS

TxME predicts cracking development of asphalt pavements by considering cracking initiation and cracking propagation. The cracking parameters characterizing cracking initiation and propagation are fracture properties of asphalt mixes: A and n . The Overlay test (OT) can be used to determine the cracking parameters of asphalt mixes (Hu et al. 2012b). Figure 24 shows an example of OT and associated fracture properties: A and n .

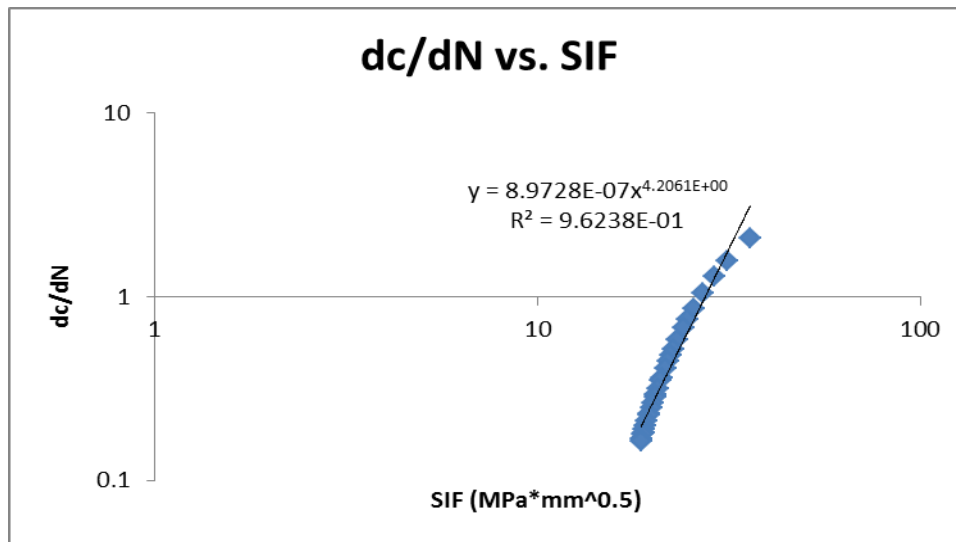


Figure 24. OT Result and Determination of Fracture Properties: A and n .

Table 10 lists the recommended default values of fracture properties for most often used virgin asphalt mixes in Texas.

Table 10. Default Fracture Properties for Typical Virgin Asphalt Mixes Often Used in Texas.

PG	Mix Type	A	n
64-22	Type B	6.4359E-06	3.8374
70-22	Type B	6.8551E-06	3.8201
76-22	Type B	7.3171E-06	3.8023
64-28	Type B	3.1557E-06	4.0323
70-28	Type B	3.7800E-06	3.9828
64-22	Type C	5.2041E-06	3.8948
70-22	Type C	5.5095E-06	3.8792
76-22	Type C	5.8430E-06	3.8630
64-28	Type C	2.8039E-06	4.0645
70-28	Type C	3.3231E-06	4.0179
64-22	Type D	4.2081E-06	3.9531
70-22	Type D	4.4280E-06	3.9391
76-22	Type D	4.6659E-06	3.9248
64-28	Type D	2.4914E-06	4.0969
70-28	Type D	2.9215E-06	4.0532
64-22	Superpave B	6.0544E-06	3.8541
70-22	Superpave B	6.4359E-06	3.8374
76-22	Superpave B	6.8551E-06	3.8201
64-28	Superpave B	3.0241E-06	4.0440
70-28	Superpave B	3.6074E-06	3.9956
64-22	Superpave C	4.9238E-06	3.9100
70-22	Superpave C	5.2041E-06	3.8948
76-22	Superpave C	5.5095E-06	3.8792
64-28	Superpave C	2.6934E-06	4.0755
70-28	Superpave C	3.1804E-06	4.0299
64-22	Superpave D	4.0044E-06	3.9667
70-22	Superpave D	4.2081E-06	3.9531
76-22	Superpave D	4.4280E-06	3.9391
64-28	Superpave D	2.3989E-06	4.1073
70-28	Superpave D	2.8039E-06	4.0645
76-22	SMA-C	9.2769E-08	4.9996
76-22	SMA-D	8.1315E-08	5.0358
76-22	SMA-F	6.0576E-08	5.1166
70-28	SMA-C	9.2769E-08	4.9996
70-28	SMA-D	8.1315E-08	5.0358
70-28	SMA-F	6.0576E-08	5.1166
64-22	RBL	1.1519E-07	4.9402

Figure 25 shows the comparison between the default (TxME recommended) and the measured fracture properties in the Texas Flexible Pavement Database.

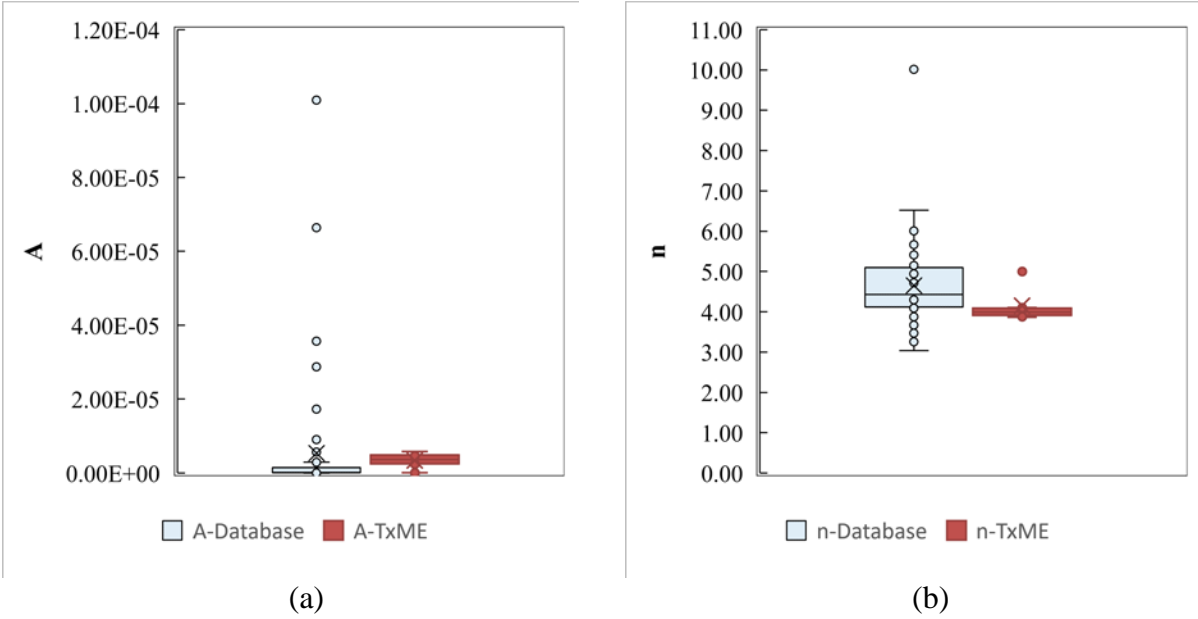


Figure 25. Overall Comparison of Virgin Asphalt Mixtures Default and Measured Fracture Properties: (a) A Values and (b) n Values.

Furthermore, this study also evaluated the impact of RAP/RAS on cracking parameters of asphalt mixes. The two cracking parameters, A and n , are both affected by the addition of RAP/RAS into asphalt mixes. Based on the observation, the following A and n equations are recommended for RAP/RAS mixes:

$$A = A_{virgin} e^{(\lambda_1 P_{RAP} + \lambda_2 P_{RAS})} \quad (3-8)$$

$$n = n_{virgin} (1 - \xi_1 P_{RAP}) (1 - \xi_2 P_{RAS}) \quad (3-9)$$

where

A_{virgin} and n_{virgin} = the fracture parameters for the virgin (zero-RAP and zero-RAS contents) asphalt mixes (see Table 10).

P_{RAP} and P_{RAS} = the percentages of RAP and RAS contents in the asphalt mixes.

λ_1 and λ_2 = the adjustment factors for the A -parameter due to RAP and RAS contents.

ξ_1 and ξ_2 = the adjustment factors for the n -parameter due to RAP and RAS contents.

Least-square regression method were used to determine λ_1 , ξ_1 , λ_2 , and ξ_2 , and Figure 26 shows the comparison between the predicted from Equations 3-8 and 3-9 and the measured A and n .

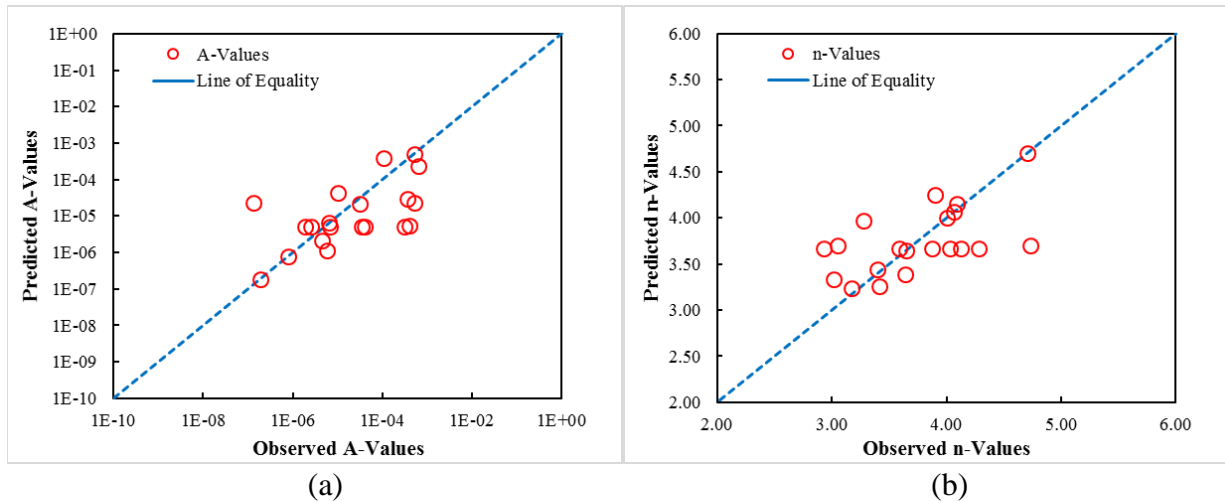


Figure 26. Comparison between the Predicted and Observed (Measured) RAP/RAS Mixes Fracture Properties (a) A and (b) n .

Table 11 lists the optimized λ_1 , ζ_1 , λ_2 , and ζ_2 values.

Table 11. RAP/RAS Adjustment Factors for Fracture Properties.

λ_1	λ_2	ζ_1	ζ_2
0.091611	0.689790	0.004856	0.030354

INCORPORATE DEFAULT VALUES INTO TXME

Figure 27 shows the TxME screen of incorporating default material properties. In this screen, when users select/input different binder type, gradation, RAP content, or RAS content (the input boxes marked as numbers 1, 2, 3, and 4 in the red circle, respectively), the values in the dynamic modulus, fracture property, and the rutting property input items (marked as numbers 5, 6, and 7 in the red circle, respectively) will be changed automatically. When both the RAP and RAS content are 0 (virgin mixture), these default values will be directly obtained from Table 1, Table 6, and Table 10, respectively. Otherwise, Equations 3-4, 3-6, 3-7, 3-8, and 3-9 will be used to calculate the corresponding default values according to the user-defined RAP/RAS contents.

Layer 1: SMA C, PG 76-22	
Layer Information	
Layer Number	1
Layer Thickness (inches)	4
Cost (\$/Cubic Yard):	130
Material Information	
Binder Type	PG 76-22
Gradation	SMA C
RAP %	0
RAS %	0
Material Properties	
Dynamic Modulus	Level 2 input : default value
Fracture Property	@77 F: A=9.2769E-8, n=4.9996
Rutting Property	@104 F: alpha=0.7106, mu=0.7761
Poisson Ratio	0.35
Thermal Coefficient of Expansion (1e-6 in/in/F):	13.5

Figure 27. TxME Screen of Incorporating Default Material Properties.

CHAPTER 4. DEVELOP DEFAULT AXLE LOAD SPECTRA FOR TXME

Traffic loading is one of the key inputs required by TxME. Two options are available in TxME for traffic inputs: traditional ESAL and load spectra. Compared to ESALs, load spectra input is preferable, because it characterizes traffic in more details. However, collecting and analyzing traffic data for determining load spectra is expensive and time-consuming. Thus, it is necessary to determine default traffic load spectra for any mechanistic-empirical-based pavement designs, including TxME. Texas has various types of highways including IH, US/SH, and FM roads and each of them has its own specific traffic loading characteristics. Additionally, there are many areas associated with oil/gas development in Texas. Thus, the main objective of this chapter is to analyze all available WIM data and then develop default load spectra for IH, US/SH, FM, and oil/gas energy sectors so that pavement engineers can design pavements with TxME for each different application using specific load spectra information. This chapter will first describe the methodology and the traffic data source, and then provide the details of developing default load spectra for IH, US/SH, FM, and energy sector road, respectively, and at last illustrate how these default load spectra are incorporated into the TxME software.

METHODOLOGY

TxME needs the following main inputs when the load spectra option is chosen for traffic input:

- AADTT and traffic growth rate.
- VCD. According to the Federal Highway Administration vehicle class classification, truck types are classified as Class 4 to Class 13. VCD factors are the percentage of each type of truck within the total truck volume.
- Axle per truck (APT). APT represents the average number of axles for each truck class (Class 4 to 13) and each axle type (steering single, other single, tandem, tridem and quad axles). Note that steering single is single axle with single tire at each side while other single is the single axle with dual tires at each side. The tandem-, tridem-, or quad-axle is also axle with dual tires.
- MAF. MAF represents the proportion of the annual truck traffic for a given truck class (Class 4 to 13) that occurs in a specific month. For each truck class, the sum of the MAF of all months must equal 12.
- ALD. ALD factors represent the percentage of the total axle applications within each load interval for a specific axle type and vehicle class. A definition of load intervals for single, tandem, tridem, and quad is 3,000 lb to 40,000 lb at 1,000-lb intervals, 6,000 lb to 80,000 lb at 2,000-lb intervals, and 12,000 lb to 102,000 lb at 3,000-lb intervals, respectively.

Among these five categories of traffic inputs, the AADTT and traffic growth rate are relatively easier to be measured and they could be much different from site to site. In order to maximize the resources and maintain the accuracy, the development of default load spectra inputs focused

on four major traffic characteristics: VCD, ALD, APT, and MAF for each type of roads. The traffic data from both permanent and portable WIM stations were used to develop default load spectra for IH, US/SH, FM, and energy sector roads. When developing the default values for load spectra inputs, sensitivity analyses were performed for each traffic characteristic (VCD, ALD, APT, and MAF) to identify how significant each traffic characteristic impacts pavement performance. In this study, a parameter is significant if the pavement life is changed (either decreased or increased) by two or more years. According to this criterion, the analysis results can be divided into one or multiple groups, and then one set of default values are provided for each group.

SOURCES OF TRAFFIC DATA

TxDOT has deployed more than 41 permanent WIM sensors in 20 districts. Most of WIM stations are located on IH and US/SH highways, while only a few WIM stations are located on FM roads. In recent years, rapid energy development in Texas has caused significant premature damage to road networks. Characterization of traffic data in the energy sectors is critical for designing adequate pavements. Thus, portable WIM is used for this study. Traffic data from 27 permanent WIM and portable WIM stations were analyzed and used in this study, as listed in Table 12. The AADTT for each road is presented in Table 12. As can be seen from the table, IHs have very high AADTT while FM roads have the lowest values. FMs in the energy sector obviously have a much larger AADTT than in the non-energy sector.

Table 12. WIM Stations Used for Data Analysis.

Types of Roads	Road #	WIM Station ID	AADTT
IH	I-20	533	14822
	I-35	513	10867
	I-10	502	8005
	I-20	526	7704
	I-10	524	7523
	I-45	539	6834
	I-35	531	6299
	I-40	547	6127
	I-20	544	5767
	I-37	534	5053
US/SH	SH 6	554	5611
	US 281	523	4720
	US 84	537	3630
	US 287	528	3247
	SH 114	527	2656
	US 380	549	2593
	SH 130	532	2269
	US 59	535	2000
	US 82	530	919
	US 96	142	846
	SH 121	546	550
	US 90	551	544
	US 82	543	372
FM	3129	541	251
	2223	800	142
Energy Sector	US 281	TS005 (Portable WIM)	2958
	FM 468	TS004 (Portable WIM)	714

DEVELOPMENT OF DEFAULT LOAD SPECTRA INPUTS FOR IH

In this section, the sensitivity analysis was conducted first. Based on the sensitivity analysis results, the default load spectra inputs for IHS are then recommended for each load spectra input: VCD, APT, MAF, and ALD. A total of 10 permanent WIM stations were used. These WIM stations are located on six IHS: I-10, I-20, I-35, I-37, I-40, and I-45 in Texas.

Vehicle Class Distribution

Figure 28 presents VCD for IH based on the traffic data from the WIM stations, and the percentage ranges of each truck class are also summarized in the table. All the WIM stations have the percentage of C9 in the range between 60 percent and 80 percent and the percentage of C5 in the range between 10 percent and 30 percent except for IH20_533.



Figure 28. VCDs for IH WIM Stations.

Researchers conducted a sensitivity analysis to investigate how change of percentage of each truck class in the VCD impacts the predicted pavement performance. The varied percentage of each truck class used in the sensitivity analysis is in the ranges as shown in Table 13. For the sensitivity analysis, all the design inputs including pavement structure, mixture type and properties, and climate were held constant except the traffic load spectra parameters. When evaluating the VCD, all load spectra parameters were held constant except the input of VCD. A typical pavement structure of 6-inch AC and 12-inch FB was used for sensitivity analysis, and AADTT was 7000. Figure 29 shows the sensitivity analysis results, which indicate that C9 plays a more significant role in the VCD than other truck classes, while there is no substantial difference in the predicted results for other truck classes when changing the percentage. A trend is also observed for C9 that the difference in the predicted performances becomes smaller between high percentages of C9 with the same increment. Based on the sensitivity analysis results for the VCD, if no significant difference is observed for a specific truck class, the average value for all the IH WIM stations was used as the default value for the specific truck class. Thus, the average values were used as the default values for all the truck classes except C5 and C9 in the default VCD input. Then, the next step is to determine the values for C5 and C9 in the default VCD input. In Figure 29b, there is a substantial difference in the predicted pavement

performance between an increment of 10 percent for C9. As observed in Figure 28, all the WIM stations except Station 533 have the percentage of C9 in the range between 60 percent and 80 percent. Station 533 was excluded when determining the default inputs since the default input is defined as the most frequently observed values. Based on the discussion, it is reasonable to have three default VCD inputs for IH, and each default input has the percentage of C9 corresponding to 60 percent, 70 percent, and 80 percent, respectively. As mentioned, for each default VCD input, the average values for all the IH WIM stations were used for all the truck classes except C5 and C9 in each default VCD input. All the values for all the truck classes except C5 were determined in the three default VCD inputs; and since the sum of percentages for all the truck classes is 100, the percentage of C5 can be determined for each default VCD input.

Table 13. Percentage Ranges for Each Truck Class Based on All WIM Stations.

Vehicle Class	Min (%)	Max (%)
C4	0.5	1.5
C5	11.0	50.5
C6	1.6	4.9
C7	0.0	0.3
C8	0.9	5.1
C9	36.4	80.2
C10	0.3	1.2
C11	1.2	3.7
C12	0.4	2.3
C13	0.2	0.8

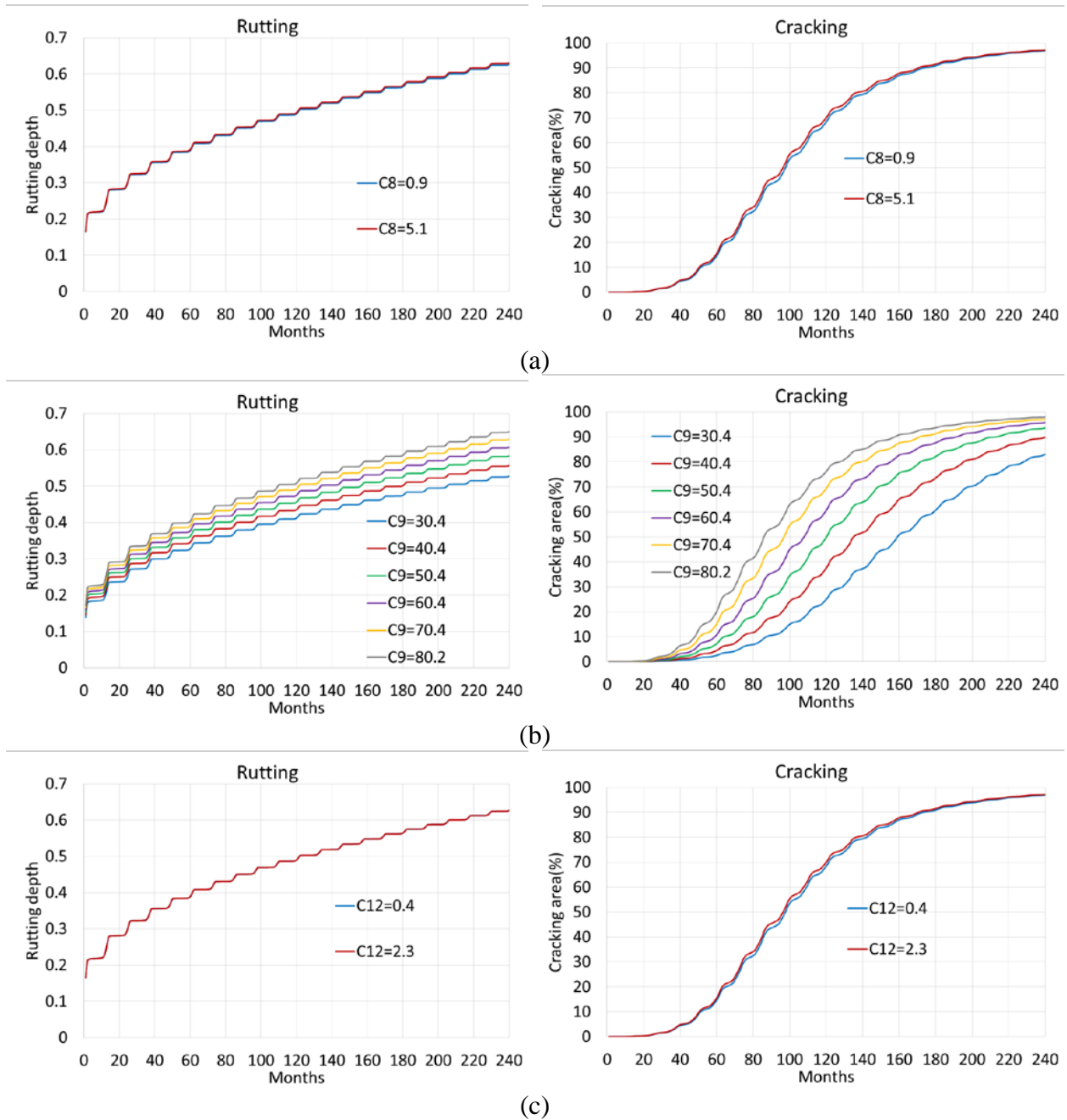


Figure 29. Examples of TxME Predicted Results: (a) C8 Ranged from 0.9 Percent to 5.1 Percent, (b) C9 Ranged from 30.4 Percent to 80.2 Percent, and (c) C12 Ranged from 0.4 Percent to 2.3 Percent.

Table 14 presents the three sets of default inputs for IH.

Table 14. Default Inputs of VCD for IH.

Vehicle class	#1 (Low)	#2 (Medium)	#3 (High)
	Distribution (%)	Distribution (%)	Distribution (%)
C4	1.3	1.3	1.3
C5	28.2	18.2	8.2
C6	2.8	2.8	2.8
C7	0.1	0.1	0.1
C8	2.9	2.9	2.9
C9	60.0	70.0	80.0
C10	0.5	0.5	0.5
C11	2.7	2.7	2.7
C12	1.3	1.3	1.3
C13	0.3	0.3	0.3

Axle per Truck

The number of tandem APT for C9 is the most important factor among all the axle types since C9 plays a more significant role in the VCD due to its large percentage. Figure 30 presents comparison of axle per truck for tandem axle. All the stations have comparable values of tandem APT. Researchers conducted a sensitivity analysis to evaluate how the input of axle per truck impacts the pavement performances. In the analysis, the input of axle per truck uses the data from individual station while all the other inputs are fixed. Figure 31a and Figure 31b present the results. As can be seen, there is no significant difference between different WIM stations when evaluating the impact of axle per truck. Thus, the average values of axle per truck for all the stations are used as the default input for IH, as shown in Table 15.

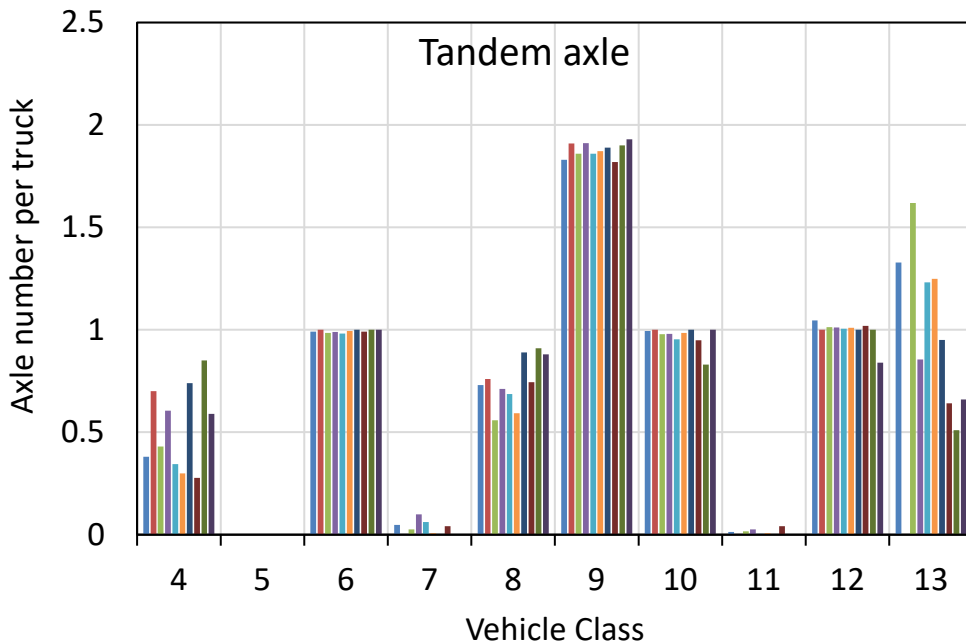
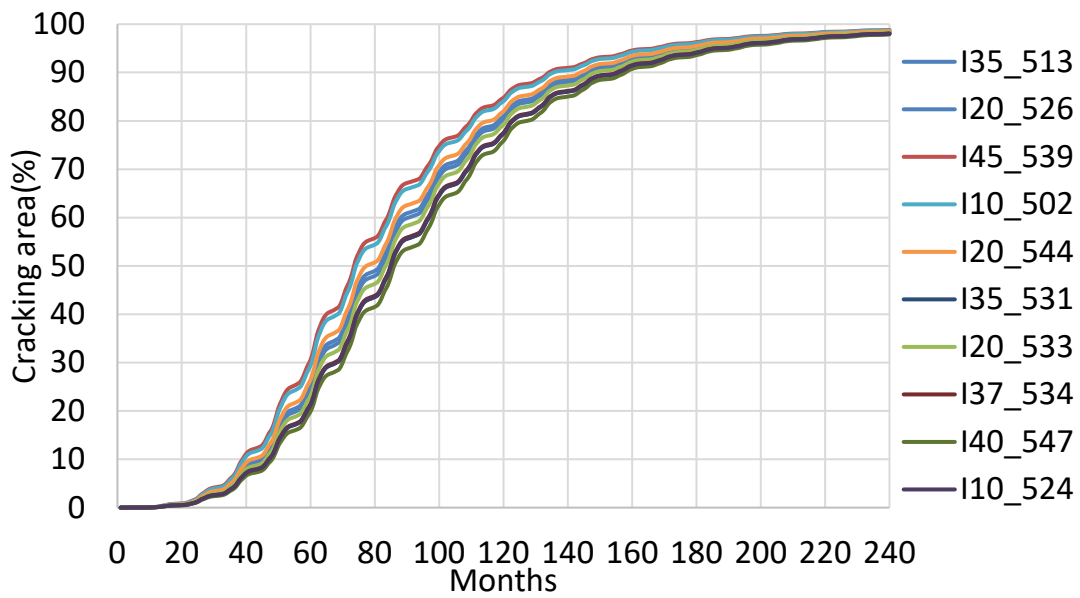
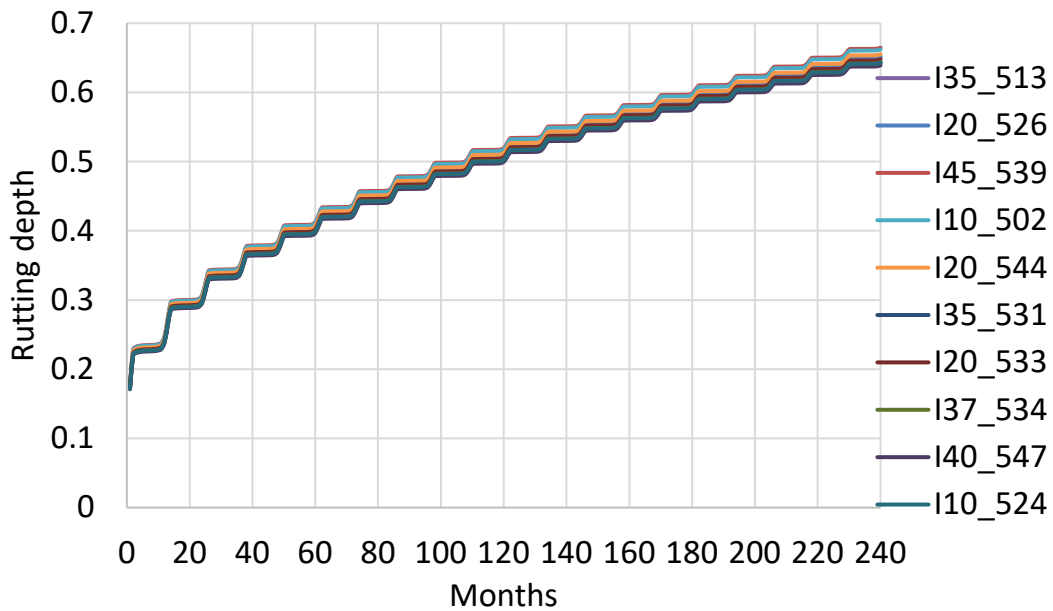


Figure 30. Comparison of the Number of APT for Tandem Axle.



(a)



(b)

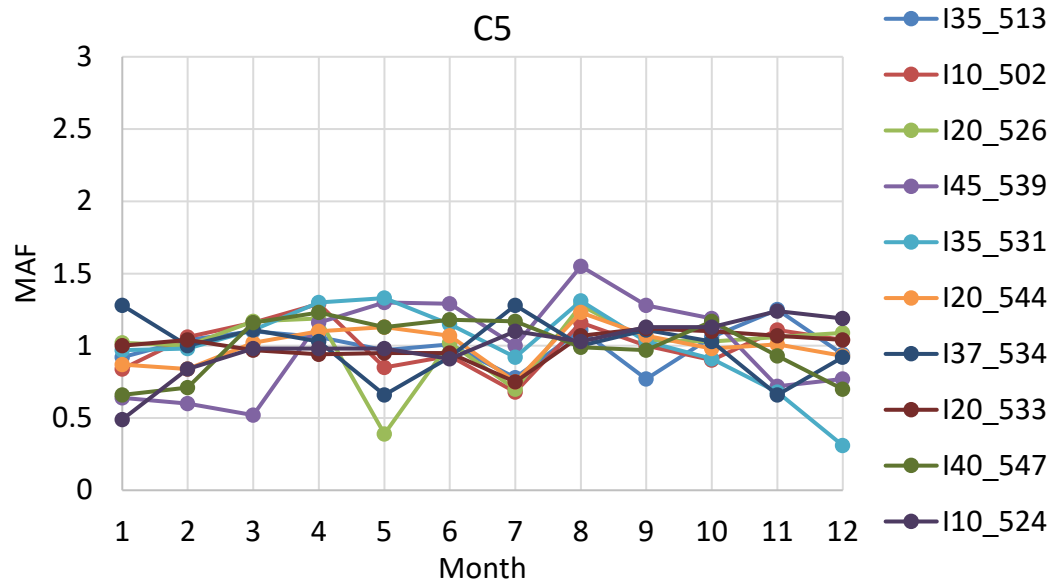
Figure 31. Sensitivity Analysis Results: (a) Rutting and (b) Cracking.

Table 15. Default Input of APT for IH.

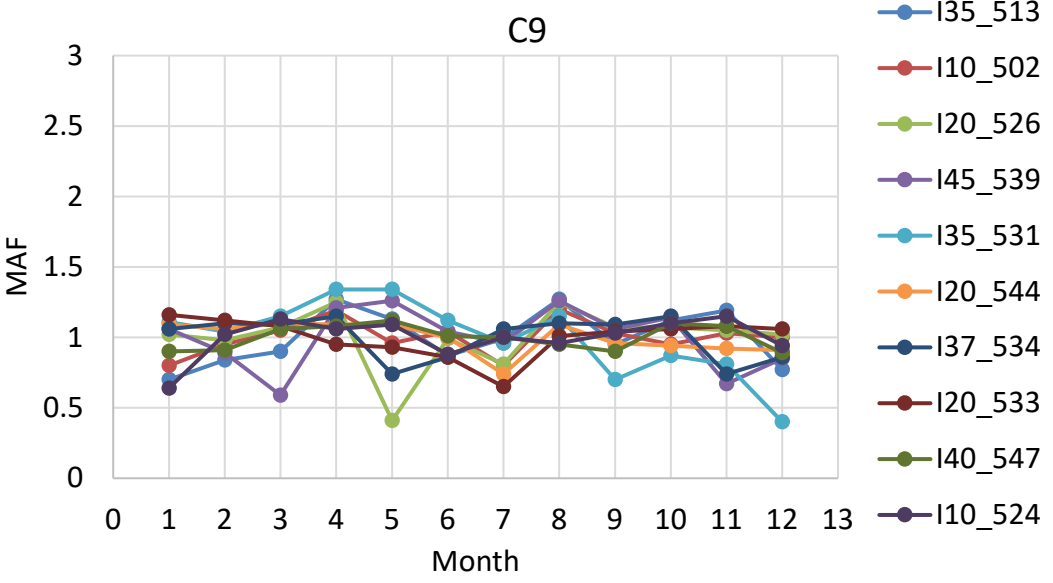
Vehicle class	Steering Axle	Single	Tandem	Tridem	Quad
C4	1	0.48	0.52	0.00	0.00
C5	1	1.00	0.00	0.00	0.00
C6	1	0.01	0.99	0.00	0.00
C7	1	0.03	0.03	0.97	0.00
C8	1	1.29	0.75	0.00	0.00
C9	1	0.24	1.88	0.00	0.00
C10	1	0.03	0.97	0.87	0.02
C11	1	4.00	0.01	0.00	0.00
C12	1	2.88	0.99	0.00	0.00
C13	1	1.12	0.90	0.47	0.35

Monthly Adjustment Factor

Researchers conducted a sensitivity analysis to investigate how the input of MAFs impacts the predicted pavement performances. The MAF from individual WIM station is used for each case. Figure 32 shows examples of MAF for C8 and C9. Figure 33 presents the sensitivity analysis results, which indicate that there is no significant difference when evaluating the impact of the input of MAF. Thus, the average values of MAFs from all the stations are used as the default input for IH, as shown in Table 16.

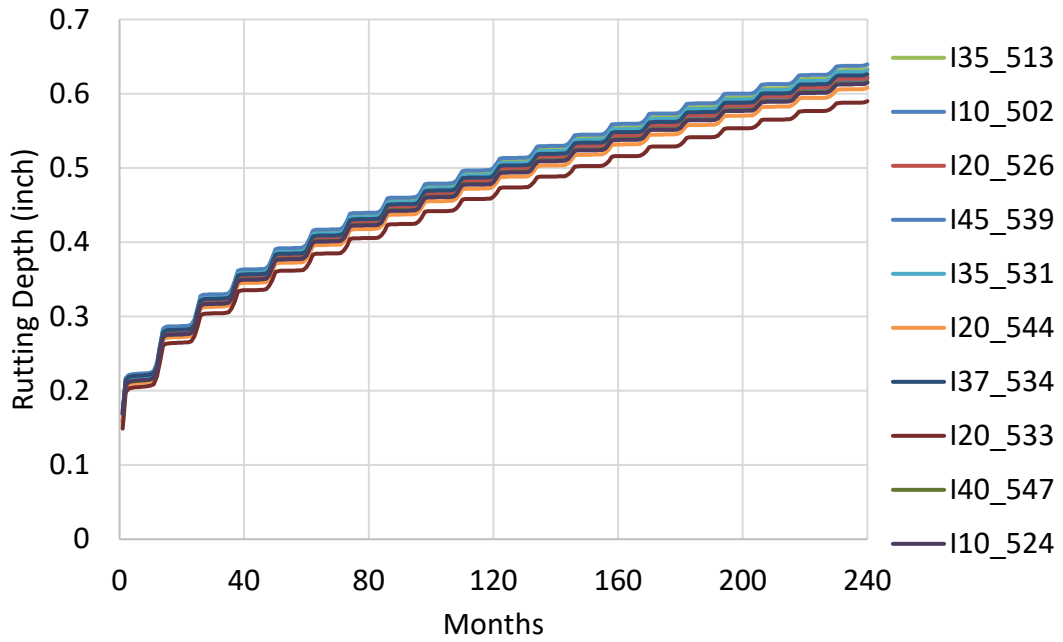


(a)

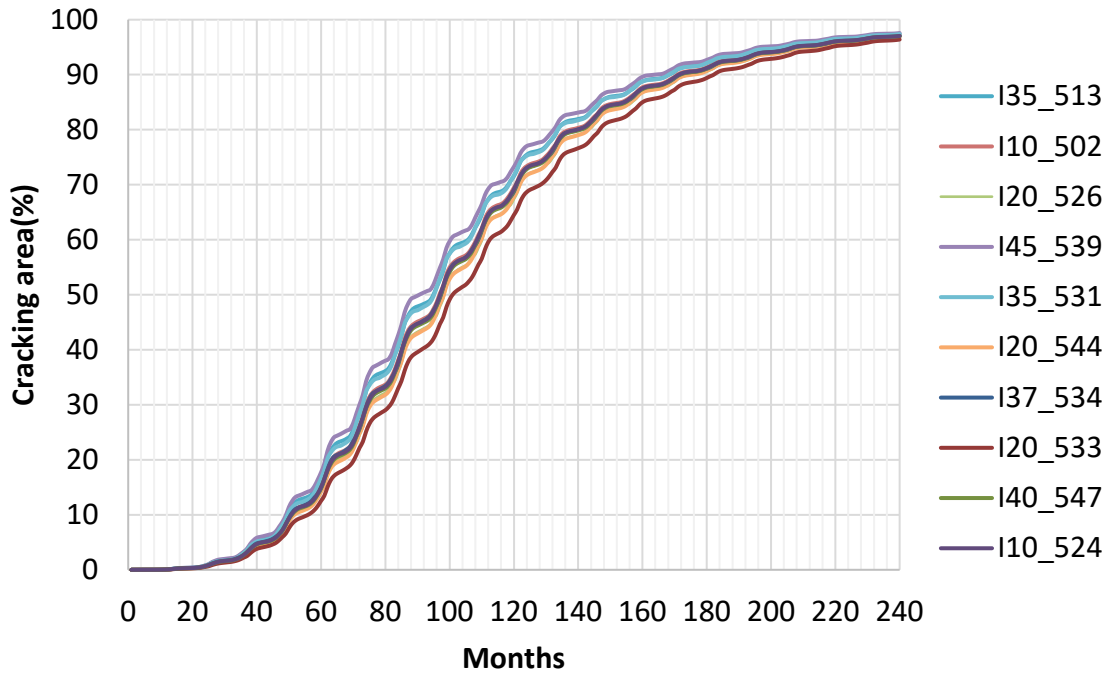


(b)

Figure 32. Examples of MAF for (a) C5 and (b) C9.



(a)



(b)

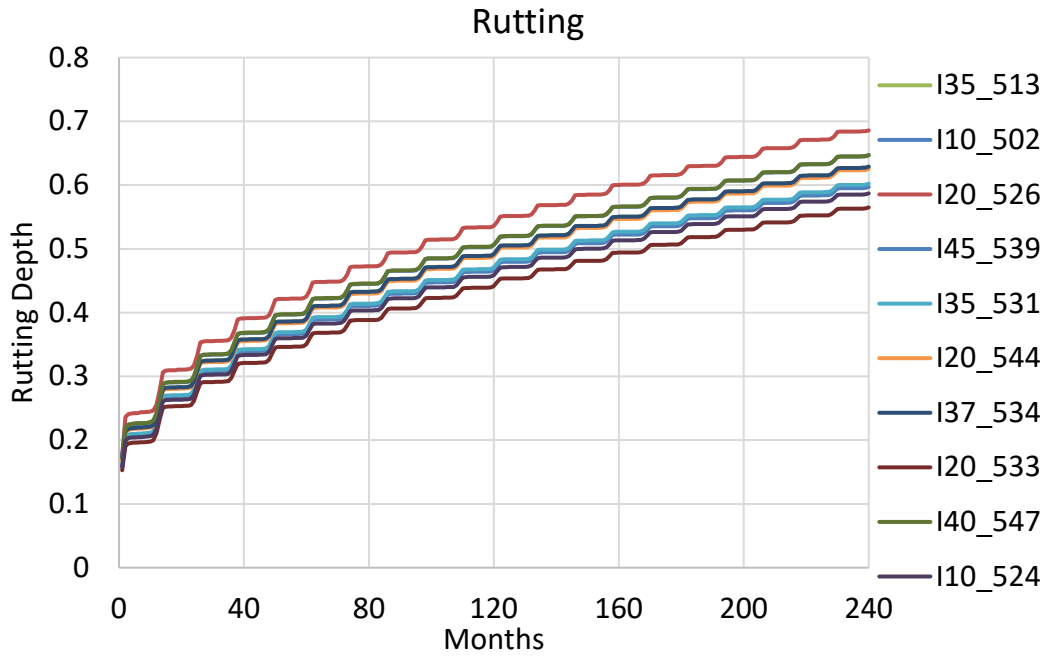
Figure 33. Sensitivity Analysis Results for MAF: (a) Rutting and (b) Cracking.

Table 16. Average Values of MAF.

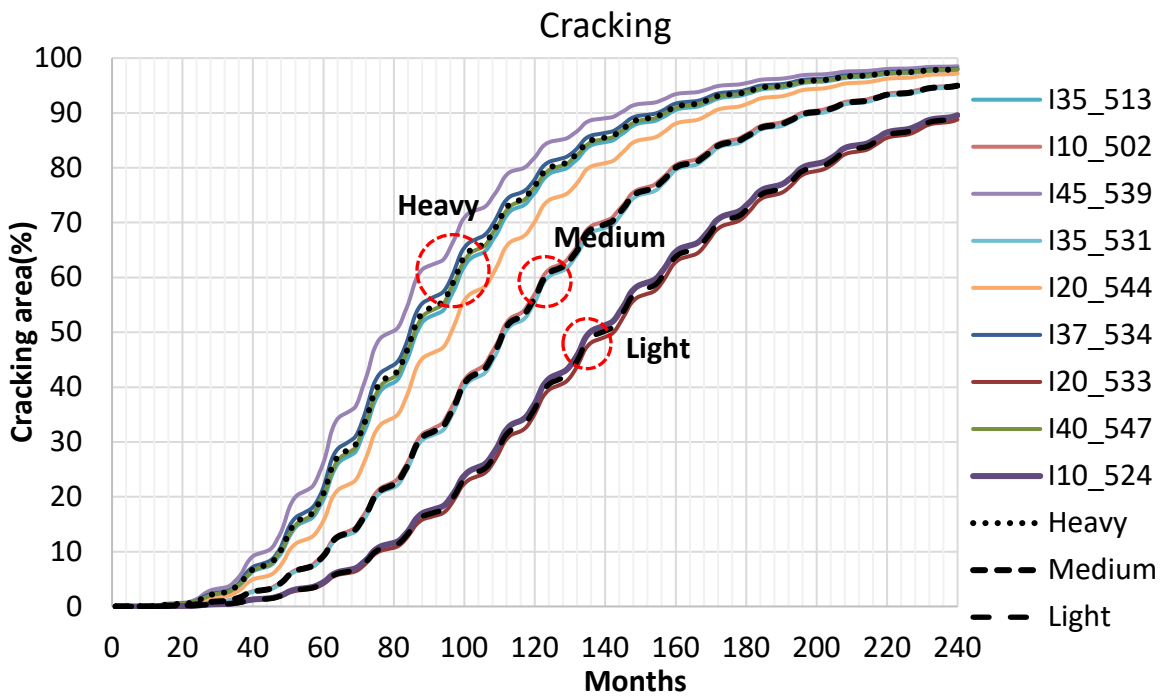
Month	Class 4	Class 5	Class 6	Class 7	Class 8	Class 9	Class 10	Class 11	Class 12	Class 13
January	1.01	0.87	0.83	0.52	0.81	0.95	0.37	0.97	0.38	0.31
February	1.12	0.91	0.88	0.49	0.92	0.99	0.42	1.01	0.43	0.30
March	1.21	1.03	0.93	0.52	1.00	1.02	0.44	1.07	0.42	0.36
April	1.01	1.13	1.16	1.28	1.20	1.16	1.64	1.14	1.63	1.38
May	0.87	0.97	1.03	1.19	1.02	1.01	1.41	0.99	1.41	1.15
June	1.19	1.04	0.91	0.60	0.95	0.97	0.49	1.02	0.35	0.95
July	1.30	0.91	0.95	1.09	1.12	0.90	0.65	0.88	0.59	0.51
August	0.96	1.17	1.22	1.34	1.10	1.12	1.59	1.12	1.60	1.44
September	0.90	1.05	1.07	1.42	1.01	0.98	1.37	1.01	1.30	1.71
October	0.92	1.05	1.10	1.41	1.07	1.05	1.37	1.07	1.45	1.40
November	0.83	0.97	1.00	1.06	0.93	0.97	1.19	0.94	1.31	1.27
December	0.69	0.89	0.92	1.09	0.88	0.87	1.07	0.79	1.15	1.22

Axle Load Distribution

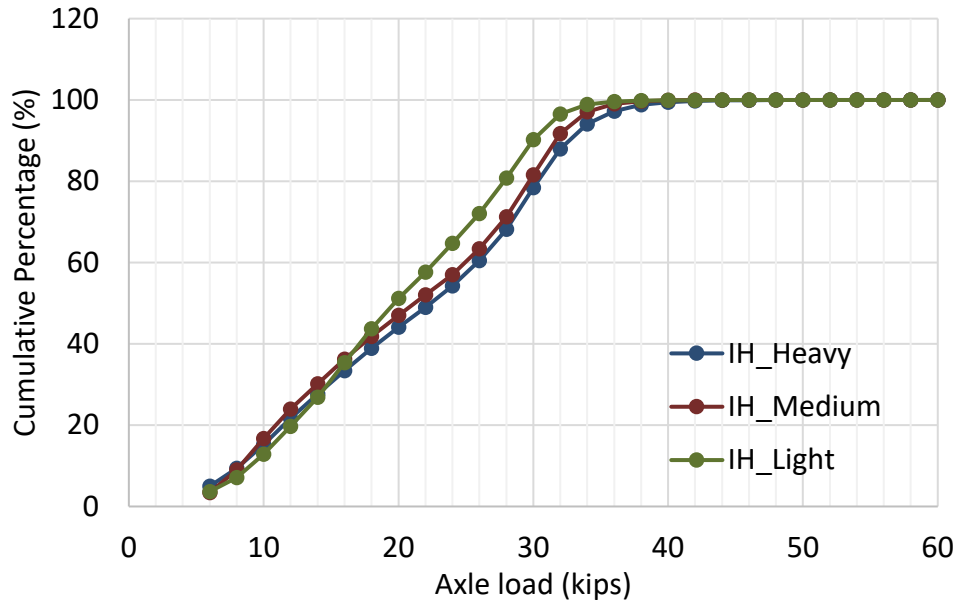
Researchers conducted a sensitivity analysis to investigate how the input of ALD impacts the predicted pavement performance. In this analysis, all inputs are fixed except the ALD. The input of ALD uses the data from individual WIM stations. The pavement structure is 6-inch AC and 12-inch FB. AADTT was 7000. Station 526 is excluded since its ALD is obviously different from other stations, which could be an outlier. Figure 34 presents the results, which indicate that the input of ALD has a significant impact on the performances, especially in the cracking results. Based on the results, the ALDs from the WIM stations are categorized into three groups: heavy, medium, and light. The average of ALDs from each group is determined as the default input, so there are three default inputs corresponding to heavy, medium, and light ALD. In order to better understand the three default ALD inputs, the ALD of tandem axle for C9 is examined and compared. Figure 34c compares cumulative percentage versus axle load. The legal limit of axle load for tandem axle is 34 kips. The cumulative percentages for the axle load over the legal limit corresponding to heavy ALD, medium ALD, and light ALD is 5.9 percent, 2.9 percent, 1.1 percent, respectively. Table 17 presents the location information of WIM stations, which are categorized into three groups (i.e., three default ALDs), which can be used as a reference for the designers in the decision-making process about which ALD should be used for a specific location.



(a)



(b)



(c)

Figure 34. Sensitivity Analysis Results of ALD: (a) Rutting, (b) Cracking, and (c) ALDs of Heavy, Medium and Light Default Input for Tandem Axle.

Table 17. Location Information for Three Default ALDs.

Default ALD Inputs	Station ID	Hwy#	County	District
IH_Heavy	539	I-45	Navarro	Dallas
	534	I-37	Nueces	Corpus Christi
	547	I-40	Gray	Amarillo
	544	I-20	Eastland	Brownwood
	513	I-35	Bell	Waco
IH_Medium	502	I-10	Guadalupe	San Antonio
	531	I-35	LaSalle	Laredo
IH_Light	533	I-20	Ector	Odessa
	524	I-10	El Paso	El Paso

DEVELOPMENT OF DEFAULT LOAD SPECTRA INPUTS FOR US/IH

A total of 13 permanent WIM stations was used for determining the default load spectra inputs for US/SH highways. Following the same approach for IH, researchers developed default inputs for US/SH highways, as described below.

Vehicle Class Distribution

Figure 35 presents the VCD based on the traffic data from the WIM stations, and the range for each truck class in the VCD based on all the WIM stations is summarized in Table 18. The percentage of C9 is between 32.4 percent and 64.8 percent.

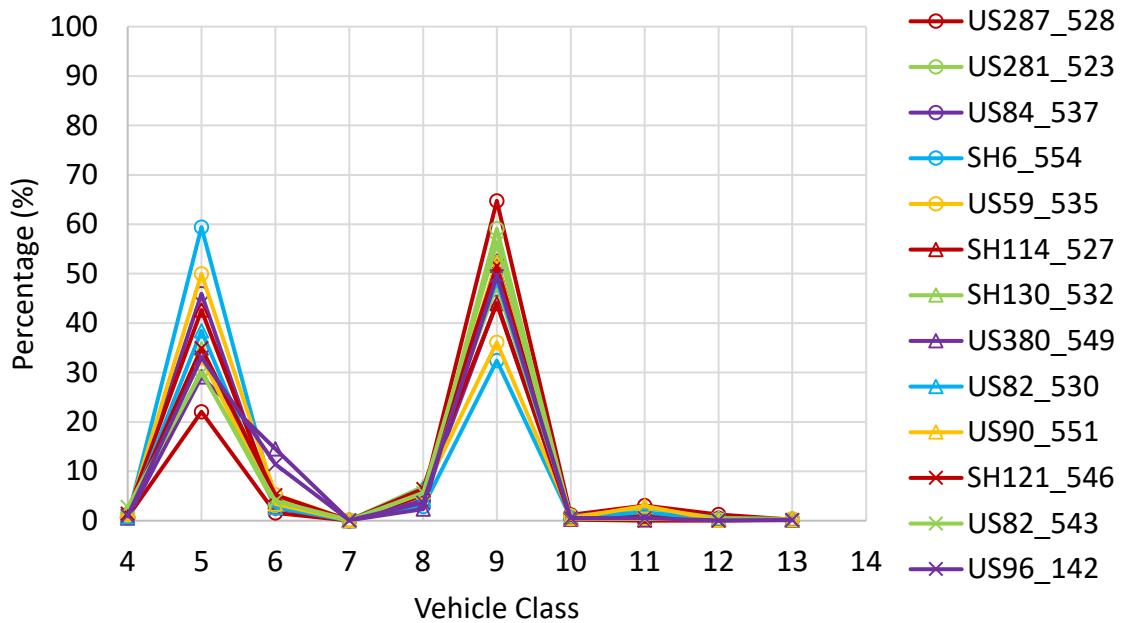


Figure 35. VCDs for US/SH.

Table 18. Percentage Ranges for Each Truck Class Based on All the WIM Stations.

Vehicle Class	Min (%)	Max (%)
C4	0.5	2.8
C5	22.1	59.4
C6	1.6	14.5
C7	0.0	0.2
C8	2.4	6.9
C9	32.4	64.8
C10	0.2	1.2
C11	0.0	3.1
C12	0.0	1.3
C13	0.1	0.4

Similarly, researchers conducted a sensitivity analysis to investigate how change of percentage of each truck class in the US/SH VCD impacts the predicted pavement performance. Figure 36 shows some examples of the results. The results indicate that C9 plays a more significant role in the VCD than other truck classes, while there is no substantial difference in the predicted results for other truck classes when changing the percentage. A typical pavement structure of 6-inch AC and 12-inch FB is used for sensitivity analysis, and AADTT was 4182. Most of WIM stations have the percentage of C9 ranged from 40 percent to 60 percent. The default values are defined as the most frequently observed values. Similar with the method used for IH, three sets of default inputs of VCD were determined for US/SH. Each set of input used the same average values for

all the truck classes except C9 and C5, and the percentage of C9 for each set is 40 percent, 50 percent, and 60 percent, as shown in Table 19.

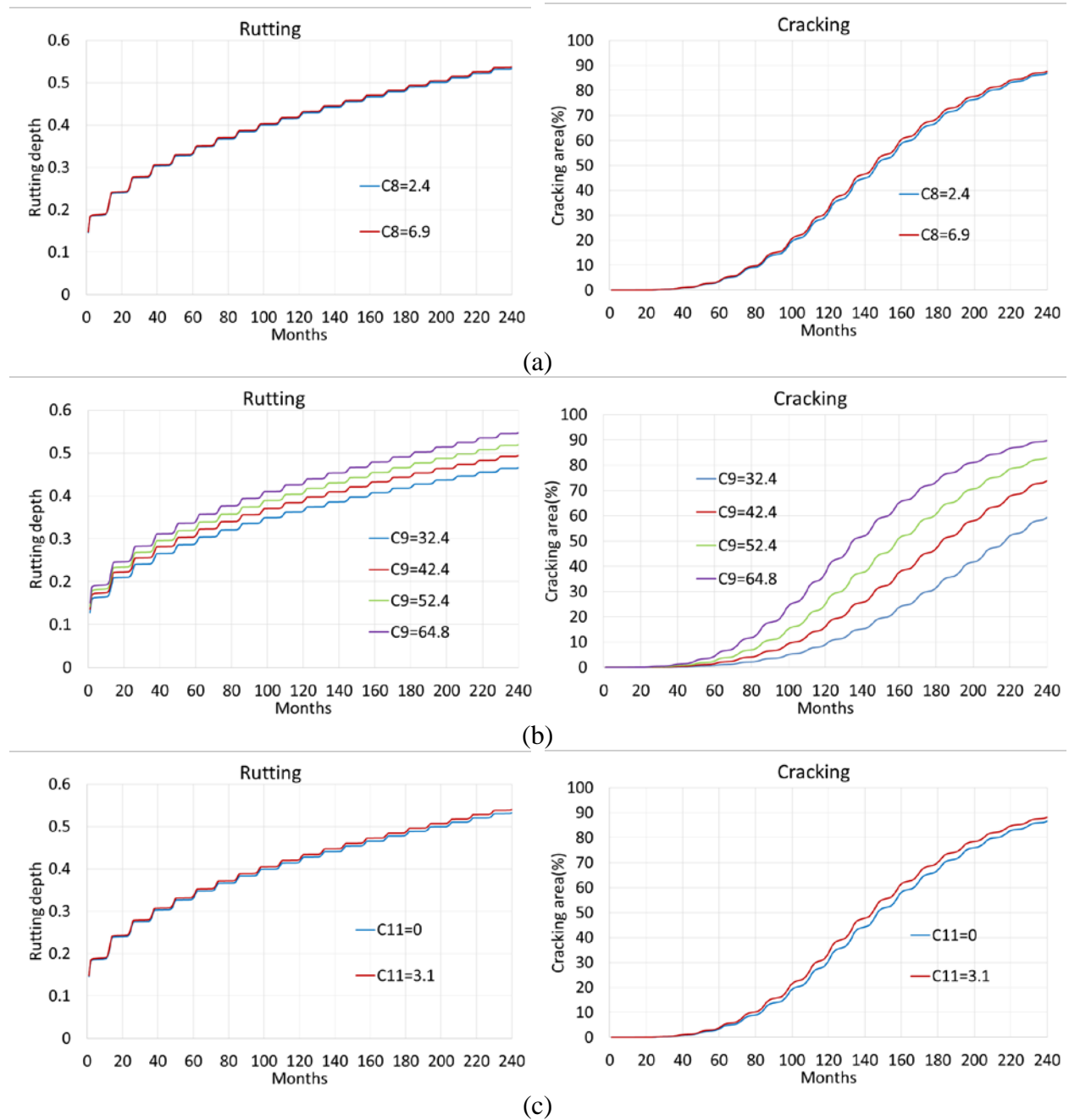


Figure 36. Sensitivity Analysis Results: (a) C8, (b) C9, and (c) C11.

Table 19. Default Inputs of VCD for US/SH.

Vehicle class	#1 (40% 18-wheeler)	#2 (50% 18-wheeler)	#3 (60% 18-wheeler)
	Distribution (%)	Distribution (%)	Distribution (%)
C4	1.2	1.2	1.2
C5	46.4	36.4	26.4
C6	5.0	5.0	5.0
C7	0.1	0.1	0.1
C8	5.0	5.0	5.0
C9	40.0	50.0	60.0
C10	0.6	0.6	0.6
C11	1.2	1.2	1.2
C12	0.3	0.3	0.3
C13	0.2	0.2	0.2

Axle per Truck

Researchers conducted a sensitivity analysis to evaluate how the input of APT impacts the pavement performances for US/SH. Like the results in the IH section, there is no significant difference between different WIM stations when evaluating the impact of APT. Thus, the average values of APTs from all the stations were used as the default input for US/SH, as listed in Table 20.

Table 20. Average Value of APT.

Vehicle class	Steering	Single	Tandem	Tridem	Quad
Class 4	1	0.58	0.42	0.00	0.00
Class 5	1	1.00	0.00	0.00	0.00
Class 6	1	0.01	0.99	0.00	0.00
Class 7	1	0.01	0.01	1.03	0.00
Class 8	1	1.32	0.69	0.00	0.00
Class 9	1	0.24	1.87	0.00	0.00
Class 10	1	0.04	0.99	0.98	0.01
Class 11	1	3.90	0.03	0.00	0.00
Class 12	1	2.69	1.05	0.00	0.00
Class 13	1	0.88	1.14	0.44	0.44

Monthly Adjustment Factor

Researchers conducted a sensitivity analysis to investigate how the input of MAF impacts the predicted pavement performances for US/SH highways. Similarly, there is no significant

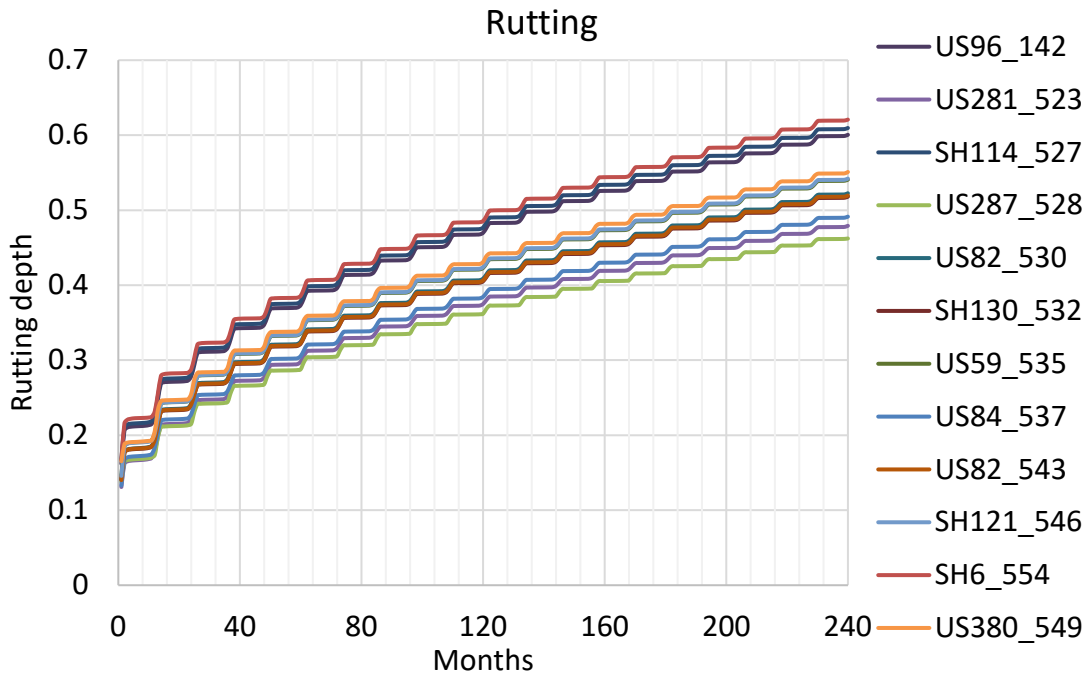
difference in the results between different WIM stations. Thus, the average values of MAFs from all the stations, as tabulated in Table 21, were used as the default input for US/SH.

Table 21. Average Values of MAF.

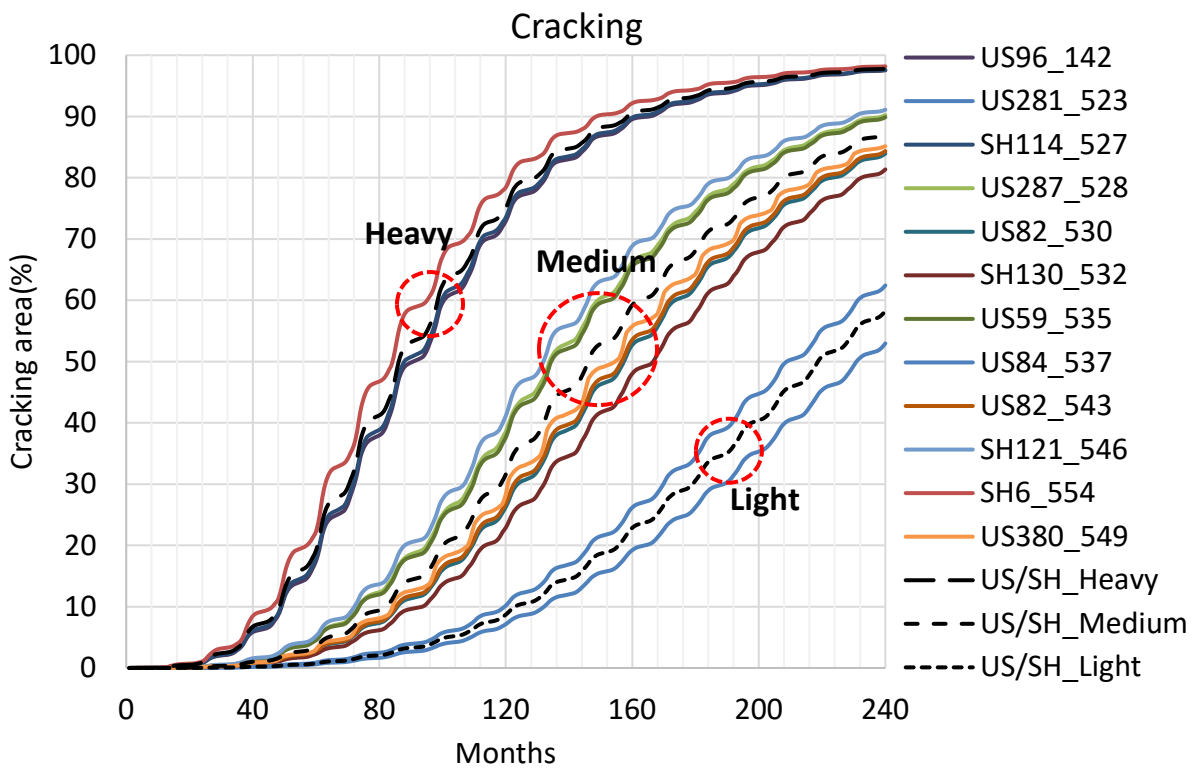
Month	Class_4	Class_5	Class_6	Class_7	Class_8	Class_9	Class_10	Class_11	Class_12	Class_13
January	1.16	0.87	0.75	0.32	0.68	0.94	0.32	0.95	0.38	0.23
February	1.23	0.83	0.71	0.34	0.75	0.89	0.31	0.85	0.41	0.26
March	1.40	0.98	0.87	0.63	0.90	0.97	0.34	1.01	0.37	0.42
April	0.79	1.02	1.06	1.59	1.10	1.13	1.62	1.08	1.47	1.64
May	0.77	1.06	1.12	1.42	1.08	1.12	1.53	1.09	1.38	1.70
June	1.38	1.11	0.95	0.44	0.97	0.97	0.35	1.00	0.30	0.37
July	1.31	0.98	1.07	1.18	1.40	0.96	0.62	0.90	0.57	0.42
August	0.74	1.17	1.24	1.23	1.13	1.12	1.55	1.04	1.45	1.56
September	0.71	0.99	1.02	1.07	0.98	0.97	1.15	0.84	1.41	1.17
October	0.82	1.02	1.11	1.28	1.10	1.02	1.38	1.18	1.68	1.38
November	0.99	1.08	1.15	1.31	1.06	1.04	1.42	1.24	1.46	1.52
December	0.70	0.89	0.94	1.19	0.85	0.86	1.39	0.83	1.11	1.33

Axle Load Distribution

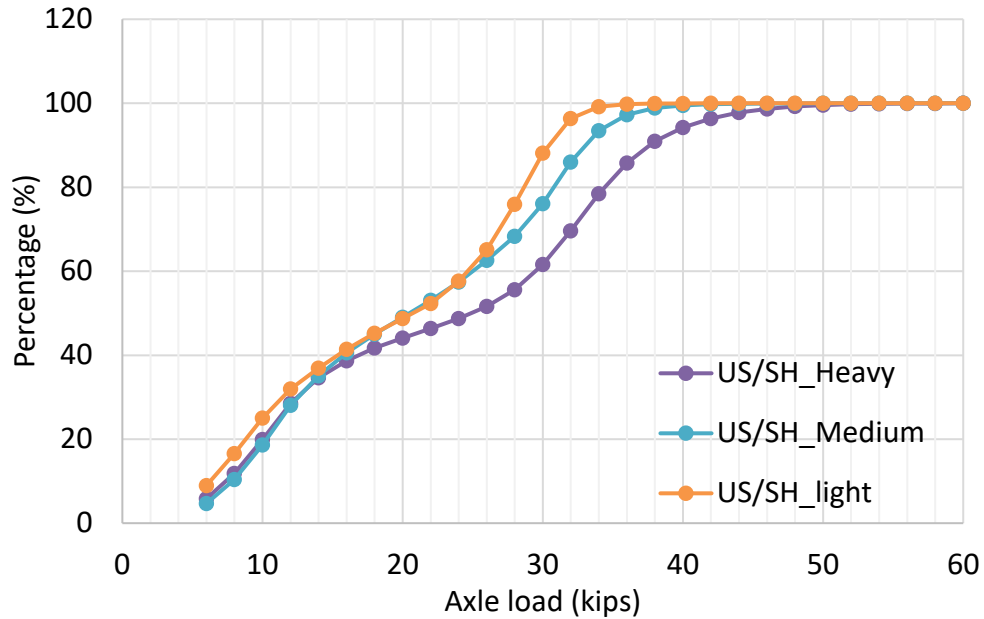
Similarly, researchers performed a sensitivity analysis. For each case, all the TxME inputs are fixed except the input of ALD. The input of ALD uses the data from individual WIM stations. The pavement structure is 6-inch AC and 12-inch FB. AADTT is 4182. Figure 37 presents the sensitivity analysis results, which indicate that the ALDs from the WIM stations can be categorized into three groups: heavy, medium and light, as shown in Figure 37b. The average of ALDs from each group was determined as the default input. Figure 37c compares cumulative percentage versus axle load. The legal limit of axle load for tandem axle is 34 kips. The cumulative percentages for the axle load over the legal limit corresponding to heavy ALD, medium ALD, and light ALD is 21.6 percent, 6.6 percent, 0.9 percent, respectively. Furthermore, Table 22 presents the location information of WIM stations, which are categorized into three groups (i.e., three default ALDs), which can be used as a reference for the designers in the decision-making process about which ALD should be used for a specific location.



(a)



(b)



(c)

Figure 37. Sensitivity Analysis Results of ALD for US/SH: (a) Rutting, (b) Cracking, and (c) ALDs of Heavy, Medium, and Light Default Input for Tandem Axle.

Table 22. Location Information for Three Default ALDs.

Default ALD Inputs	Station ID	Hwy#	County	District
US/SH_heavy	142	US 96	Jasper	Beaumont
	527	SH 114	Wise	Fort Worth
	554	SH 6	Brazos	Bryan
US/SH_medium	528	US 287	Wichita	Wichita Falls
	530	US 82	Archer	Wichita Falls
	532	SH 130	Williamson	Austin
	535	US 59	Live Oak	Corpus Christi
	543	US 82	Terry	Lubbock
	546	SH 121	Fannin	Paris
	549	US 380	Wise	Fort Worth
US/SH_light	523	US 281	Hidalgo	Pharr
	537	US 84	Lubbock	Lubbock

DEVELOPMENT OF DEFAULT LOAD SPECTRA INPUTS FOR FM ROADS

There are very few WIM stations located on FM roads. The traffic data from two WIM stations were used for FM roads. Similar works were performed to develop default load spectra inputs for FM roads, as noted below.

Vehicle Class Distribution

The percentage of C9 in the VCD for the two WIM stations are 29 percent and 72 percent, respectively. When the roads have low volume traffic, there is generally a large variation in the VCD. For FM roads based on the limited traffic data, 30 percent was selected for the percentage of C9 in the default input. Table 23 presents the default input of VCD for FM roads.

Table 23. Default Input of VCD for FM.

Vehicle class	#1 (30% 18-wheeler)
	Distribution (%)
Class 4	0.8
Class 5	54.7
Class 6	7.8
Class 7	0.1
Class 8	4.5
Class 9	30.0
Class 10	1.4
Class 11	0.0
Class 12	0.0
Class 13	0.7

Axle per Truck

The sensitivity analysis results indicate that there is no significant difference between the two stations. Thus, the average values listed in Table 24 were used as the default input.

Table 24. Average Value of APT.

Vehicle class	Steering Axle	Single	Tandem	Tridem	Quad
Class 4	1.00	0.90	0.10	0.00	0.00
Class 5	1.00	1.00	0.00	0.00	0.00
Class 6	1.00	0.00	1.00	0.00	0.00
Class 7	1.00	0.08	0.08	0.92	0.00
Class 8	1.00	1.26	0.75	0.00	0.00
Class 9	1.00	0.07	1.97	0.00	0.00
Class 10	1.00	0.02	0.98	1.02	0.01
Class 11	1.00	3.80	1.05	0.00	0.00
Class 12	1.00	1.17	1.92	0.00	0.00
Class 13	1.00	0.60	1.09	0.11	0.85

Monthly Adjustment Factor

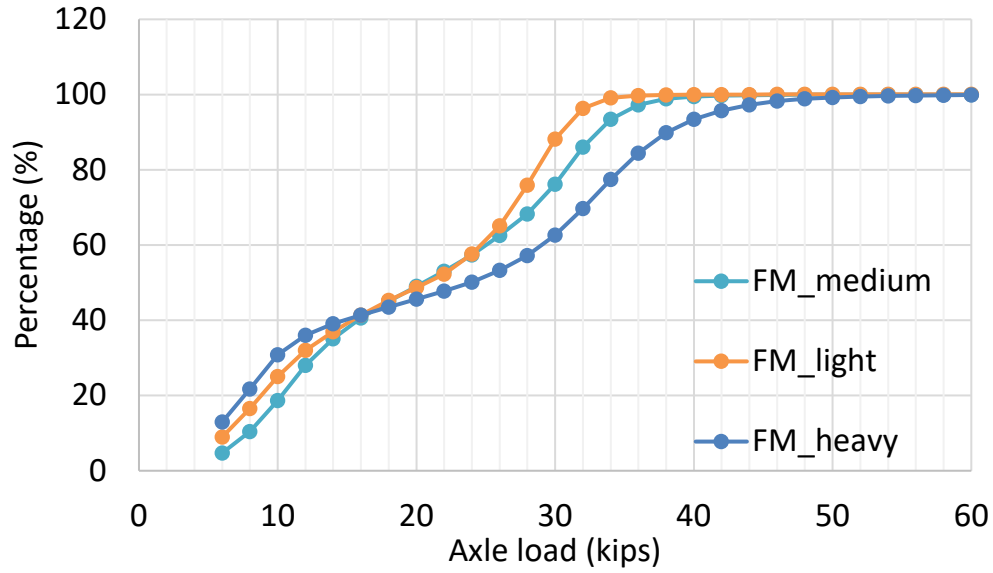
The sensitivity analysis results indicate that there is no significant difference between the two stations. Thus, the average values presented in Table 25 were used as the default input.

Table 25. Average Values of MAF.

Month	Class_4	Class_5	Class_6	Class_7	Class_8	Class_9	Class_10	Class_11	Class_12	Class_13
January	1.73	0.79	0.71	0.39	0.60	0.79	0.00	3.60	0.00	0.00
February	2.39	0.88	0.69	0.20	0.78	0.82	0.00	1.20	0.00	0.00
March	1.91	0.90	0.83	0.07	0.71	0.73	0.00	0.00	0.00	0.00
April	0.90	1.17	1.22	2.19	1.23	1.00	2.97	3.00	1.00	2.66
May	1.11	1.23	1.29	0.79	1.15	1.09	1.37	0.00	1.50	1.16
June	1.10	1.27	1.19	0.29	1.11	0.89	0.00	0.00	0.00	0.00
July	0.58	0.84	1.12	0.42	1.32	1.06	0.31	0.00	3.00	0.06
August	0.40	1.33	1.48	2.04	1.44	1.45	1.99	1.20	1.50	3.88
September	0.67	1.15	1.07	1.24	1.19	1.30	1.64	3.00	4.00	0.86
October	0.69	1.04	1.00	1.59	0.84	1.05	1.65	0.00	1.00	1.91
November	0.30	0.80	0.90	2.36	0.96	1.19	1.38	0.00	0.00	0.59
December	0.24	0.63	0.52	0.46	0.70	0.66	0.71	0.00	0.00	0.89

Axle Load Distribution

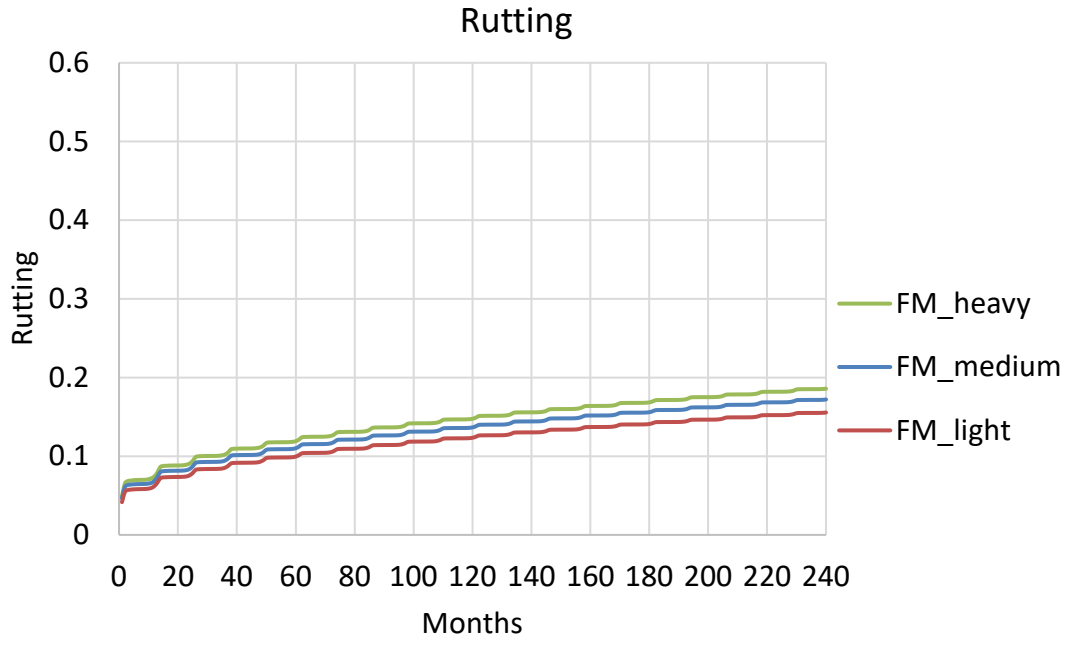
The sensitivity analysis results indicate the ALDs from the two WIM stations are similar with the ALD of US/SH_heavy default input. The average of ALDs from the two WIM stations were used as the default input labeled as FM_heavy ALD (see Figure 38). In order to provide more choices for different scenarios, the ALDs of US/SH_medium and US/SH_light were used as the default inputs corresponding to FM_medium ALD and FM_light ALD, respectively. For each case, all the TxME inputs are fixed except the input of ALD. The input of ALD uses the data of individual WIM stations. The pavement structure is 3-inch AC and 8-inch FB. AADTT is 200.



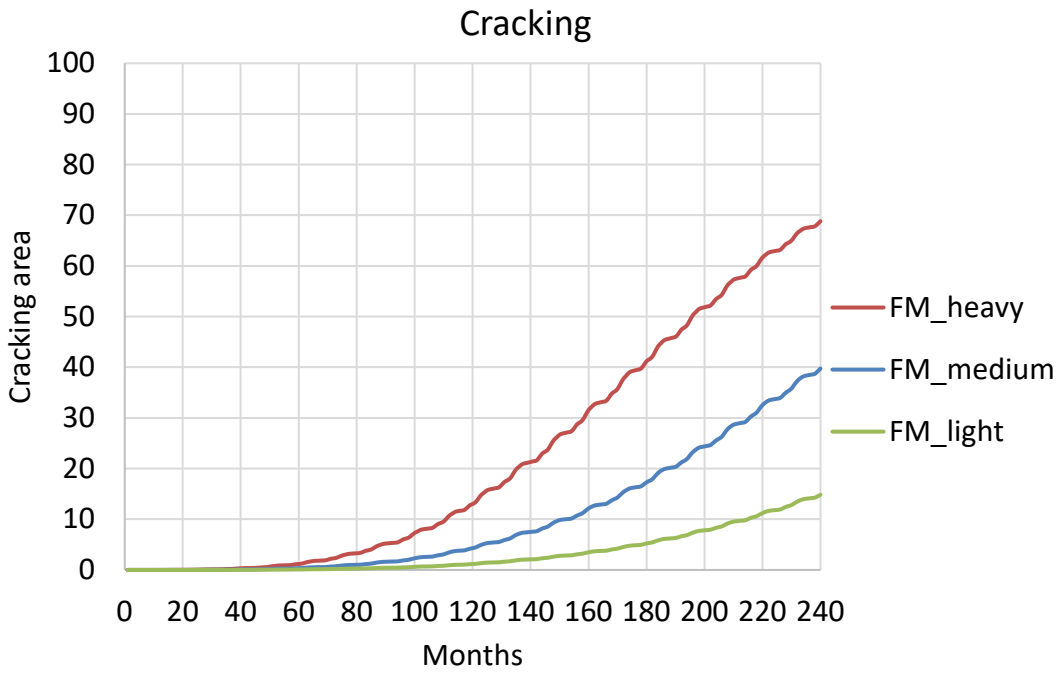
(c)

Figure 38. Comparison of Cumulative Tandem ALDs of C9 for Three Default ALD Inputs.

Figure 39 presents the comparison of three default ALDs in terms of predicted rutting and cracking performances.



(a)



(b)

Figure 39. Three Default ALDs for FM: (a) Rutting and (b) Cracking.

DEVELOPMENT OF DEFAULT LOAD SPECTRA INPUTS FOR ROADS IN ENERGY SECTORS

The traffic data from two sites using portable WIM were used for roads in the energy sectors. Similar works were performed to develop default load spectra inputs for FM roads, as noted below.

Vehicle Class Distribution

The VCDs from the two sites are similar, and the percentage of C9 is about 80 percent. The average of the VCDs from the two sites were used as the default input for roads in energy sectors (see Table 26).

Table 26. Default Input of VCD for FM.

Vehicle class	#1 (80% 18-wheeler)
	Distribution (%)
Class 4	0.6
Class 5	7.2
Class 6	3.0
Class 7	0.3
Class 8	5.3
Class 9	80
Class 10	2.1
Class 11	0.5
Class 12	0.6
Class 13	0.4

Axle per Truck

The sensitivity analysis results indicate that there is no significant difference between the two stations. Thus, the average values (see Table 27) were used as the default input.

Table 27. Average Value of APT.

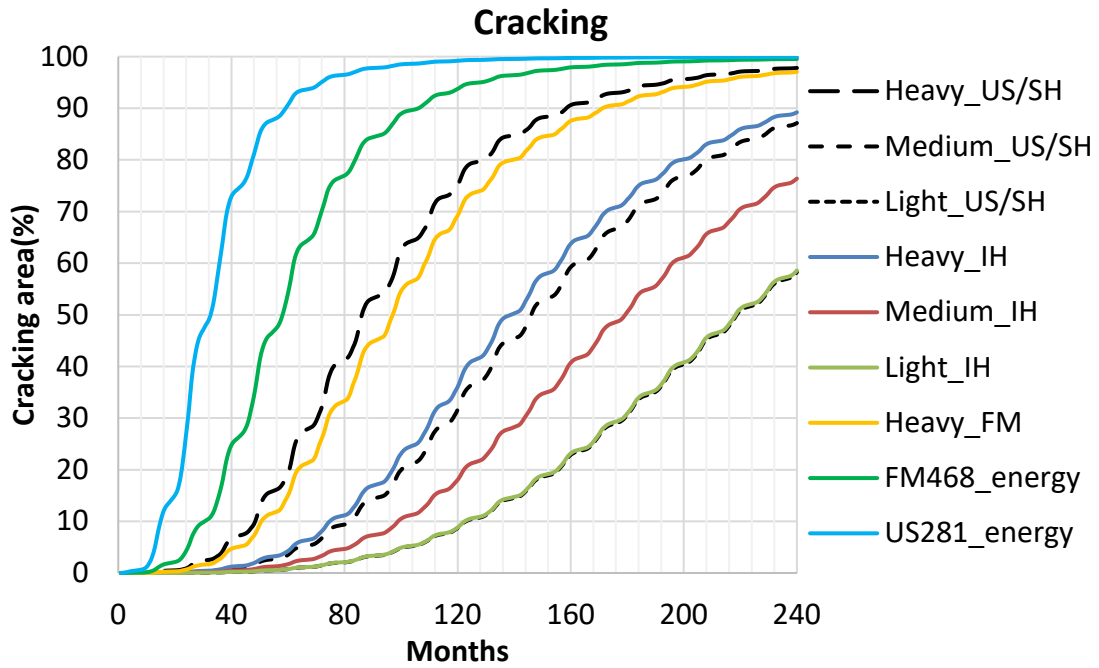
Vehicle class	Steering Axle	Single	Tandem	Tridem	Quad
Class 4	1	0.23	0.75	0.00	0.00
Class 5	1	1.00	0.00	0.00	0.00
Class 6	1	0.00	1.00	0.00	0.00
Class 7	1	0.00	0.00	0.88	0.00
Class 8	1	1.12	0.88	0.00	0.00
Class 9	1	0.09	1.96	0.00	0.00
Class 10	1	0.00	0.86	0.92	0.18
Class 11	1	4.00	0.00	0.00	0.00
Class 12	1	2.17	1.10	0.50	0.00
Class 13	1	0.00	0.00	2.00	0.00

Monthly Adjustment Factor

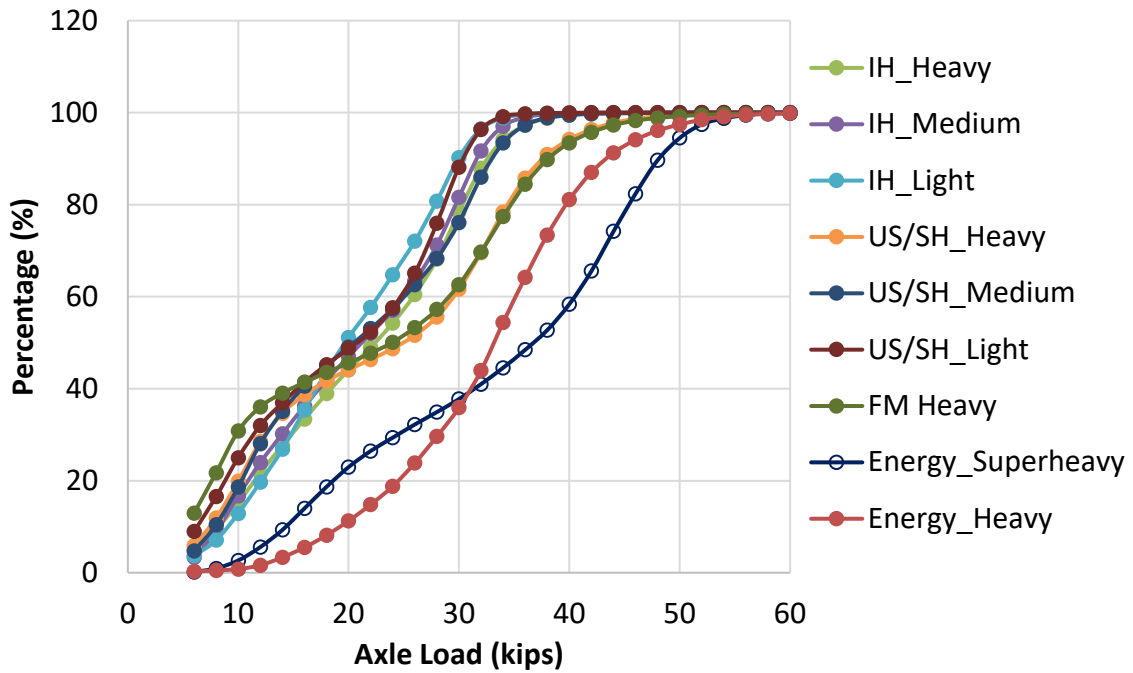
There were not enough portable WIM data to develop MAFs for roads in the energy sectors. Therefore, one is set for every month.

Axle Load Distribution

Researchers conducted the sensitivity analysis. Figure 40a compares cracking performance with different ALDs from IH, US/SH, FM, and energy sectors. For this comparison, for each case, all the TxME inputs are fixed except the input of ALD. The pavement structure is 6-inch AC and 12-inch FB. AADTT is 4182. FM 468 and US 281 have the smallest cracking fatigue life. Thus, for roads in energy sectors, the ALDs from US 281 and FM 468 are used as the default inputs of super-heavy ALD and heavy ALD, respectively. Figure 40b compares the curves of cumulative percentage versus axle load for C9 tandem axle. The legal limit of axle load for tandem axle is 34 kips. Super-heavy ALD and heavy ALD have a much larger cumulative percentage over the legal axle load limit than others.



(a)



(b)

Figure 40. (a) Comparison of Predicted Cracking Performances with Use of Different ALDs for IH, US/SH, FM, and Roads in Energy Sectors, and (b) Comparison of ALDs.

INCORPORATE DEFAULT VALUES INTO TXME

Figure 41 shows the TxME screen of incorporating default load spectra. In this screen, the highway types are divided into four categories: energy sector, IH, US/SH, and FM. The VCDs are divided into three categories according to the volume of 18-wheelers (vehicle class C9): high, medium, and low. Similarly, the ALDs are divided into three categories based on the weight of the 18-wheelers (vehicle class C9): heavy, medium, and light. As discussed before, each highway type has one set of corresponding averaged MAFs and one set of APT factors.

When users select one combination of highway type, VCD type, and ALD type, TxME software will automatically load all the corresponding factors. Users can also edit these factors if they have specific WIM data available.

Traffic Characteristics

Highway Type	Vehicle Class Distribution Volume of 18-Wheelers	Axle Load Distribution Weight of 18-Wheelers	Monthly Adjustment Factor (MAF)	Axles Per Truck (APT)
US/SH ▾	High ▾	Heavy ▾	MAF-US/SH	APT-US/SH

US/SH ▾ Energy Section IH US/SH FM	High ▾ High Medium Low	Heavy ▾ Heavy Medium Light	<table border="1" style="width: 100%; border-collapse: collapse; font-size: 8px;"> <thead> <tr> <th colspan="5">Vehicle Class Distribution and Growth (US/SH, High Volume of 18-Wheelers)</th> </tr> <tr> <th>Vehicle Class</th> <th>Pictorial View</th> <th>Distribution (%)</th> <th>Growth Rate (%)</th> <th>Growth Function</th> </tr> </thead> <tbody> <tr><td>Class 4</td><td></td><td>1.2</td><td>3</td><td>Compound ▾</td></tr> <tr><td>Class 5</td><td></td><td>26.4</td><td>3</td><td>Compound ▾</td></tr> <tr><td>Class 6</td><td></td><td>5.0</td><td>3</td><td>Compound ▾</td></tr> <tr><td>Class 7</td><td></td><td>0.1</td><td>3</td><td>Compound ▾</td></tr> <tr><td>Class 8</td><td></td><td>5.0</td><td>3</td><td>Compound ▾</td></tr> <tr><td>Class 9</td><td></td><td>60</td><td>3</td><td>Compound ▾</td></tr> <tr><td>Class 10</td><td></td><td>0.6</td><td>3</td><td>Compound ▾</td></tr> <tr><td>Class 11</td><td></td><td>1.2</td><td>3</td><td>Compound ▾</td></tr> <tr><td>Class 12</td><td></td><td>0.3</td><td>3</td><td>Compound ▾</td></tr> <tr><td>Class 13</td><td></td><td>0.2</td><td>3</td><td>Compound ▾</td></tr> </tbody> </table> <p style="text-align: right; margin-top: 10px;">Sum of Distribution (%): 100.0</p> <div style="margin-top: 10px;"> <p style="background-color: #fff2cc; padding: 2px; text-align: center;">View/Edit Axle Load Distribution</p> <p style="color: #4f81bd; font-size: 8px; margin-left: 20px;">US/SH, Heavy Weight of 18-Wheelers</p> <p style="background-color: #fff2cc; padding: 2px; text-align: center; margin-top: 10px;">View/Edit Monthly Adjustment Factors</p> <p style="color: #4f81bd; font-size: 8px; margin-left: 20px;">US/SH</p> <p style="background-color: #fff2cc; padding: 2px; text-align: center; margin-top: 10px;">View/Edit Axles Per Truck</p> <p style="color: #4f81bd; font-size: 8px; margin-left: 20px;">US/SH</p> </div>	Vehicle Class Distribution and Growth (US/SH, High Volume of 18-Wheelers)					Vehicle Class	Pictorial View	Distribution (%)	Growth Rate (%)	Growth Function	Class 4		1.2	3	Compound ▾	Class 5		26.4	3	Compound ▾	Class 6		5.0	3	Compound ▾	Class 7		0.1	3	Compound ▾	Class 8		5.0	3	Compound ▾	Class 9		60	3	Compound ▾	Class 10		0.6	3	Compound ▾	Class 11		1.2	3	Compound ▾	Class 12		0.3	3	Compound ▾	Class 13		0.2	3	Compound ▾
Vehicle Class Distribution and Growth (US/SH, High Volume of 18-Wheelers)																																																															
Vehicle Class	Pictorial View	Distribution (%)	Growth Rate (%)	Growth Function																																																											
Class 4		1.2	3	Compound ▾																																																											
Class 5		26.4	3	Compound ▾																																																											
Class 6		5.0	3	Compound ▾																																																											
Class 7		0.1	3	Compound ▾																																																											
Class 8		5.0	3	Compound ▾																																																											
Class 9		60	3	Compound ▾																																																											
Class 10		0.6	3	Compound ▾																																																											
Class 11		1.2	3	Compound ▾																																																											
Class 12		0.3	3	Compound ▾																																																											
Class 13		0.2	3	Compound ▾																																																											

Figure 41. TxME Screen of Incorporating Default Load Spectra.

CHAPTER 5. DEVELOP DEFAULT INITIAL CONSTRUCTION COST

Initial construction cost analysis can provide preliminary comparisons among different pavement structure and layer materials. It helps pavement designers to balance the pavement performance with cost and choose an optimal design. The current version of FPS 21 has incorporated typical initial construction costs for each pavement layer such as AC mixture, base, and subbase materials. However, FPS does not consider the influence of binder or gradation variations on the cost of AC mixture. Neither does FPS 21 consider the RAP/RAS influence, although a certain amount of cost saving can be achieved by using some percentages of RAP/RAS materials.

This chapter summarizes how the initial construction costs of pavement layer materials especially the AC mixtures with RAP/RAS were determined and incorporated into the TxME software.

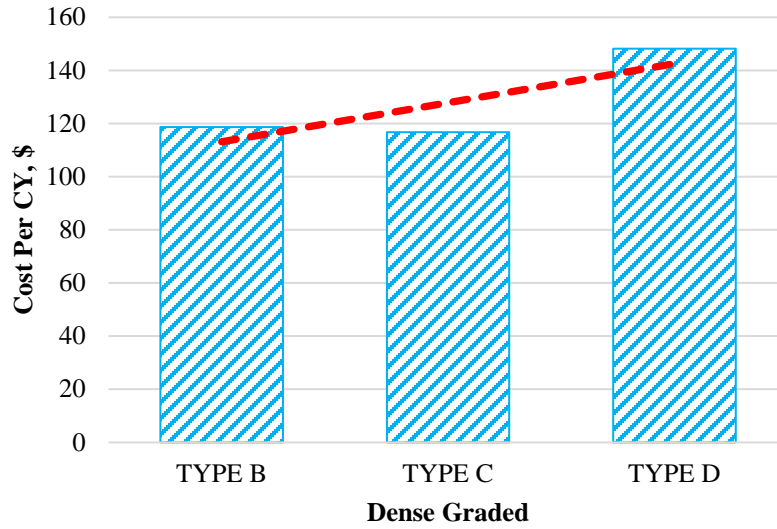
INITIAL CONSTRUCTION COSTS OF AC MIXTURES WITH NO RAP/RAS

As mentioned before, the cost of AC mixture was incorporated in the current FPS system without considering any specified binder grade or aggregate gradation type. To be consistent with FPS, it was assumed in the TxME that the AC mixture costs listed in the FPS system was for a typical mixture with PG64-22 binder and a Type C (intermediate) aggregate gradation. Hence, the cost of this mixture was used as a baseline price for estimating the cost of other mixtures with various binder PGs and gradation types.

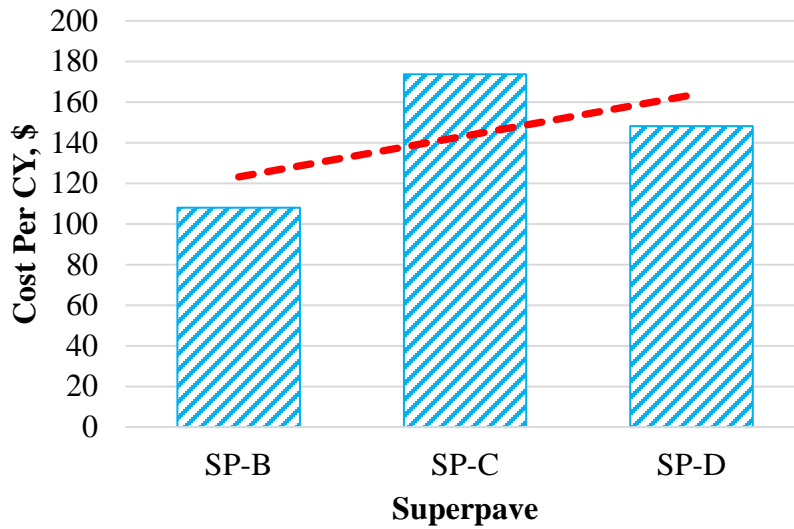
Regarding the cost of asphalt binder, it is normal that the prices of various binders with different PGs vary over the year, so it is not possible to obtain some exact cost figures. However, a common trend can always be observed and found to be rational to apply for defining costs of various binders. The trend is that binders that are modified for achieving adequate lower or higher temperature grade costs more than the base binder grade. These rational trends were used in this study as a guideline to determine and establish the costs of the materials. For example, a 10 percent increase in price can be observed when a mix design recommends the use of a PG64-28 binder rather than a PG64-22 binder. Similar rise in price can also be observed in case of a replacement of a PG70-22 binder with a PG70-28 binder. For the present case, one of the objectives is to establish only some tentative prices of the binders to implement binder specific mixture costs in the current version of TxME. Such initiative was considered in this study, and the binder prices for three different binders (i.e., PG64-22, PG70-22, and PG76-22) are gathered from current market evaluation. These prices were used as references for the estimation of binder specific asphalt-aggregate mix costs.

Another issue was to determine how the AC prices varies with the type of aggregate gradation used in the mixture. To acquire knowledge on this subject matter, the study conducted a thorough evaluation on the prices of the asphalt-aggregate mixture with same binder grade but with different types of aggregate gradations. The 12-month average low bid unit prices archived

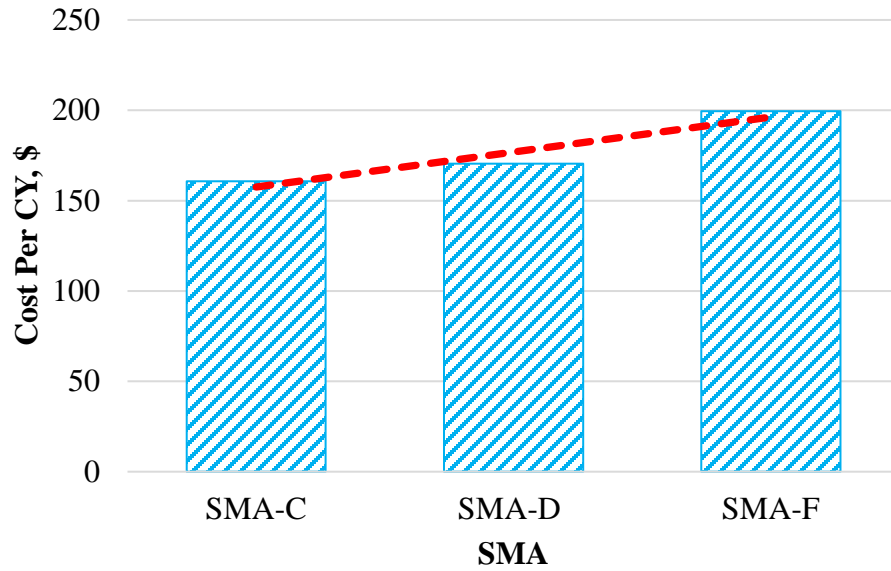
in the TxDOT website (TxDOT n.d.) were used as benchmarks for this purpose. Figure 42 shows the 12-month low-bid unit prices for the dense-graded, Superpave, SMA mixtures. A linear increase in prices from the coarse-graded to the fine-graded of AC mixtures can be approximated from this figure.



(a)



(b)



(c)

Figure 42. Twelve-Month Average Low Bid Prices of (a) Dense Graded, (b) Superpave, and (c) SMA Mixtures.

In general, a rational approach was adopted in this study to determine the costs for binder specific AC mixtures. Table 28 shows the typical calculations involved while estimating binder-specific mixture costs for Type C dense-graded asphalt-aggregate mixtures.

Table 28. Costs for Binder-Specific Dense-Graded Type C AC Mixtures.

Cost of Dense-Graded Asphalt Concrete Mixture					
Items Description	Unit	Value	Measurement	Comment	
Cost of Asphalt Concrete Pavement from FPS (Assumed typical dense graded mix with PG64-22 binder)	\$	115.00	Per CY	(CY = Cubic yd.)	
Computation of Mixture Cost Per Ton					
Unit weight of Mixture (assumed)	lb-ft ³	145.00			
Mixture volume in cubic feet for each CY volume	cft	27.00			
Mix Weight in pounds and Tons	lb.	3915.00			
	Ton	1.96			
Unit Cost = (115/1.96) =	\$	58.75	Per Ton		
Calculation of Aggregate and Binder Cost Partial for the Reference Prices					
Tentative cost					
Cost of PG 64-22 binder	\$	584.00	Per Ton		
Cost of Aggregate (any gradation)	\$	12.00	Per Ton		
Partial cost of binder (x) per ton of mix = 0.05 x 584 = (Assumed 5% by weight binder in the mixture)	\$	29.20	Per Ton of Mix		
Partial cost of aggregate (y) per ton of mix = 0.95 x 12 =	\$	11.40	Per Ton of Mix		
Total cost for the PG 64-22 Mix = 29.20 + 11.40	\$	40.60	Per Ton		
Calculation of Aggregate and Binder Cost Partial for the dense-graded AC mixture with PG64-22 binder					
Ratio Old:	$X_{ref}/Y_{ref} = 29.20/11.40 =$		2.56	Times	
New:	$X_{actual}/Y_{actual} = 115/1.96 =$	\$	58.75	Per Ton	
Partial cost of binder (x) = (58.75 - 16.50) =	\$	42.25	Per Ton of Mix		
Unit cost fraction of Aggregate (y) = 58.75/(1+2.56) =	\$	16.50	Per Ton of Mix		
Total cost for the PG64-22 Mix (check) = 42.25+16.5 =	\$	58.75	Per Ton		
Calculations of Costs for the Binder Specific Dense Graded Mixtures					
Reference Binder Prices					
Binder PG 64-22	\$	584.00	Per Ton		
Binder PG 70-22	\$	688.00	Per Ton		
Binder PG 76-22	\$	736.00	Per Ton		
New Binder Prices (By Rational Approach)					
Binder PG 64-22 = 42.25/0.05 =	\$	845.00	Per Ton		
Binder PG 70-22 = (688/584)*845 =	\$	995.48	Per Ton		
Binder PG 76-22 = (736/688)*995.48 =	\$	1064.93	Per Ton		
PG 64-28 (assumed 10% increase from 64-22)	\$	929.50	Per Ton		
PG 70-28 (assumed 10% increase from 70-22)	\$	1095.03	Per Ton		
Priced Per Ton of Mix					
Aggregate Price	\$	16.50	Per Ton of Mix		
Mix with PG 64-22 Binder = (845.00*0.05)+16.50 =	\$	58.75	Per Ton		
Mix with PG 70-22 Binder = (995.48*0.05)+16.50 =	\$	66.27	Per Ton		
Mix with PG 76-22 Binder = (1064.93*0.05)+16.50 =	\$	69.75	Per Ton		
Mix with PG 64-28 Binder = (929.50*0.05)+16.50 =	\$	62.98	Per Ton		
Mix with PG 70-28 Binder = (1095.03*0.05)+16.50 =	\$	71.25	Per Ton		
Unit Volume (CY) Prices of Asphalt Concrete Mixtures					
Mix with PG 64-22 Binder	\$	115.00	Per CY		
Mix with PG 70-22 Binder	\$	129.73	Per CY		
Mix with PG 76-22 Binder	\$	136.53	Per CY		
Mix with PG 64-28 Binder	\$	123.27	Per CY		
Mix with PG 70-28 Binder	\$	139.47	Per CY		

Similar approaches were employed to calculate the initial construction cost of other AC mixtures. Table 29 summarizes default initial costs for the AC mixtures incorporated in the TxME.

Table 29. TxME Default Initial Construction Cost of AC Mixtures.

PG	Mix Type	Cost (\$/Cubic Yard)
64-22	Type B	105.00
70-22	Type B	118.45
76-22	Type B	124.66
64-28	Type B	112.55
70-28	Type B	127.34
64-22	Type C	115.00
70-22	Type C	129.73
76-22	Type C	136.53
64-28	Type C	123.27
70-28	Type C	139.47
64-22	Type D	125.00
70-22	Type D	141.01
76-22	Type D	148.40
64-28	Type D	133.99
70-28	Type D	151.60
64-22	Superpave B	115.00
70-22	Superpave B	129.73
76-22	Superpave B	136.53
64-28	Superpave B	123.27
70-28	Superpave B	139.47
64-22	Superpave C	125.00
70-22	Superpave C	141.01
76-22	Superpave C	148.40
64-28	Superpave C	133.99
70-28	Superpave C	151.60
64-22	Superpave D	135.00
70-22	Superpave D	152.29
76-22	Superpave D	160.27
64-28	Superpave D	144.71
70-28	Superpave D	163.73
76-22	SMA-C	130.00
76-22	SMA-D	140.00
76-22	SMA-F	150.00
70-28	SMA-C	132.97
70-28	SMA-D	143.21
70-28	SMA-F	153.44
64-22	RBL	138

INITIAL CONSTRUCTION COSTS OF AC MIXTURES WITH RAP/RAS

The inclusion of RAP/RAS in AC mixtures saves money in terms of material costs compared to the virgin mixtures. There are two basic types of savings by using RAP/RAS: recycled material saving and binder substitution saving. When determining the initial construction cost of AC mixture with RAP/RAS, these two savings needs to be calculated to estimate the total savings and the final cost. Table 30 listed the cost factors of the AC mixture with different percentage of RAP/RAS. Note that the cost factor is the ratio of cost of AC mixture with RAP/RAS over the cost of virgin AC mixture (no RAP/RAS).

Table 30. Cost Factors for Various AC Mixtures with Recycled Materials.

Virgin Mix %	RAP%	RAS%	Cost Factor (Normalized Cost)
100.00	0.00	0.00	1.00
95.00	5.00	0.00	0.97
90.00	10.00	0.00	0.95
85.00	15.00	0.00	0.92
80.00	20.00	0.00	0.90
75.00	25.00	0.00	0.87
70.00	30.00	0.00	0.84
65.00	35.00	0.00	0.82
99.00	0.00	1.00	0.97
94.00	5.00	1.00	0.95
89.00	10.00	1.00	0.92
84.00	15.00	1.00	0.89
79.00	20.00	1.00	0.87
74.00	25.00	1.00	0.84
69.00	30.00	1.00	0.82
64.00	35.00	1.00	0.79
98.00	0.00	2.00	0.95
93.00	5.00	2.00	0.92
88.00	10.00	2.00	0.89
83.00	15.00	2.00	0.87
78.00	20.00	2.00	0.84
73.00	25.00	2.00	0.82
68.00	30.00	2.00	0.79
63.00	35.00	2.00	0.76
97.00	0.00	3.00	0.92
92.00	5.00	3.00	0.89
87.00	10.00	3.00	0.87
82.00	15.00	3.00	0.84
77.00	20.00	3.00	0.81
72.00	25.00	3.00	0.79
67.00	30.00	3.00	0.76
62.00	35.00	3.00	0.74
96.00	0.00	4.00	0.89
91.00	5.00	4.00	0.87
86.00	10.00	4.00	0.84
81.00	15.00	4.00	0.81
76.00	20.00	4.00	0.79
71.00	25.00	4.00	0.76
66.00	30.00	4.00	0.74
61.00	35.00	4.00	0.71
95.00	0.00	5.00	0.87
90.00	5.00	5.00	0.84
85.00	10.00	5.00	0.81
80.00	15.00	5.00	0.79
75.00	20.00	5.00	0.76
70.00	25.00	5.00	0.74
65.00	30.00	5.00	0.71
60.00	35.00	5.00	0.68

According to Table 30, a sigmoid function was proposed to estimate the cost of an AC mixture with given RAP/RAS contents, as follows:

$$C_{RS} = C_v * CF = C_v * \left[a_1 + \frac{a_2}{1 + e^{a_3 + a_4 P_{RAS} + a_5 P_{RAP}}} \right] \quad (5-1)$$

where

C_{RS}	= Cost of RAP/RAS included AC mixture.
C_v	= Cost of virgin mixture.
CF	= Cost Factor.
P_{RAP}	= Percentage of RAP in the AC mixture.
P_{RAS}	= Percentage of RAS in the AC mixture.
$a_1, a_2 \dots$	= Regression coefficients, where
a_1	= -1.741228.
a_2	= 4.685146.
a_3	= -0.341911.
a_4	= 0.022901.
a_5	= 0.004500.

Figure 43 shows the comparison between cost factors estimated from Equation 5-1 (predicted CF) and the cost factors from the Table 30 (actual CF). All the data points are found on the line of equality, confirming the cost model gives a very good estimation of adjusted cost for RAP/RAS included mixtures.

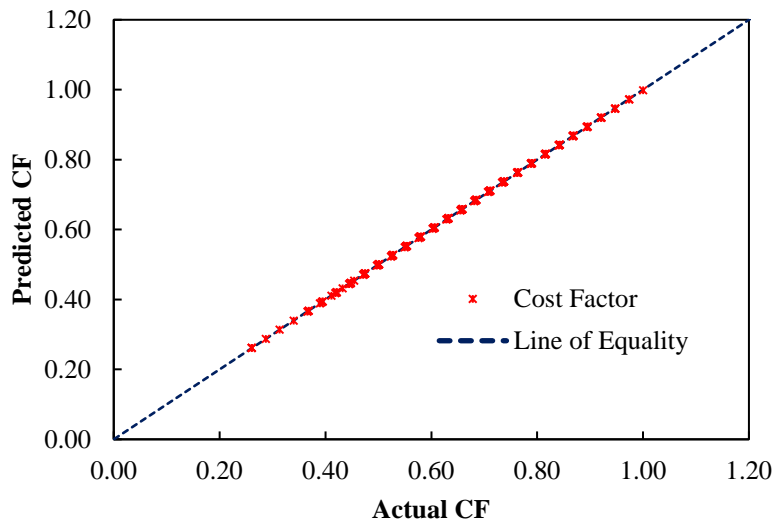


Figure 43. Comparison between the Actual CF and Predicted CF.

COST OF OTHER LAYER MATERIALS

A total of six types of base layer materials three types subbase/subgrade material were found in both TxME and the FPS system. To be consistent, these costs from FPS system were adopted in the TxME pavement design system too. Table 31 lists these layer material costs.

Table 31. Costs of Base/Subbase/Subgrade Layer Materials

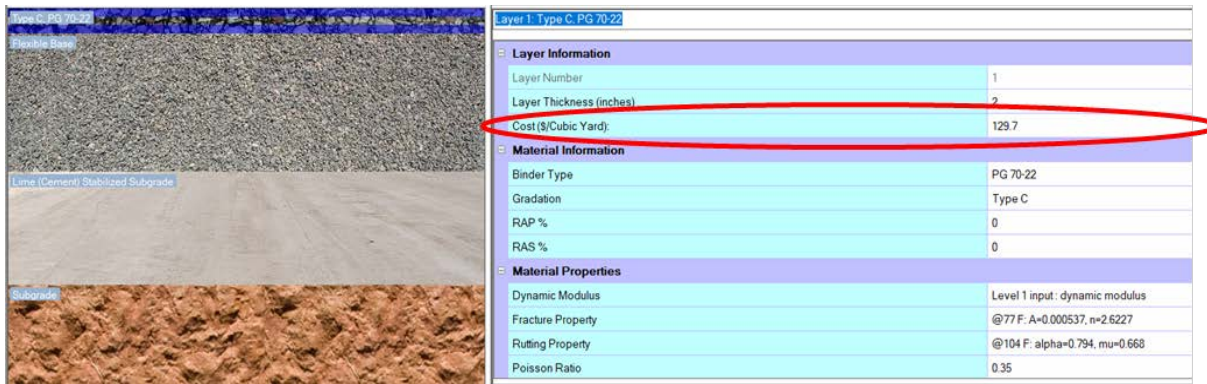
Item	Cost (\$/Cubic Yard)
FA or LFA Stabilized Base	42.00
Asphalt Treated Base	80.00
Emulsion Asphalt Treated Base	45.00
FB	37.00
Lime Stabilized Base	42.00
Cement Stabilized Base	45.00
Lime (Cement) Stabilized Subgrade	15.00
Emulsion Asphalt Treated Subgrade	18.00
Shallow Subgrade	2.00

INCORPORATE INITIAL CONSTRUCTION COST INTO TXME

Figure 44 shows the TxME Initial Construction Cost analysis input and output screens. In Figure 44a, when users select different binder type, gradation type, or input different RAP/RAS contents, the number in the cost (\$/cubic yard) input box will change accordingly. This number is determined based on the Table 29 and Equation 5-1. Users can also input a specific number if they have a more accurate cost estimation for a given mixture. Figure 44b shows the initial construction cost analysis result in the Excel spreadsheet format. In this spreadsheet, the initial construction cost of each layer is tabulated (in the unit of \$/Cubic Yard), and the final pavement initial construction cost (in the unit of \$/Square Yard) is determined based on the following calculation:

$$\text{Total Initial Construction Cost (\$Y)} = \Sigma [\text{Layer Material Initial Construction Cost (\$/CY)} * \text{Layer Thickness (Yard)}].$$

The AC layer(s) initial construction cost (\$SY) was also determined and provided in the spreadsheet for comparison among different AC mixture types.



(a)

	A	B	C	D	E	F	G	H
1								
2			AC Layer(s) Intital Construction Cost (\$/SY):	7.21				
3			Total Intital Construction Cost (\$/SY):	22.26				
4								
5								
6								
7			Pavement Layer	Thickness (in.)		Material		Cost (\$/CY)
8			Layer1--AC Layer	2		Type C, PG 70-22, 0.0% RAP, 0.0% RAS		129.7
9			Layer2--Base Layer	11		FlexibleBase		37
10			Layer3--Subbase Layer	9		LSS		15
11			Layer4--Subgrade	--		--		--
12								
13								
14								
15								
--								

(b)

Figure 44. TxME Initial Construction Cost Analysis (a) Input and (b) Output.

CHAPTER 6. TXME PERFORMANCE MODEL CALIBRATION

In this study, the Texas Flexible Pavement Database were used to calibrate the TxME performance models. After thorough investigation, researchers found that although the flexible pavement database has many test sections, most of them are asphalt overlay sections. For some newly constructed flexible pavements, the material properties and observed field performance data in the database are abnormal; and some test sections do not have complete data required for TxME model calibration. Researchers reported the findings to the database team. Thus, only the test sections that have reasonable performance data were identified for this calibration purpose. When determining calibration factors (CFs) for performance models, researchers consider two scenarios:

- Performance prediction with TxME embedded default materials properties.
- Performance prediction with laboratory measured materials properties.

Only one set of CFs for each performance model should be developed and such CF should apply for both scenarios. Otherwise, the TxME system will become very complex and may potentially make users confused. Based on the identified test sections, available material properties, and performance data in the database, the rutting model and fatigue cracking model were calibrated in this study. A detailed calibration process is presented in the following sections.

CALIBRATION OF BASE/SUBGRADE RUTTING MODEL

Rutting in surface treatment pavements is mainly from the base and subgrade. Thus, surface pavements provide a perfect situation for calibrating the rutting models for base and subgrade. Table 32 lists all the available surface treated sections in the flexible pavement database for which monthly rut measurements exist in the database. However, sections UTEP-11 and UTEP-12 were excluded from model calibration because of abnormal rutting development. Sections TTI-27 and TTI-59 are on the same road but with different traffic, which is true for sections TTI-30 and TTI-50 and for sections TTI-35 and TTI-52. Regarding sections TTI-27 and TTI-59, excessive rut depth was observed within 16 months. This indicated that the rutting development is abnormal and may be caused by improper construction process. Therefore, these two sections were excluded from calibrating rutting model.

Table 32. Surface Treated Sections with Measured Rut Performance Data.

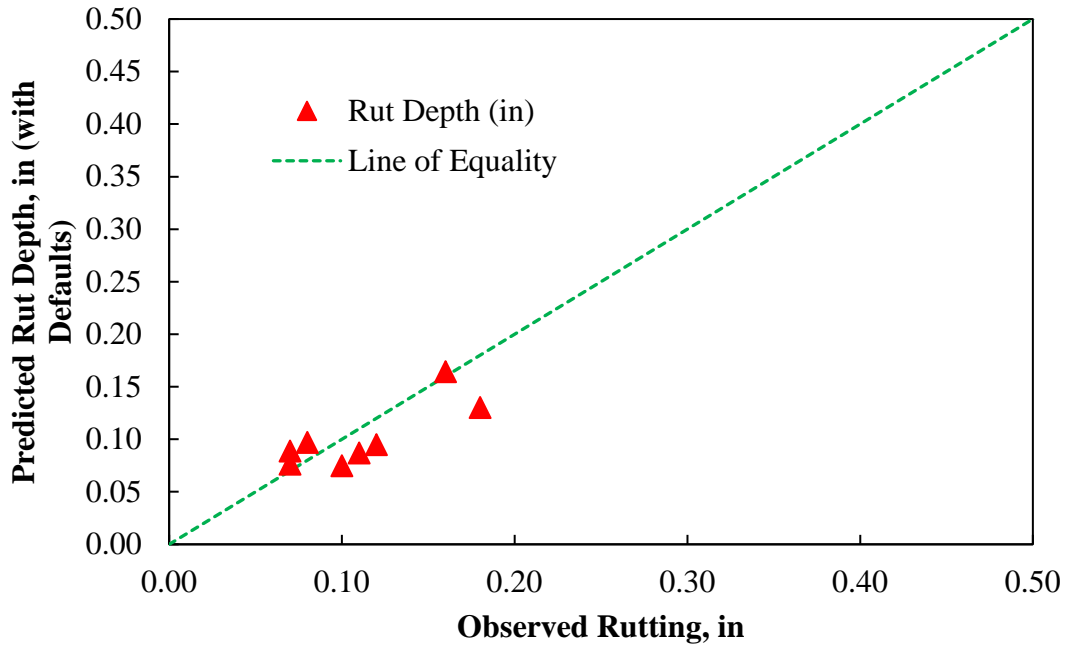
Section	Month	Observed rut depth, in.	Predicted Rut Depth with TxME Defaults, in.	Predicted Rut Depth with Database, in.
TxDOT_TTI-00027 (Surface Treated)	5	0.16	0.102669801	0.435247413
	16	0.34	0.128603415	0.633624185
	29	0.32	0.144676334	0.770791031
	45	0.33	0.157794603	0.891530035
	54	0.41	0.164211806	0.950379852
	56	0.35	0.16520697	0.960866865
TxDOT_TTI-00030 (Surface Treated)	38	0.16	0.164376317	0.275297611
TxDOT_TTI-00035 (Surface Treated)	12	0.07	0.076451449	0.796507654
	24	0.07	0.088720213	0.94773587
	36	0.08	0.096920595	1.050493814
TxDOT_TTI-00050 (Surface Treated)	38	0.18	0.130377922	0.22106714
TxDOT_TTI-00052 (Surface Treated)	12	0.10	0.074954008	0.786145763
	24	0.11	0.086965862	0.935458418
	36	0.12	0.094992591	1.036917725
TxDOT_TTI-00059 (Surface Treated)	29	0.38	0.123548398	0.587184023
	45	0.39	0.134905532	0.679137829
	54	0.48	0.140309611	0.723945141
	56	0.45	0.141215037	0.731935754
TxDOT_UTEP-00011 (Surface Treated)	48	0.18	0.013183067	0.025064539
	59	0.11	0.013776079	0.026965565
	65	0.17	0.014068643	0.028000366
	72	0.13	0.014345929	0.028652464
TxDOT_UTEP-00012 (Surface Treated)	34	0.19	0.021561744	0.017010661
	39	0.13	0.022047751	0.017154562
	43	0.13	0.022566809	0.018209606
	50	0.18	0.023236573	0.018586052
	61	0.13	0.024251887	0.019810385
	67	0.07	0.024749723	0.02063529
	74	0.08	0.025239975	0.02091898

Table 33 summarizes the values of laboratory measured rut parameters for the surface treated sections. Observing the values in this table, one can recognize that section TTI-35/52 has an unusual value of α and μ . Also, no information was found for the subgrade rut parameters. Again, in the case of sections TTI-27/59, unusual values of rut parameters for the base and subgrade layers can be observed. To overcome these data limitations, test sections TTI-27/59 were excluded for TxME calibration, and test sections TTI-35 and TTI-52 were modeled in TxME by using the TxME embedded default rut parameter values for the base and subgrade layers. The analysis results were then used for calibration purposes.

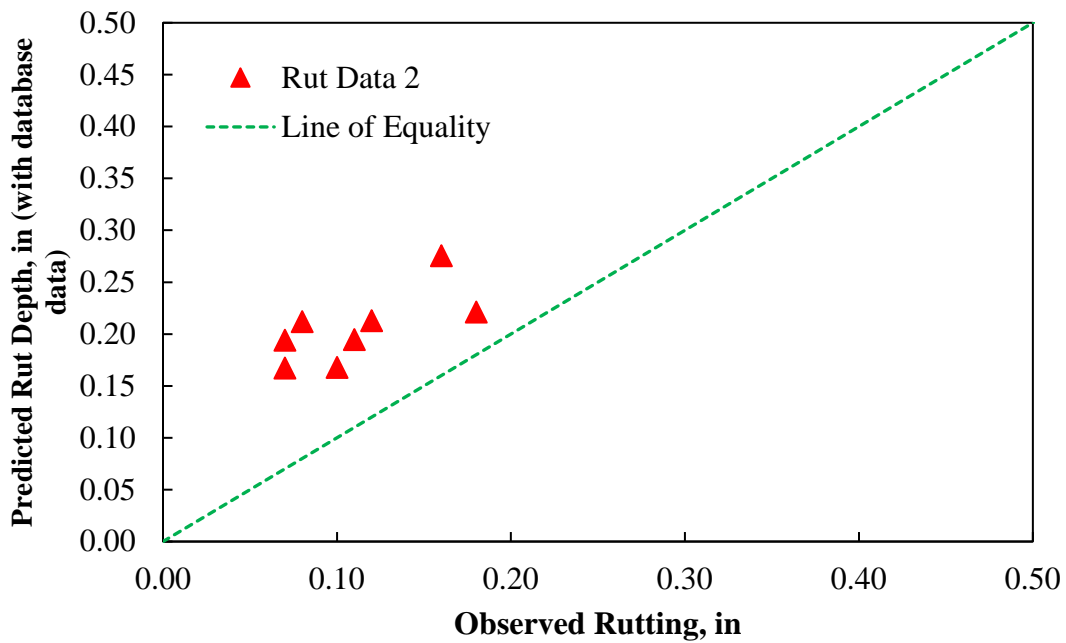
Table 33. Tests Sections and Their Rut Parameters from TxDOT Database.

Sections	Layer	α	μ	Comment
TTI-35/TTI-52	Base	0.82	0.42	Unusual values of α and μ for base layer; No information about subgrade rut parameters.
	Subgrade	No info	No info	
TTI-27/TTI-59	Base	0.73	0.16	Unusual values of α and μ for subgrade layer.
	Subgrade	0.96	0.01	
TTI-30/TTI-50	Base	0.88	0.08	Reasonable α and μ values for this section.
	Subgrade	0.81	0.07	

Figure 45a shows the observed versus TxME predicted rut depths when TxME default parameters were used for the selected test sections. Also, Figure 45b shows the observed versus TxME predicted rut depths when database parameters were used. In both plots, the data points can be found more or less around the line of equality. In case of Figure 45b, a slightly higher rut depth prediction can be observed and can be seen as a conservative measure. With the current data available, researchers decided to use 1.0 as the CF for base and subgrade rutting models.



(a)



(b)

Figure 45. Observed versus TxME Predicted Rut Depths for Surface Treated Pavement Sections when (a) TxME Defaults Are Used and (b) Database Parameters Are Used.

CALIBRATION OF ASPHALT LAYER RUTTING MODEL

Since the base and subgrade rutting models are calibrated separately above, the calibration here focuses on asphalt layer rutting model. A thorough search in the database was conducted and the 15 tests sections were found to have monthly performance measurement data (i.e., monthly rutting measurement). Performance measurement data of these test sections were further evaluated for any obsolete or irregular data. Only those with justifiable values were selected for calibration purposes. All 15 test sections were modeled with TxME, considering two scenarios. The first one in which TxME defaults were considered for the material property inputs, whereas, in the second scenario, the laboratory measured material parameters listed in the flexible pavement database were used. Table 34 summarizes the observed and predicted rut depths for the months in which rut performance measurements of the associated test section were conducted. For some of the sections listed in Table 34, the rut parameters (μ and α) for asphalt and base layers from the database were absent or abnormal. In those cases, the default values of the rutting parameters in the TxME were considered to be the most representative parameter values, and so used while predicting rutting developments based on the TxDOT database.

Table 34. Test Sections Considered for TxME Rutting Calibration.

Section ID	Month (n)	Observed rut depth, (in.)	Rut Depth Predicted with TxME Defaults (in.)	Rut Depth Predicted with Database Parameters (in.)
TxDOT_TTI-00004	5	0.02	0.01	0.01
TxDOT_TTI-00004	26	0.04	0.014913619	0.019898277
TxDOT_TTI-00004	40	0.04	0.016551454	0.022167828
TxDOT_TTI-00005	60	0.01	0.040807281	0.063680345
TxDOT_TTI-00008	20	0.06	0.024828322	0.026201418
TxDOT_TTI-00008	31	0.17	0.029644307	0.032390894
TxDOT_TTI-00015	13	0.05	0.02943475	0.021395609
TxDOT_TTI-00015	29	0.09	0.03451617	0.025642007
TxDOT_TTI-00015	43	0.04	0.037913947	0.028401155
TxDOT_TTI-00015	55	0.07	0.040619067	0.030641267
TxDOT_TTI-00017	12	0.05	0.014569647	0.01934757
TxDOT_TTI-00017	25	0.06	0.017344753	0.022739419
TxDOT_TTI-00017	37	0.07	0.019196398	0.024929373
TxDOT_TTI-00028	6	0.02	0.009622824	0.00944418
TxDOT_TTI-00028	12	0.02	0.042818014	0.03554088
TxDOT_TTI-00028	21	0.03	0.044457387	0.036990311
TxDOT_TTI-00046	5	0.02	0.005691339	0.007853993
TxDOT_TTI-00046	26	0.01	0.01534726	0.025208008
TxDOT_TTI-00046	40	0.03	0.017036742	0.027852045
TxDOT_TTI-00048	12	0.01	0.042702255	0.08282029
TxDOT_TTI-00048	21	0.02	0.044221015	0.089176741
TxDOT_TTI-00051	7	0.03	0.012446321	0.023746526
TxDOT_TTI-00057	12	0.03	0.019333389	0.022158951
TxDOT_TTI-00057	25	0.05	0.02312062	0.02611358
TxDOT_TTI-00057	37	0.06	0.02565312	0.028681507
TxDOT_TTI-00065	9	0.00	0.028269337	0.05180025
TxDOT_TTI-00065	24	0.02	0.035106448	0.061428203
TxDOT_TTI-00065	50	0.02	0.044114787	0.074156175
TxDOT_TTI-00065	59	0.02	0.045460969	0.075992129
TxDOT_TTI-00071	7	0.03	0.011934327	0.022896545
TxDOT_TTI-00071	18	0.06	0.024929276	0.030664639
TxDOT_TTI-00071	31	0.06	0.029442701	0.034832654
TxDOT_UTEF-00005	65	0.03	0.079593409	0.035465974
TxDOT_UTEF-00005	72	0.04	0.081725311	0.036165817
TxDOT_UTEF-00006	78	0.14	0.112765812	0.074757732
TxDOT_UTEF-00008	61	0.18	0.200781074	0.302735483
TxDOT_UTEF-00008	67	0.17	0.209523273	0.318394656
TxDOT_UTEF-00008	74	0.21	0.212892771	0.323930323

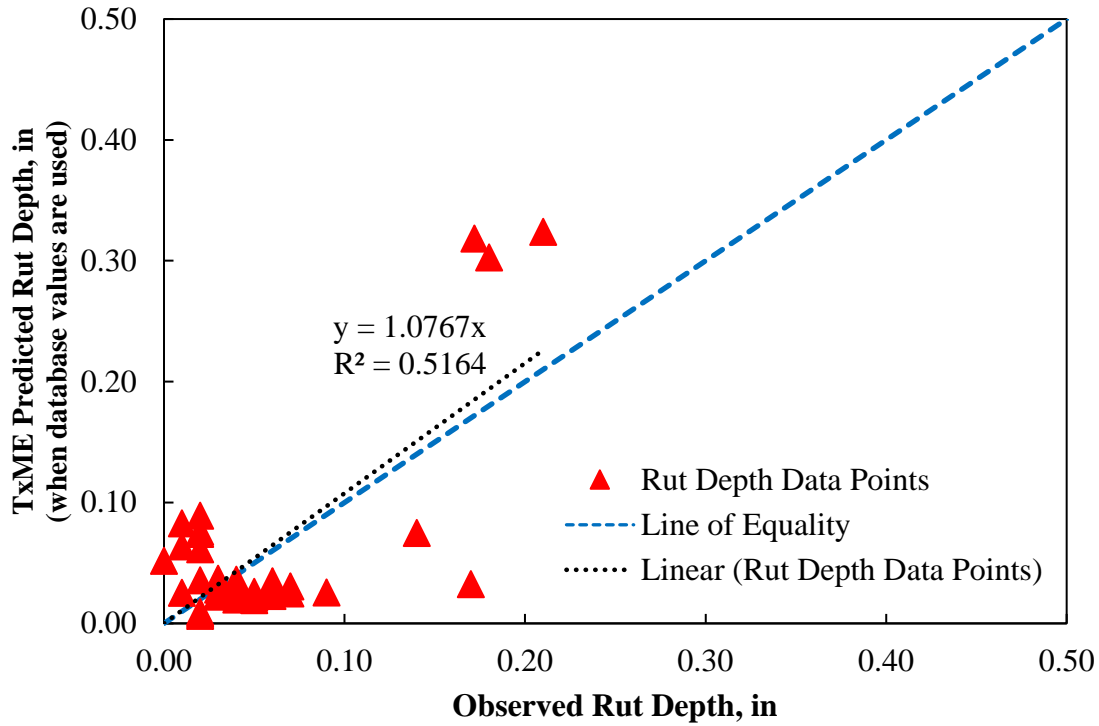
Figure 46a shows the observed versus TxME predicted rut depths when the laboratory measured material properties were used. It is very difficult to measure smaller rut depths in the field (i.e., rut depths smaller than 0.1 inch). Therefore, the observed rut depths in Figure 46 should be considered as best measurement as it could be possible. Then again, in Figure 46a, the predicted values are pretty close to the observed values after considering the difficulty in measuring rut depths less than 0.1 inch. A best fitted line can be drawn through these rut depth data points, which confirms a slightly higher rut depth prediction by TxME at the higher rut depth region.

Figure 46b shows the observed versus TxME predicted rut depths when the default material properties were used. In Figure 46b, the predicted values are very close to the observed values. A best fitted line confirms a slightly lower rut depth prediction by TxME at the higher rut depth region.

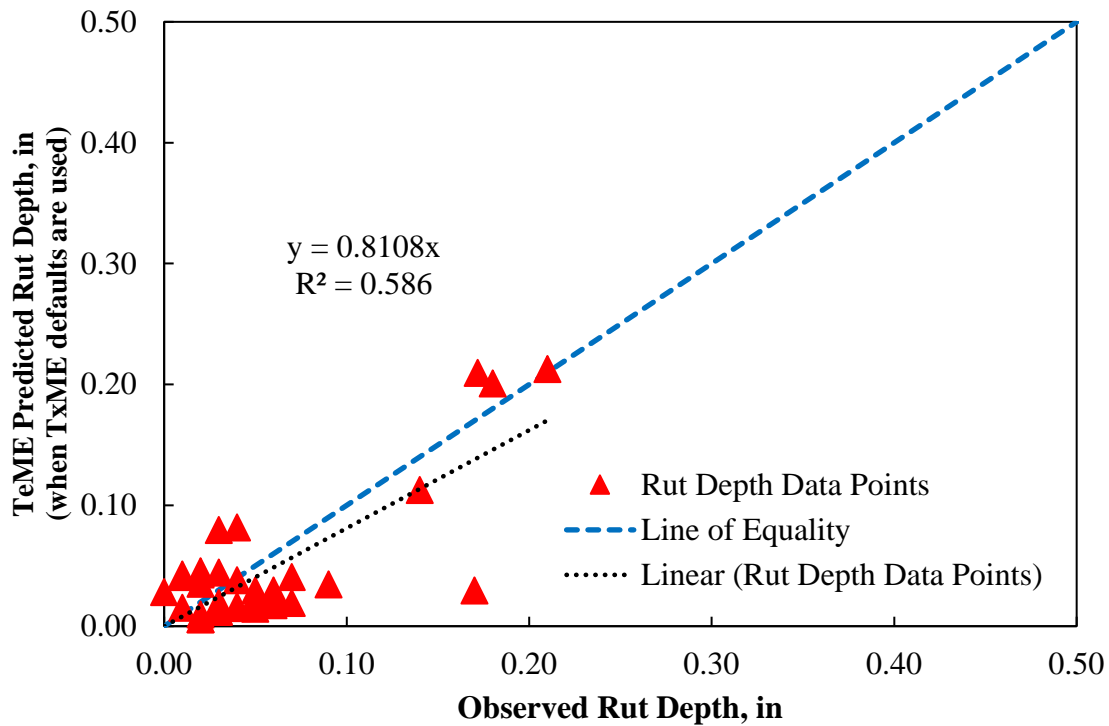
As discussed previously, a single CF is preferred to represent both default values and laboratory measured material properties. It means that the single CF should be able to provide the smallest difference between the TxME predicted and the field observed rut depths, whether the rutting is predicted using default material properties or laboratory measured material properties.

In Figure 46a, a CF value reciprocal to the slope of the line (i.e., $CF = 1/1.0767 = 0.9288$) can give the minimum difference in TxME predicted and observed rut depths. Similarly, in Figure 46b, a CF value reciprocal to the slope of the line (i.e., $CF = 1/0.8108 = 1.2346$) can give the minimum difference in TxME predicted and observed rut depths. A fair justification is to use the average of these two factors as the final CF. This will give the minimum difference between TxME predicted and observed rut depths considering both the TxME input scenarios. Therefore, the final CF is calculated as follows:

$$CF = \frac{0.9288+1.2346}{2} = 1.0817. \quad (6-1)$$



(a)



(b)

Figure 46. Observed versus TxME Predicted Rut Depths when (a) Database Material Parameter Values Used and (b) TxME Default Material Parameter Values Used.

Figure 47 shows the predicted versus observed rut depth plots when the CF in Equation 6-1 is multiplied with the TxME predicted rut depths from the two scenarios. More or less, all the data points are around the line of equality, which confirms that observed rut depths and the predicted rut depths by the TxME system are in good agreement.

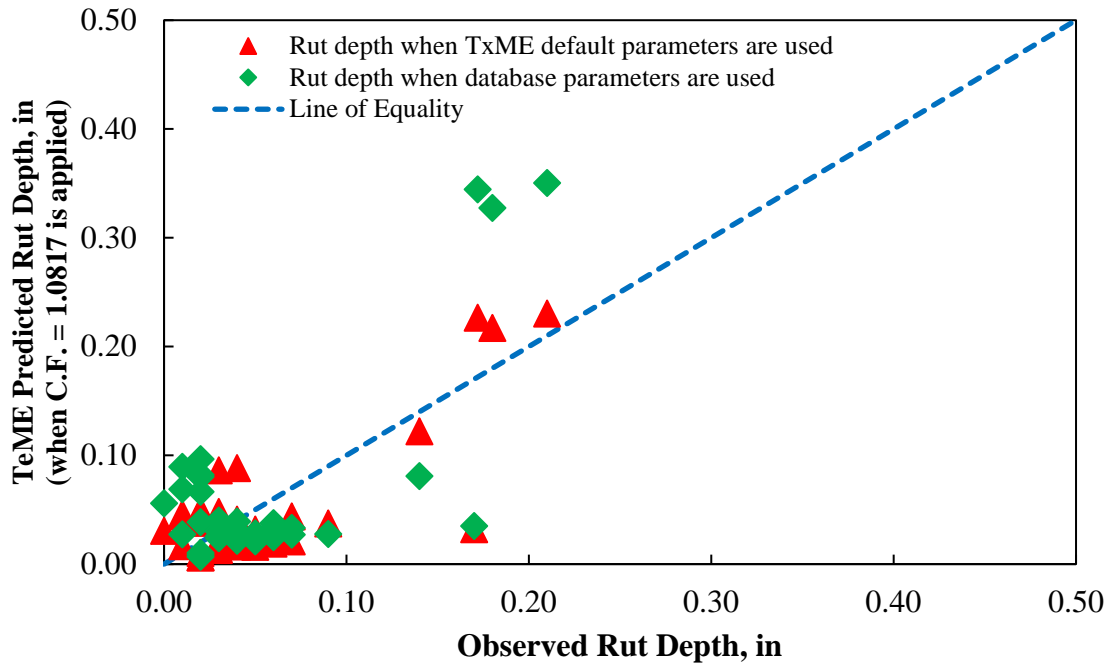


Figure 47. Observed versus TxME Predicted Rut Depths.

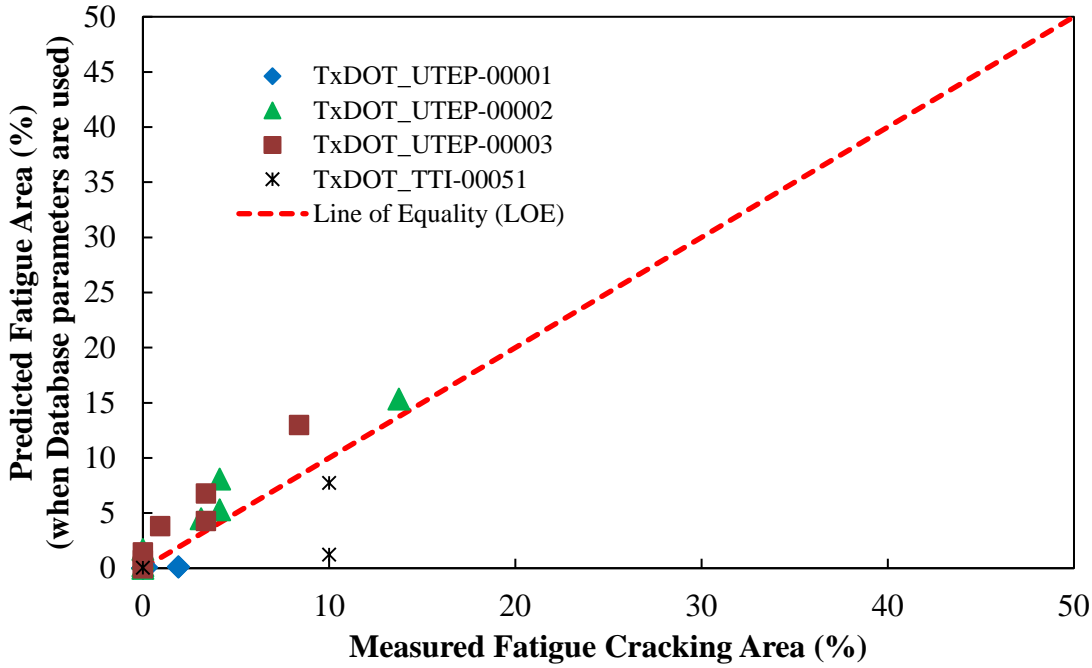
CALIBRATION OF FATIGUE CRACKING MODEL

The test sections in the flexible pavement database are selected on regular TxDOT roads and they are not intended to have fatigue cracking within a short period of time. Thus, most of the test sections with performance data show zero fatigue cracking area. This is a good thing, but it makes the model calibration become very challenging because the accuracy of the fatigue cracking model cannot be judged without actual fatigue data to check with. Out of the 15 sections, only four sections showed fatigue cracking. These sections are UTEP-1, UTEP-2, UTEP-3, and TTI-51. Table 35 lists the TxME model outputs for these four sections with the observed fatigue cracking values.

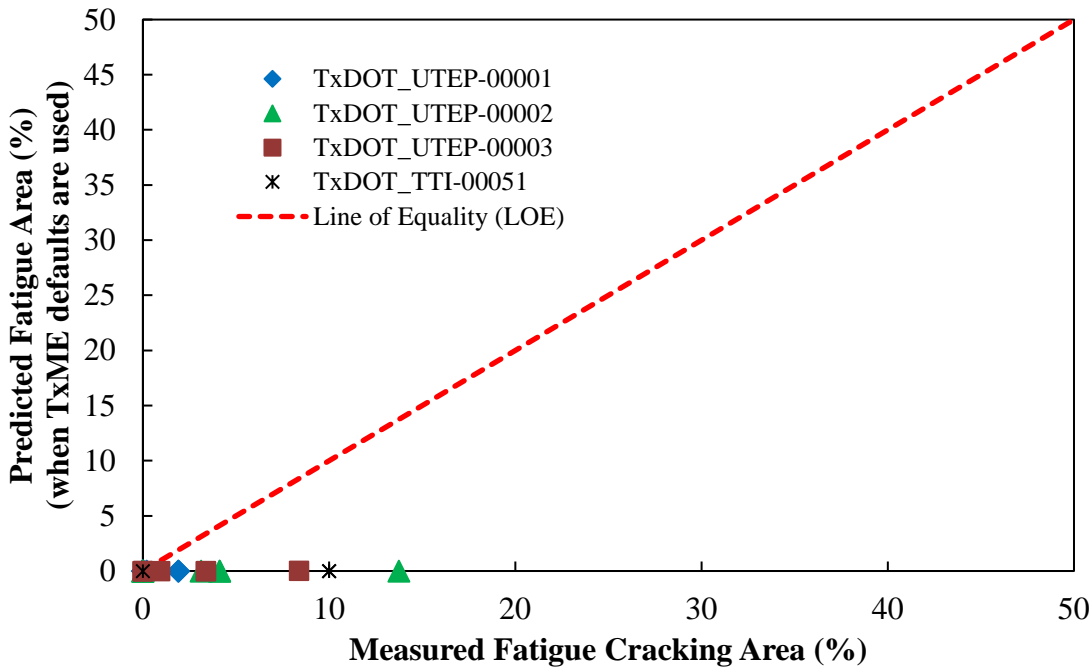
Table 35. Tests Sections and Their Fatigue Performance Data.

Sections	Month (N)	Observed AC Fatigue Cracking Area (%)	Predicted AC Fatigue Cracking Area with TxME Default Parameters (%)	Predicted AC Fatigue Cracking Area with Database Parameters (%)
TxDOT_UTEP-00001	0.0000	0.0000	0.0000	0.0000
	8.0000	0.0000	0.0000	0.0002
	18.0000	0.0000	0.0000	0.0033
	27.0000	0.0000	0.0000	0.0140
	33.0000	0.0000	0.0000	0.0294
	43.0000	0.2000	0.0000	0.0729
	47.0000	1.9000	0.0000	0.1019
	52.0000	1.9000	0.0000	0.1439
TxDOT_UTEP-00002	0.0000	0.0000	0.0000	0.0000
	17.0000	0.0000	0.0000	0.2192
	27.0000	0.0000	0.0000	0.8854
	32.0000	0.0000	0.0001	1.6861
	43.0000	3.1300	0.0002	4.4854
	47.0000	4.1300	0.0002	5.2854
	52.0000	4.1300	0.0004	8.0778
	64.0000	13.7500	0.0009	15.3413
TxDOT_UTEP-00003	0.0000	0.0000	0.0000	0.0000
	17.0000	0.0000	0.0003	0.2024
	27.0000	0.0000	0.0011	0.7402
	32.0000	0.0000	0.0021	1.4367
	43.0000	0.9200	0.0058	3.8051
	47.0000	3.3800	0.0062	4.2741
	52.0000	3.3800	0.0105	6.7834
	64.0000	8.3800	0.0213	12.9734
TxDOT_TTI-00051	7.0000	0.0000	0.0000	0.0414
	18.0000	10.0000	0.0002	1.2296
	31.0000	10.0000	0.0016	7.7402

Figure 48a shows the observed versus TxME predicted fatigue cracking when laboratory measured material properties were used. The data points are found to be very near to the line of equality. This confirms that $CF = 1$ can be considered for fatigue cracking model. However, Figure 48b shows the observed versus TxME predicted fatigue cracking area when TxME default material parameters were used. Almost all the cases, the predicted fatigue cracking area is zero. The reason is that the default value for a certain mixture is a typical or average value, but the property values of actual used material can be very different from these typical values. For example, some material used in the test section might not be a typical material especially when some special RAP/RAS is included. Considering this point of view, the results in Figure 48b are not surprising when TxME default parameters were used.



(a)



(b)

Figure 48. Observed versus TxME Predicted Fatigue Cracking Area when (a) Database Material Parameters Are Used and (b) TxME Default Parameters Are Used.

Figure 49 shows the simulation results of all three UTEP sections while using the database parameters. The figure also incorporates the observed monthly fatigue cracking area for the test sections. The observed and predicted fatigue cracking are very close to each other. This means the $CF = 1$ for fatigue cracking model is adequate enough for TxME.

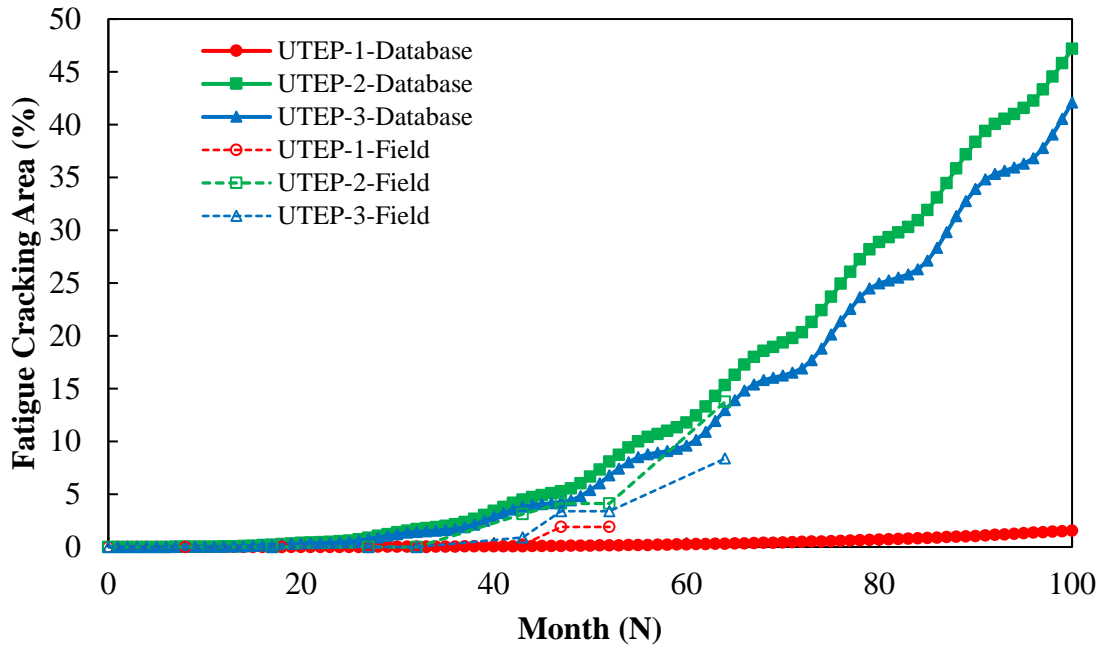


Figure 49. TxME Simulation Results and the Observed Fatigue Cracking Area for UTEP-1, UTEP-2, and UTEP-3 Test Sections.

CHAPTER 7. DEMONSTRATION AND VERIFICATION OF TXME WITH INDEPENDENT FIELD TEST SECTIONS

In total, 11 test sections in six different districts were identified in this study. Researchers visited each test section several times to document the existing pavement condition, sampled the layer material during construction, and conducted the field performance survey. Extensive lab tests were also conducted to characterize pavement layer material properties. For each test section, the pavement structure, the layer material property, and the field performance information were collected and processed. With this information, researchers used the enhanced and calibrated TxME software to conduct field performance prediction and compare the predicted result with the field survey result. This chapter describes the following steps taken:

- Identify projects/test sections already let and soon to be constructed.
- Visit each project to document existing conditions and conduct a field performance survey.
- Assemble samples of the asphalt mixes, bases, and subgrade soils, and run lab test of these samples to determine input parameters for TxME.
- Assemble traffic information for each test sections.
- Use TxME to simulate the test sections and to predict the performance.
- Compare the TxME predicted performance with the field performance and draw conclusions.

IDENTIFY PROJECTS AND TEST SECTIONS

The test sections in six districts were identified with the help of the former project advisor Joe Leidy and other TxDOT district engineers. Figure 50 shows their corresponding project locations.

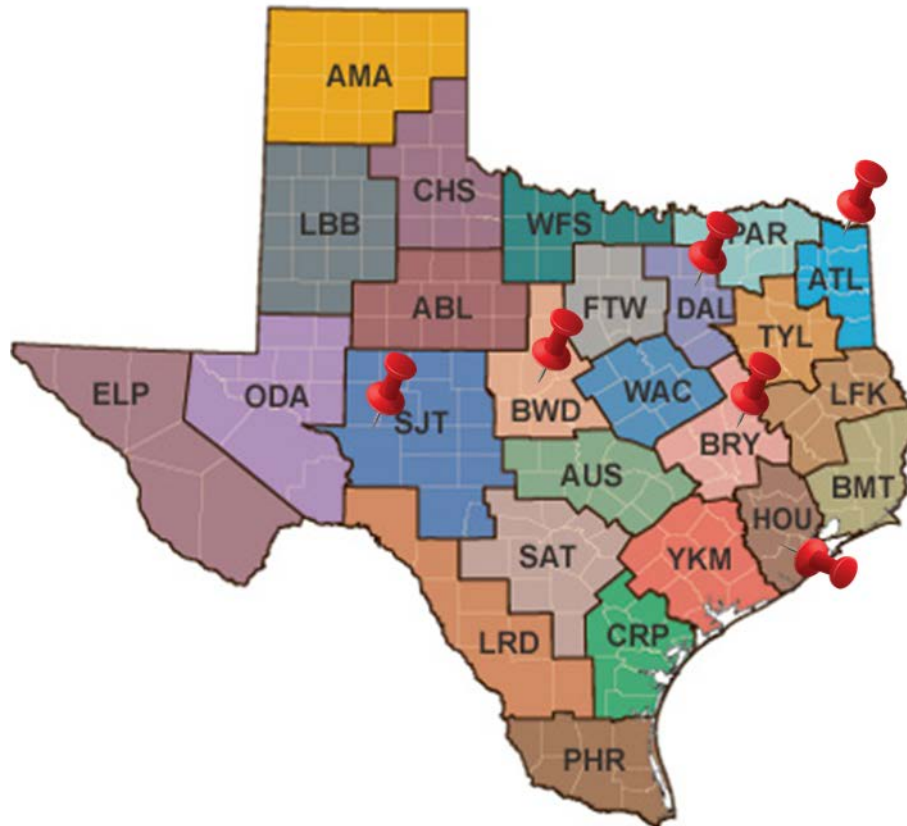


Figure 50. Projects and Test Section Location.

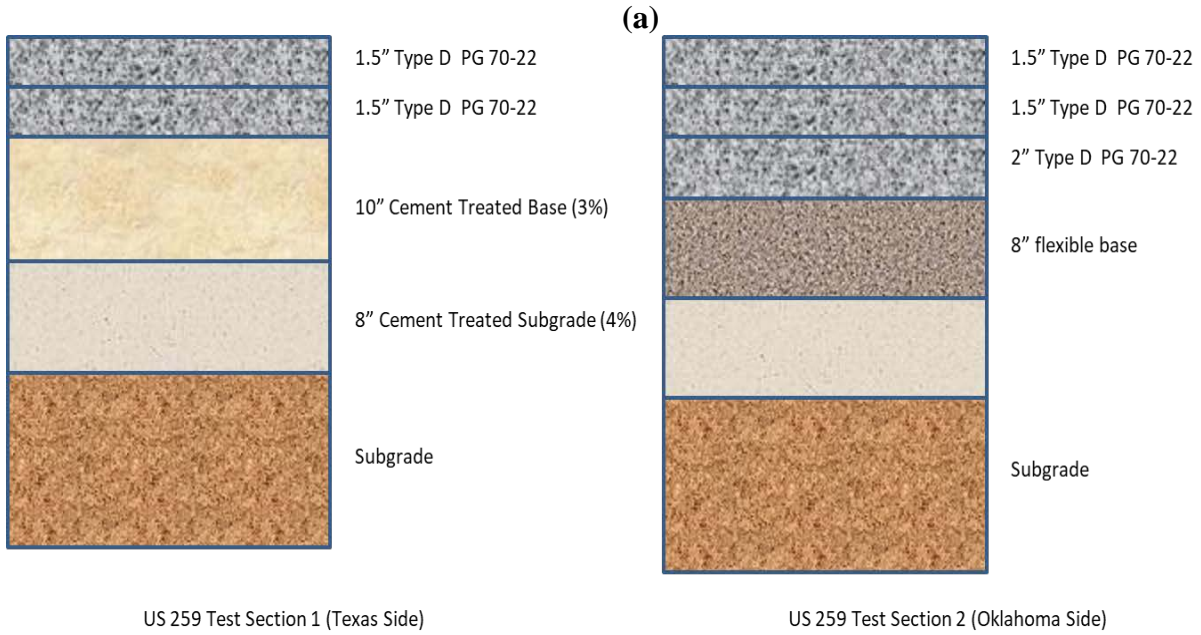
Note that some projects have more than one test section since their pavement structure or layer material might be different. The control section job (CSJ) number and let date information of each project are listed below:

- Atlanta District – US 259, CSJ: 0085-04-037, let 06/14.
- Brownwood District – SH 6, CSJ: 0257-05-042, let 09/14.
- Bryan District – SH 7, CSJ: 0335-03-048, let 02/15.
- Dallas District – FM 3549, CSJ:1015-01-022, let 03/15.
- San Angelo District – US 87, CSJ: 0069-07-103, let 02/16.
- Houston District – FM 1463, CSJ: 0188-10-023, let 02/16.

Among these projects, US 259 has two sections, SH 7 has two sections, and FM 1463 has four sections. Table 36 presents the GPS coordinates and section length of each test section. Figure 51–Figure 56 illustrate their locations in the map and their pavement structure. Note that the difference among FM 1463 sections is the surface layer material.

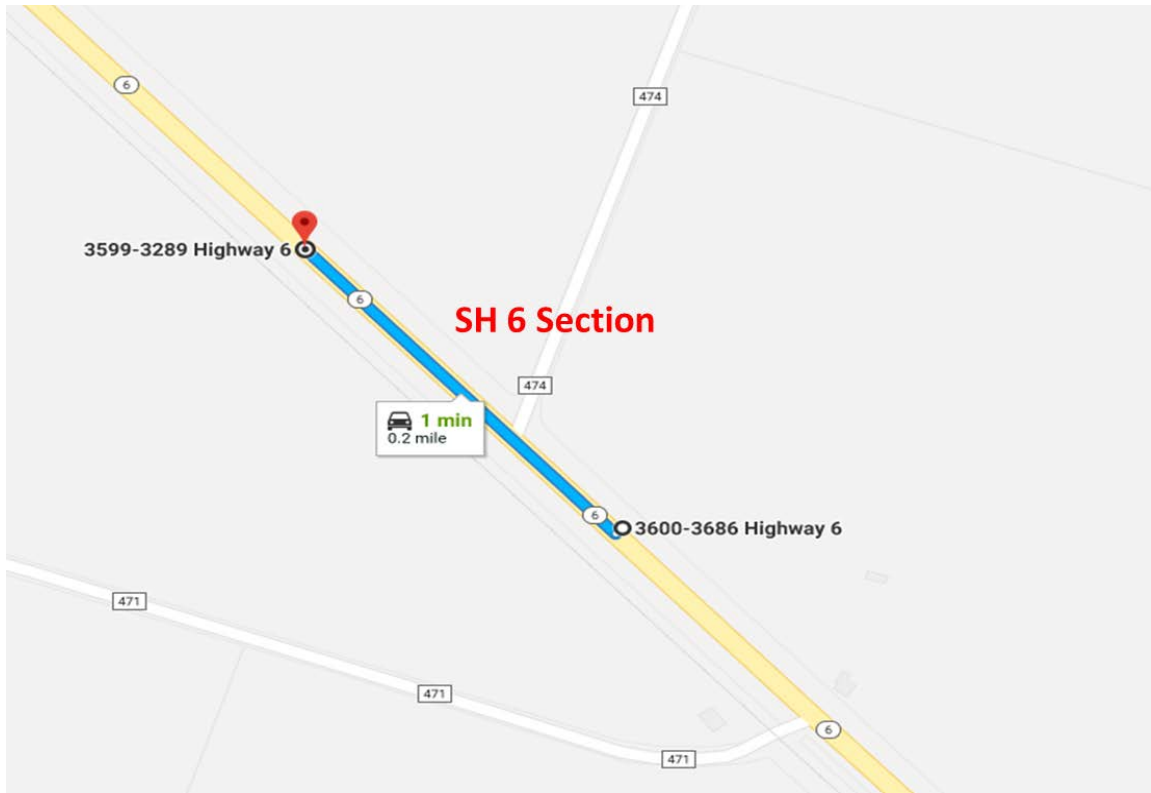
Table 36. GPS Coordinate and Length of Each Test Section.

Test Section	Latitude of Section Start	Longitude of Section Start	Latitude of Section End	Longitude of Section Start	Section Length (ft)
US 259_S1	33°40'57.9"	-94°41'39.4"	33°41'8.5"	-94°41'39.5"	1000
US 259_S2	33°41'16.4"	-94°41'39.4"	33°41'26.5"	-94°41'39.5"	1000
SH 6	32°8'17.5"	-98°34'22.7"	32°8'24.6"	-98°34'30.9"	1050
SH 7_S1	31°14'48.7"	-96°16'31.9"	31°14'50.3"	-96°16'43.2"	1000
SH 7_S2	31°14'41.6"	-96°13'51.4"	31°14'42.2"	-96°13'39.9"	1000
FM 3549	32°56'26"	-96°25'3.7"	32°56'35.8"	-96°25'2.87"	1000
US 87	31°28'33.6"	-100°27'11.8"	31°28'25"	-100°27'6.14"	1000
FM 1463_S1	29°45'52"	-95°50'30.9"	29°45'52.6"	-95°50'47.7"	1500
FM 1463_S2	29°45'52.6"	-95°50'47.7"	29°45'52.3"	-95°51'0.1"	1100
FM 1463_S3	29°45'52.3"	-95°51'0.1"	29°45'42.3"	-95°51'6.59"	1300
FM 1463_S4	29°45'42.3"	-95°51'6.59"	29°45'33.2"	-95°51'6.31"	1000

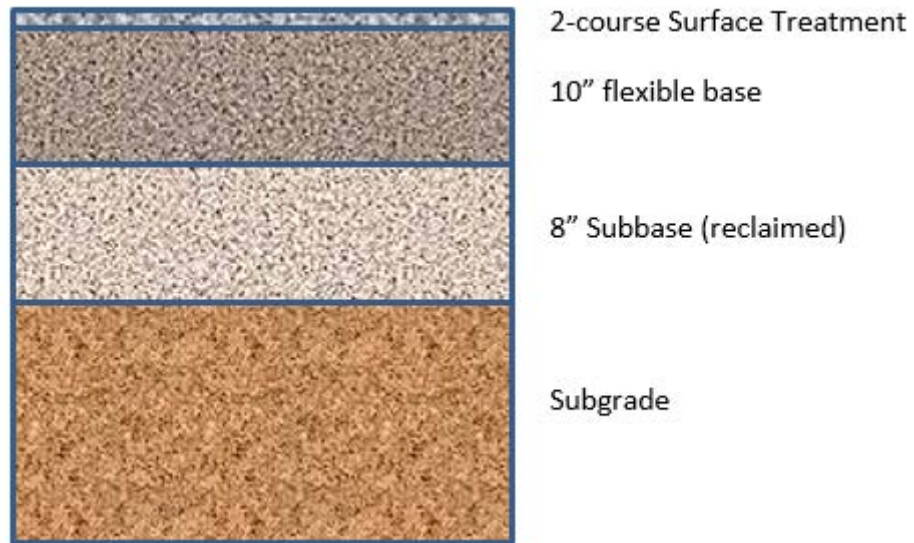


(b)

Figure 51. US 259 Test Sections (a) Map Location and (b) Pavement Structure.



(a)

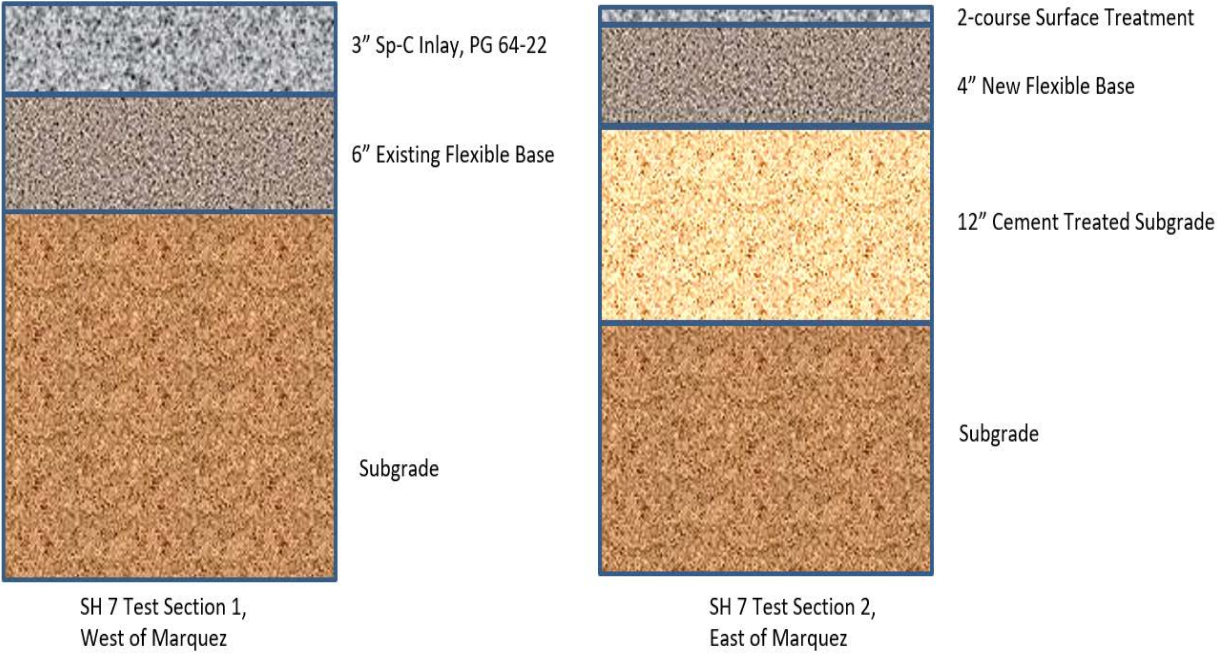


(b)

Figure 52. SH 6 Test Section (a) Map Location and (b) Pavement Structure.



(a)



(b)

Figure 53. SH 7 Test Sections (a) Map Location and (b) Pavement Structure.



(a)

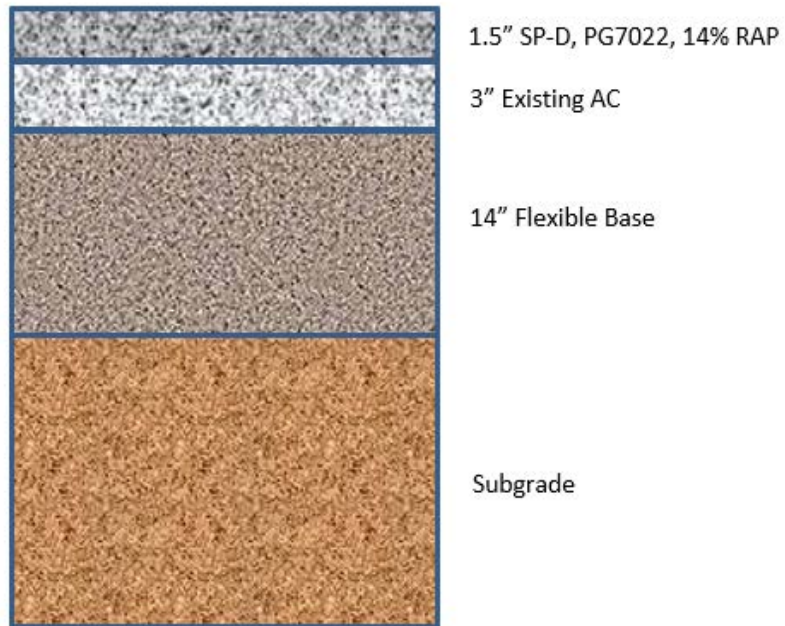


(b)

Figure 54. FM 3549 Test Section (a) Map Location and (b) Pavement Structure.

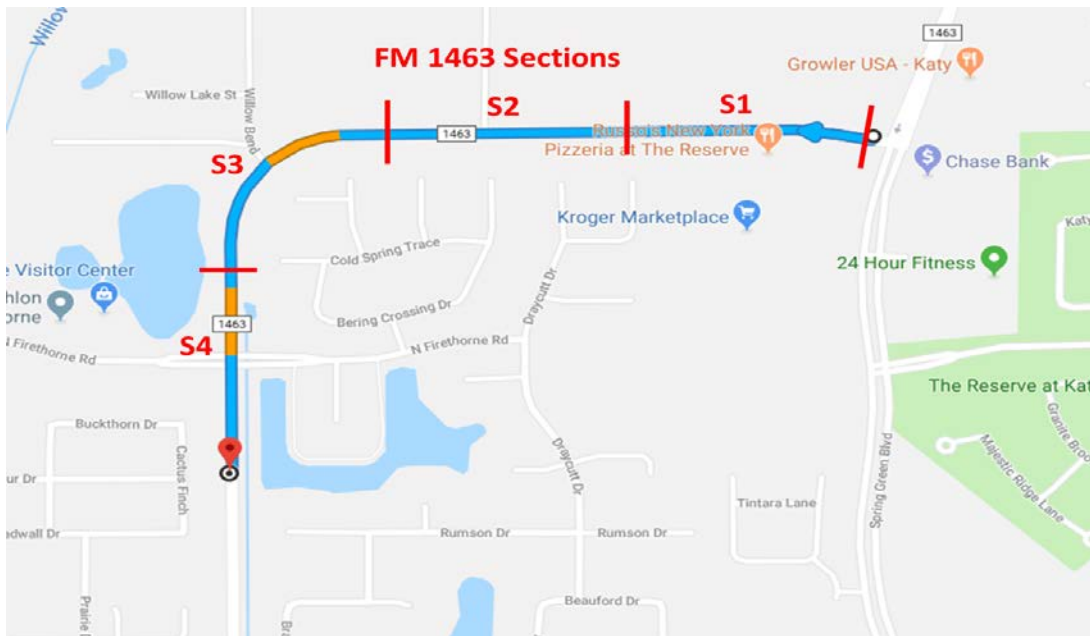


(a)

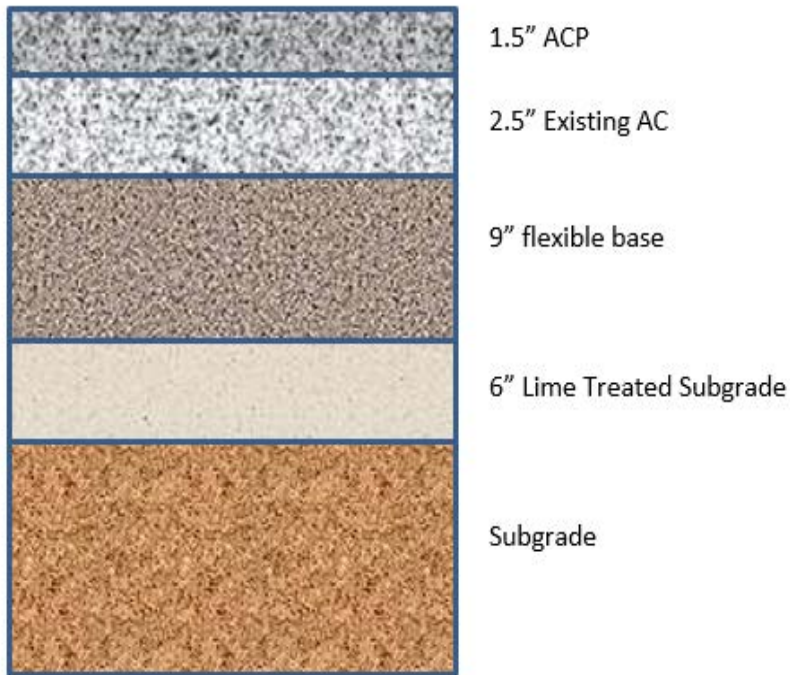


(b)

Figure 55. US 87 Test Section (a) Map Location and (b) Pavement Structure.



(a)



(b)

Figure 56. FM 1463 Test Sections (a) Map Location and (b) Pavement Structure.

VISIT TEST SECTIONS AND CONDUCT FIELD SURVEY

For each project, researchers contacted the project manager/superintendent and attended the pre-construction meeting to identify the potential test sections. Then before, during, and after

construction, researchers visited the test sections to record the existing pavement condition, sample the material, and conduct field performance survey. The test section visiting includes the following:

- US 259:
 - 2015-02-20, identified test sections.
 - 2016-01-22, sampled subgrade and base material.
- SH 6:
 - 2015-04-17, sampled base material.
 - 2016-11-19, conducted field performance survey.
 - 2018-07-19, conducted field performance survey.
- SH 7:
 - 2015-08-27, visited S1 (west of Marquez), recorded old pavement condition and sampled new HMA material during surface layer construction.
 - 2016-04-04, visited S2 (east of Marquez), sampled base material.
 - 2016-11-20, conducted field performance survey for both S1 and S2.
 - 2018-07-18, conducted field performance survey for both S1 and S2.
- FM 3549:
 - 2015-09-23, sampled subbase material during construction.
 - 2015-10-09, sampled base materials during construction.
 - 2016-01-28, sampled HMA material during construction.
 - 2016-11-20, conducted field performance survey.
 - 2017-10-07, conducted field performance survey.
 - 2018-07-17, conducted field performance survey.
- US 87:
 - 2016-11-18, sampled HMA material during construction.
 - 2017-06-06, conducted field performance survey.
 - 2018-07-20, conducted field performance survey.
- FM 1463:
 - 2016-06-15, identified test sections and recorded the existing pavement condition.
 - 2016-07-11, sampled new HMA during construction for all S1–S4 test sections.
 - 2017-04-07, conducted field performance survey for all S1–S4 test sections.
 - 2017-11-07, conducted field performance survey for all S1–S4 test sections.
 - 2018-07-22, conducted field performance survey for all S1–S4 test sections.

Figure 57–Figure 63 show the photos of the test sections before/during construction and the last survey in 07-2018 (except US 259, since the surface HMA was not completed yet since the bridge has some issues).



(a)



(b)

Figure 57. US 259 Field Visiting Photos (a) 2015-02-20, Identifying Test Section and (b) 2016-01-22, Sampling Subgrade and Base Material.



(a)



(b)

Figure 58. SH 6 Field Visiting Photos (a) 2016-11-09, Field Survey and (b) 2018-07-21, Field Survey.



(a)



(b)

Figure 59. SH 7_S1 Field Visiting Photos (a) 2015-08-27, HMA Sampling during Surface Layer Construction and (b) 2018-07-18, Field Survey.



(a)



(b)

Figure 60. SH 7_S2 Field Visiting Photos (a) 2016-04-04, Base Material Sampling during Base Layer Construction and (b) 2018-07-18, Field Survey.



(a)



(b)

Figure 61. FM 3549 Field Visiting Photos (a) 2015-09-23, Subbase Material Sampling during Construction and (b) 2018-07-17, Field Survey.



(a)



(b)

Figure 62. US 87 Field Visiting Photos (a) 2016-11-18, HMA Material Sampling during Surface Layer Construction and (b) 2018-07-20, Field Survey.



(a)



(b)

Figure 63. FM 1463 Field Visiting Photos (a) 2016-06-15, HMA Material Sampling during Surface Layer Construction and (b) 2018-07-22, Field Survey.

The test section survey results are summarized below:

- Except test section SH 6 and SH 7_S1, no obvious rutting was found on other test sections as of July 2018. The typical rutted pavement photos can be seen in Figure 58b and Figure 59b.
- FM 3549 has significant amount of transverse cracking. Also, there is one longitudinal cracking that is about 170-ft long. Based on the pavement structure information (new FB and subbase) and traffic information (low volume traffic) of this section, these transverse cracking are identified as thermal cracking. Figure 64 shows a typical pavement photo of FM 3549 during the last survey in July 2018.
- FM 1463_S4 has some longitudinal cracking, as seen in Figure 65.
- So far (as of July 2018), no crack was found on all other test sections.



Figure 64. Transverse Crack and Longitudinal Crack on FM 3549 Test Section.



Figure 65. Longitudinal Crack on FM 1463_S4 Test Section.

Table 37–Table 40 provide the rut depth survey result for SH 6 and SH 7_S1, and cracking survey result for FM 3549, and FM 1463_S4, respectively.

Table 37. SH 6 Rut Depth Survey Result.

Survey Time	Months after Traffic Open	Rut Depth (in.)
2015-06	0	0
2016-11	17	0.1
2018-07	37	0.15

Table 38. SH 7_S1 Rut Depth Survey Result.

Survey Time	Months after Traffic Open	Rut Depth (in.)
2015-08	0	0
2016-04	8	0
2016-11	15	0.06
2018-07	35	0.12

Table 39. FM 3549 Cracking Survey Result.

Survey Time	Months after Traffic Open	Fatigue Cracking (%)	Thermal Cracking (ft/mile)	Longitudinal Cracking (ft)
2016-01	0	0	0	0
2016-11	11	0	0	0
2017-10	22	0	1221	80
2018-07	31	0	1517	172

Table 40. FM 1463_S4 Cracking Survey Result.

Survey Time	Months after Traffic Open	Fatigue Cracking (%)	Thermal Cracking (ft/mile)	Longitudinal Cracking (ft)
2016-07	0	0	0	0
2017-04	9	0	0	0
2017-11	16	0	0	150
2018-07	24	0	0	248

ASSEMBLE SAMPLES AND RUN LAB TEST

Researchers sampled all the available layer material during the construction of each test section. Below are the material types sampled for each test section:

- US 259: Subgrade material and base material. No surface HMA material because the bridge had some issue and delayed the construction of surface layer.
- SH 6: Base material. This section is a surface treated pavement, so no need of sampling HMA material.
- SH 7_S1: Surface HMA material. This is a milled and in-lay pavement so only surface material was available.
- SH 7_S2: Base material. This is a surface treated pavement, so no need of sampling HMA material.
- FM 3549: subbase, base, and surface HMA material.
- US 87: Surface HMA material. This is a milled and in-lay pavement so only surface material was available.
- FM 1463_S1, S2, S3, and S4: HMA material for all four test sections. This is a milled and overlay project and each test section has different surface material.

Among these sampled material types, the dynamic modulus test, Hamburg test, OT, and repeated load test were conducted for HMA material; the repeated load test and resilient modulus test were conducted for the FB/subbase/subgrade material; and resilient modulus test and unconfined

compressive strength test were conducted for stabilized base/subbase/subgrade material. Table 41–Table 44 list the corresponding test specifications researchers followed during this study.

Table 41. HMA (Plant Mix) Tests Specification.

Test	Spec	Test Parameters	Output Data	Sample Replicates
Hamburg	Tex-242-F	As per spec, but run all samples to 20,000 load passes	Rut depth and number of wheel passes (i.e., 0, 5000, 10,000, 15,000, and 20,000)	3 (3 sets of 2)
Overlay	Tex-248-F	0.025- inch opening, 93% load drop, 77°F	Cycles to failure	5
OT fracture properties	Reports 0-5123-3 5-5123-3-1	0.017 inch @ 77°F for 100 cycles	<i>A & n</i>	5
Dynamic modulus (DM)	AASHTO TP 62-03	As per spec; 5 temps; 6 frequencies	Dynamic modulus ($ E^* $), temperature, and frequency	3
Repeated Load (RLPD)	Reports 0-6658-P3 and 0-6658-1	104°F, 20 psi, & 10000 cycles	alpha and mu	3

Table 42. FB/Subbase Material Tests Specification.

Test	Spec	Test Parameters	Output Data	Sample Replicates
Sieve Analysis	Tex-110-E	As per spec	Gradation	3
Atterberg limits	Tex-104-E , Tex-105-E , Tex-106-E	As per spec	PI, LL, and PL	3
Specific gravity	ASTM C-127, 128	As per spec	SG value	3
MD curve	Tex-113-E	6" × 8"	MDD and OMC	4
Resilient modulus	NCHRP 1-28A	6" × 12"	k- parameters	3
Repeated Load (RLPD)	NCHRP 1-28A	6" × 12"	a and m	2

Table 43. Stabilized Base/Subbase Material Tests Specification.

Test	Spec	Test Parameters	Output Data	Sample Replicates
Sieve Analysis	Tex-110-E	As per spec	Gradation	3
Atterberg limits	Tex-104-E , Tex-105-E , Tex-106-E	As per spec	PI, LL, and PL	3
Specific gravity	ASTM C-127 , 128	As per spec	SG value	3
MD curve	Tex-113-E	6" × 8"	MDD and OMC	4
Resilient modulus	NCHRP 1-28A	6" × 12"	k- parameters	3
Unconfined compressive strength	Tex-120-E , Tex-121-E	As per spec	UCS	2

Table 44. Subgrade Soil Tests Specification.

Test	Spec	Test Parameters	Output Data	Sample Replicates
Sieve Analysis	Tex-110-E	As per spec	Gradation	3
Atterberg limits	Tex-104-E , Tex-105-E , Tex-106-E	As per spec	PI, LL, and PL	3
Specific gravity	Tex-108-E	As per spec	SG value	3
MD curve	Tex-114-E	4" × 6"	MDD and OMC	4
Resilient modulus	NCHRP 1-28A	4" × 8"	k- parameters	3
Sieve Analysis	Tex-110-E	As per spec	Gradation	3

After lab test data processing and analyzing, the parameters determined for TxME inputs are summarized in Table 45–Table 47.

Table 45. HMA Dynamic Modulus of Test Sections.

Temp. (°F)	Freq. (Hz)	E* , ksi						
		SH 7 _S1	FM 3549	US 87	FM 1463_S1	FM 1463_S2	FM 1463_S3	FM 1463_S4
14	25	2500.2	3797.7	3207.0	3157.1	2665.9	2647.2	2977.1
14	10	2442.6	3669.5	3162.3	3021.8	2520.0	2515.7	2837.5
14	5	2391.6	3563.1	3121.7	2910.6	2399.8	2407.4	2723.0
14	1	2244.3	3283.7	2999.4	2623.3	2090.1	2128.4	2428.8
14	0.5	2166.8	3149.3	2932.2	2487.6	1945.4	1997.5	2290.9
14	0.1	1950.7	2806.7	2734.6	2149.1	1591.9	1675.1	1949.9
40	25	2061.2	2942.1	2815.1	2314.5	1826.6	1856.4	2137.6
40	10	1929.2	2737.7	2687.5	2116.8	1623.9	1670.0	1940.1
40	5	1818.3	2575.5	2575.9	1962.4	1468.5	1526.1	1787.0
40	1	1527.1	2180.1	2263.9	1596.6	1113.6	1192.7	1428.3
40	0.5	1390.2	2005.1	2106.9	1439.7	968.8	1053.9	1276.7
40	0.1	1060.7	1600.4	1698.6	1090.2	666.3	755.8	944.6
70	25	1189.0	1714.1	1814.9	1220.9	832.0	888.5	1089.5
70	10	1001.0	1487.8	1569.2	1028.9	666.4	726.6	907.4
70	5	862.5	1322.6	1378.6	892.5	554.5	615.1	779.7
70	1	570.9	969.6	947.3	613.7	343.5	397.8	523.5
70	0.5	464.0	834.4	777.8	512.2	273.6	323.1	432.2
70	0.1	268.7	566.7	450.5	321.6	154.7	190.7	264.6
100	25	400.4	725.1	638.4	450.4	255.8	289.2	388.0
100	10	292.3	578.9	462.1	344.7	185.3	214.2	293.3
100	5	226.4	482.9	352.5	277.8	143.6	168.6	234.2
100	1	119.8	306.5	173.9	161.8	77.5	93.8	133.8
100	0.5	90.0	248.8	125.0	126.3	59.1	72.2	103.6
100	0.1	46.4	150.1	56.2	69.2	31.5	38.9	56.1
130	25	89.4	237.7	115.4	125.3	64.4	74.4	106.1
130	10	61.2	178.5	73.3	89.3	44.9	52.4	75.1
130	5	46.1	143.1	51.8	68.6	34.3	40.1	57.5
130	1	24.6	84.8	23.6	36.9	18.7	21.8	30.7
130	0.5	19.2	67.7	17.1	28.2	14.6	16.9	23.5
130	0.1	11.4	40.5	8.8	15.3	8.5	9.6	12.8

Table 46. HMA Fracture Property and Rutting Property of Test Sections.

Test Section	Fracture Property		Rutting Property	
	A	n	alpha	Mu
SH 7	8.0959E-07	4.404900267	0.766	0.654
FM 3549	5.37E-04	2.622672839	0.794	0.668
US 87	3.80E-05	3.349091084	0.63	0.8
FM 1463_S1	7.04434E-06	3.811463015	0.778	0.636
FM 1463_S2	9.45018E-07	4.362472478	0.669	0.78
FM 1463_S3	5.51799E-07	4.510051712	0.649	0.81
FM 1463_S4	2.69019E-06	4.07550933	0.75	0.72

Table 47. Base/Subbase/Subgrade Material Property of Test Sections.

Test Section and Material	Rutting Property		Modulus (ksi)
	alpha	mu	
US 259 Subgrade	0.85	0.212	11.5
US 259 FB	0.787	0.38	39
US 259 Cement Treated Base	NA		140
SH 6 FB	0.89	0.28	69
SH 7_S2 FB	0.937	0.271	90
FM 3549 FB	0.928	0.126	72.6
FM 3549 Stabilized Subbase	NA		87

ASSEMBLE TRAFFIC INFORMATION

In this study, the TxDOT statewide planning map was used to obtain the two-way AADT and truck percentage information, which can be used to determine the 20-year ESALs. As an example, Figure 66 shows the AADT and truck percentage information of the SH 6 in Comanche County, Brownwood District. Figure 67 illustrates the ESALs calculation using the web application provided by the American Concrete Pavement Association (ACPA).

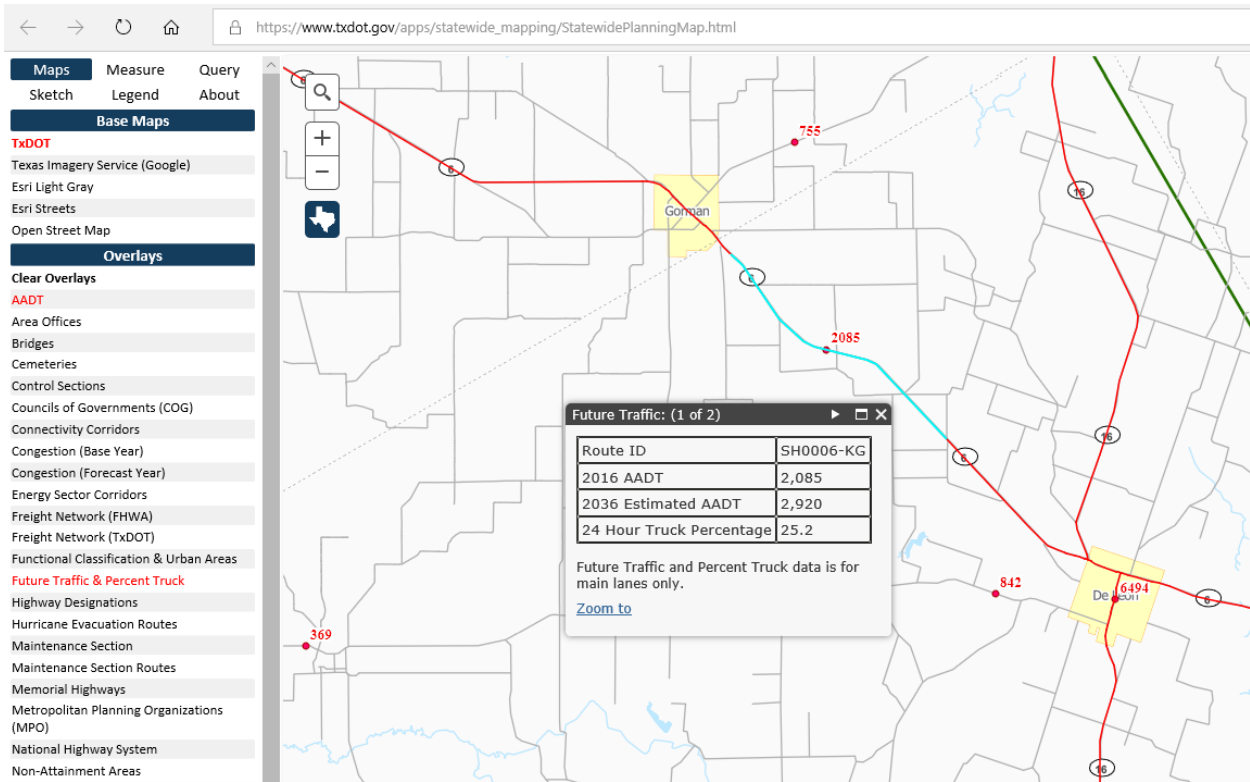


Figure 66. TxDOT Statewide Planning Map.

Traffic Calculation

No. of Years to Project Traffic (yrs): [Help](#)
 Determine Past and Future ESALs

Two-Way Average Daily Traffic (ADT): [Help](#)
 Directional Distribution Factor (%): [Help](#)
 Design Lane Distribution Factor (%): [Help](#)
 Growth Rate (%): [Help](#)

Percent Trucks (%): [Help](#)
 Truck Factor (ESALs/Truck): [Help](#)

ESAL Calculation

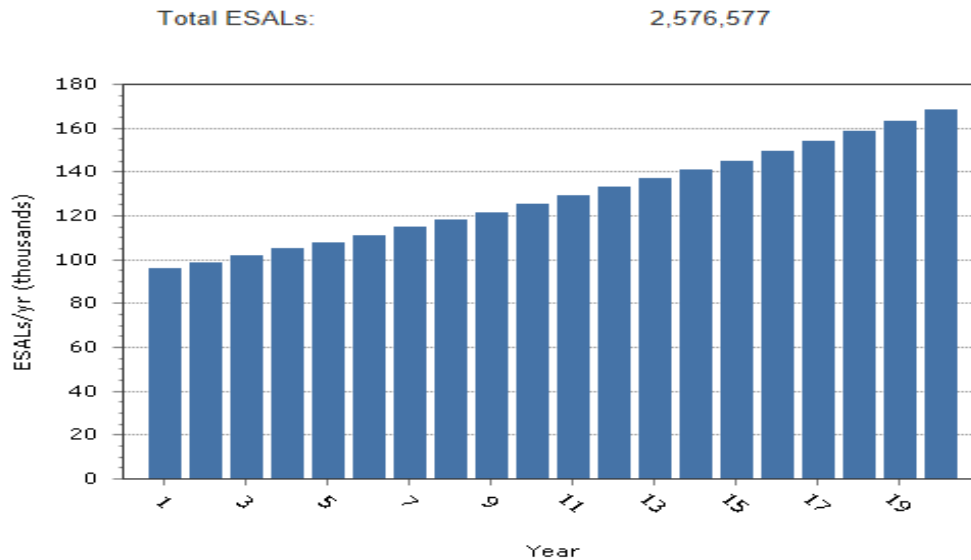


Figure 67. ESAL Calculation Using ACPA Web Application.

Using similar method, the ESALs for all test sections were determined and summarized in Table 48. Note that US 259 has two sections, named as US 259_S1 and US 259_S2, respectively; SH 7 has two sections, named as SH 7_S1 and SH 7_S2, respectively; and FM 1463 has four sections, named as FM 1463_S1, S2, S3, and S4, respectively.

Table 48. ESALs of Test Sections.

Test Section	Two-Way AADT	Lanes in one Direction	Truck Percentage	ESALs (millions)
US 259	2172	1	12.70%	1.35
SH 6	2085	1	25.20%	2.58
SH 7	3050	1	20.90%	3.13
FM 3549	2061	1	6.70%	0.6
US 87	25084	3	8.60%	6.3
FM 1463	8258	1	10%	1.83

During this study, researchers also deployed the portable weigh-in-motion (WIM) station on SH 6 test section, as seen in Figure 68.

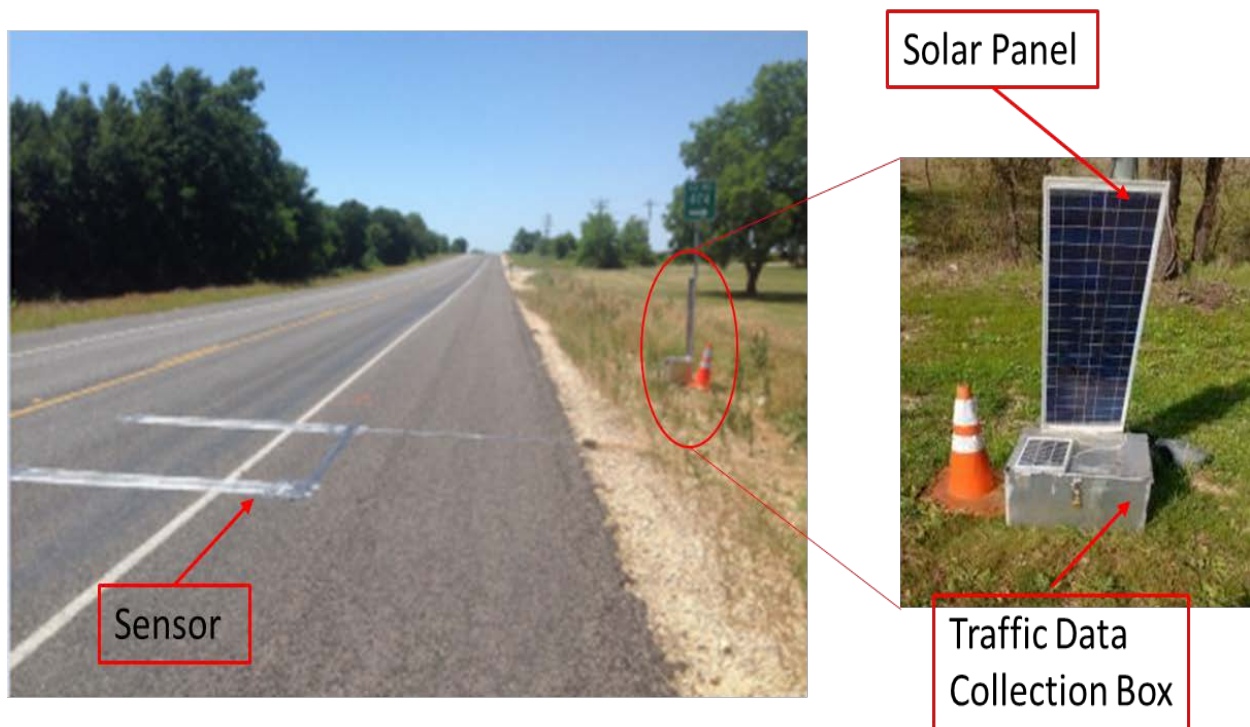


Figure 68. Portable WIM Station on SH 6.

According to the portable WIM data, the one-way AADT number was determined to be 1059 and the truck percentage to be 22.4 percent. The analyzed VCD result, the APT, the MAF result are listed in Table 49–Table 51, respectively. For the ALD, since this table has large amount of data so only part of them (January, Steering Single Axle) was listed in Table 52.

Table 49. VCD of SH 6 Test Section.

Vehicle Class	Distribution (%)
4	1.3
5	6.1
6	4.5
7	0.1
8	8.4
9	76.9
10	2.0
11	0.5
12	0.1
13	0.1

Table 50. APT of SH 6 Test Section.

Vehicle Class	Steering Single Axle	Other Single Axle	Tandem Axle	Tridem Axle	Quad Axle
4	1.00	0.18	0.59	0.00	0.00
5	1.00	1.00	0.00	0.00	0.00
6	1.00	0.00	1.00	0.00	0.00
7	1.00	0.00	0.00	1.00	0.00
8	1.00	0.00	0.00	0.00	0.00
9	1.00	0.65	1.67	0.00	0.00
10	1.00	0.00	0.00	0.00	0.00
11	1.00	4.00	0.00	0.00	0.00
12	1.00	19.00	18.00	0.00	0.00
13	1.00	0.00	0.00	2.00	0.00

Table 51. MAFs of SH 6 Test Section.

Month	Class 4	Class 5	Class 6	Class 7	Class 8	Class 9	Class 10	Class 11	Class 12	Class 13
January	1.25	1.42	0.85	0.44	0.93	1.07	1.11	0.61	0.50	0.77
February	2.39	1.90	0.87	0.10	0.84	1.16	0.89	0.11	1.28	1.72
March	1.42	0.73	0.88	1.19	1.06	1.08	0.92	1.77	0.32	0.47
April	0.33	0.72	0.95	0.44	0.97	0.83	2.27	1.43	1.70	2.29
May	0.81	1.72	1.71	1.34	1.27	1.33	0.14	1.24	1.50	0.91
June	0.64	1.56	0.81	1.93	1.44	1.23	0.33	1.75	2.51	1.25
July	0.11	0.24	1.08	2.11	0.75	0.63	1.30	0.73	1.40	1.03
August	1.13	0.28	1.03	0.65	0.77	0.80	0.99	1.12	0.30	0.53
September	1.76	0.50	1.09	0.42	0.89	0.79	1.13	0.29	1.24	1.62
October	0.82	0.53	0.83	0.65	0.98	0.99	1.01	0.96	0.61	0.21
November	0.05	1.08	0.99	1.80	1.08	0.90	0.75	0.56	0.46	0.38
December	1.30	1.33	0.92	0.92	1.02	1.19	1.17	1.43	0.20	0.80

Table 52. ALD of SH 6 Test Section (Steering Single Axle, January).

Vehicle Class	Distribution Percentage (%) for Each Axle Load in Kips															
	3	4	5	6	7	8	9	10	11	12	13	14	15	16	17	18
4	31.8	4.5	4.5	4.5	0	0	4.5	0	9.1	13.6	13.6	4.5	0	0	9.1	0
5	11.9	22.8	11.9	7.9	5.9	7.9	5.9	6.9	3	5.9	3	5	0	1	0	1
6	5.4	2.7	5.4	8.1	1.4	8.1	9.5	1.4	21.6	16.2	10.8	8.1	1.4	0	0	0
7	0	0	0	0	0	0	0	50	0	0	0	0	50	0	0	0
8	30.2	26.6	14.4	7.9	2.9	4.3	7.9	2.2	0	2.2	1.4	0	0	0	0	0
9	0.4	0.9	1.7	4.4	4.3	16.9	13.9	11.4	20.7	14.6	6.3	2.7	1.2	0.5	0.2	0
10	0	0	6.1	3	0	6.1	12.1	18.2	18.2	18.2	9.1	6.1	3	0	0	0
11	0	0	0	0	12.5	50	12.5	12.5	0	12.5	0	0	0	0	0	0
12	0	0	0	0	0	0	0	100	0	0	0	0	0	0	0	0
13	75	0	0	0	0	0	12.5	0	0	0	0	12.5	0	0	0	0

USE TXME TO SIMULATE TEST SECTIONS AND PREDICT PERFORMANCE

In this document, test section FM 3549 is used as an example to show the TxME simulation process. Below shows the pavement structure and layer material property, climate, traffic, and reliability input, and prediction results.

Pavement Structure and Layer Material Property Input

Figure 69 shows the TxME pavement structure input for FM 3549. By clicking each layer, users can input the corresponding layer material property. Figure 70 shows the surface layer HMA material property input screen.

FM3549:Structure

Pavement Type

Surface Treated

Conventional or Thin HMA

Perpetual

Design/Analysis Life (years): 20

Project Location

District: 18 Dallas

Type C, PG 70-22

Flexible Base

Lime (Cement) Stabilized Subgrade

Subgrade

Figure 69. TxME Pavement Structure Input for Test Section FM 3549.

Layer 1: Type C, PG 70-22

Layer Information	
Layer Number	1
Layer Thickness (inches)	2
Cost (\$/Cubic Yard):	129.7

Material Information	
Binder Type	PG 70-22
Gradation	Type C
RAP %	0
RAS %	0

Material Properties	
Dynamic Modulus	Level 1 input: dynamic modulus
Fracture Property	@77 F: A=0.000537, n=2.6227
Rutting Property	@104 F: alpha=0.794, mu=0.668
Poisson Ratio	0.35

Modulus Input

Level 2 (Default Value) Level 1 (Test Data)

Test Data

Dynamic Modulus (E*, ksi)

Number of Temperatures: 5 Number of frequencies: 6

Temperature (F)	Frequency (Hz)					
	25	10	5	1	0.5	0.1
14	3798	3670	3563	3284	3149	2807
40	2942	2738	2576	2180	2005	1600
70	1714	1488	1323	970	834	567
100	725	579	483	307	249	150
130	238	179	143	85	68	41

OK

Figure 70. TxME HMA Material Property Input for Test Section FM 3549.

Climate Input

Figure 71 shows the climate input for FM 3549. In this input screen, the Dallas weather station was selected, and the right side of the screen shows the annual average and monthly average temperature.

FM3549:Structure FM3549:Climate

Climatic data for a specific weather station

Select Weather Station

- AMARILLO, TX
- ANGLETON/LAKE JACKSON, TX
- ARLINGTON, TX
- AUSTIN/CITY, TX
- AUSTIN/BERGSTROM, TX
- BEAUMONT/PORT ARTHUR, TX
- BORGER, TX
- BROWNSVILLE, TX
- BURNET, TX
- CHILDRESS, TX
- COLLEGE STATION, TX
- CONROE, TX
- CORSICANA, TX
- CORPUS CHRISTI, TX
- COTULLA, TX
- DALLAS, TX**

Station Location:
DALLAS LOVE FIELD
Available Data Months: 99

32.51 Latitude (degrees.minutes)
-96.51 Longitude (degrees.minutes)
509 Elevation (ft)

Summary Hourly data

Annual Summary

Mean annual temperature (deg F)	67.5
Mean annual precipitation (in.)	32.5
Number of wet days	112.1
Freezing index (deg F-days)	72.1
Average annual number of freeze/thaw cycles	13.3

Monthly Temperatures

January (deg F)	49.1
February (deg F)	51.4
March (deg F)	57.2
April (deg F)	67.3
May (deg F)	75.6
June (deg F)	81.6
July (deg F)	86.5
August (deg F)	86.9
September (deg F)	79.5
October (deg F)	68.7
November (deg F)	58.0
December (deg F)	48.1

Figure 71. TxME Climate Input for Test Section FM 3549.

Traffic Input

Figure 72 shows the traffic input for FM 3549. In this input screen, the Level 2 – ESALs input was selected and the ESAL number (0.6) was filled into the corresponding input textbox.

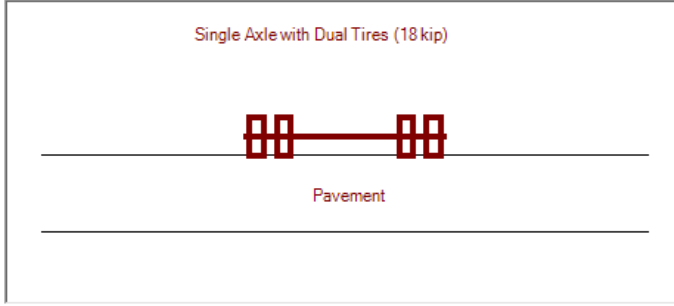
FM3549:Structure FM3549:Climate **FM3549:Traffic***

Traffic Input

Level 2: ESALs Level 1: Load Spectra

Level 2: ESALs

Single Axle with Dual Tires (18 kip)



Pavement

Tire Pressure (psi):	<input type="text" value="100"/>	18 kip ESALs 20 YR (1 DIR) (millions):	<input type="text" value="0.6"/>
ADT-Beginning (Veh/Day):	<input type="text" value="2061"/>	Operational Speed (mph):	<input type="text" value="69"/>
ADT-End 20 YR (Veh/Day):	<input type="text" value="3610"/>		

Figure 72. TxME Traffic Input for Test Section FM 3549.

Reliability/Performance Criteria Input

Figure 73 shows the reliability/performance criteria input for FM 3549. Note in this analysis, the input parameters such as layer thickness or modulus are deterministic, and no variability was provided. Thus, this is a deterministic analysis and no reliability level input is needed. The performance limit value in the screen indicates the maximum distress that a pavement can have before a major rehabilitation.

Performance Criteria			Variability of Input Parameters		
Performance	Limit	Reliability (%)	Use	Parameter	Coefficient of Variation (%)
Rutting (inch)	0.5		<input checked="" type="checkbox"/>	Layer 1 (AC: DenseGraded) - Thickness	
Thermal cracking (ft/mile)	2112		<input type="checkbox"/>	Layer 1 (AC: DenseGraded) - Modulus	
Fatigue cracking of AC layer (percent)	50		<input type="checkbox"/>	Layer 1 (AC: DenseGraded) - Fracture Property A	
			<input type="checkbox"/>	Layer 1 (AC: DenseGraded) - Fracture Property n	
			<input type="checkbox"/>	Layer 1 (AC: DenseGraded) - Rutting Property Alpha	
			<input type="checkbox"/>	Layer 1 (AC: DenseGraded) - Rutting Property Mu	
			<input type="checkbox"/>	Layer 2 (Base: FlexibleBase) - Thickness	
			<input type="checkbox"/>	Layer 2 (Base: FlexibleBase) - Modulus	
			<input type="checkbox"/>	Layer 2 (Base: FlexibleBase) - Rutting Property Alpha	
			<input type="checkbox"/>	Layer 2 (Base: FlexibleBase) - Rutting Property Mu	
			<input type="checkbox"/>	Layer 3 (Subbase: LSS) - Thickness	
			<input type="checkbox"/>	Layer 3 (Subbase: LSS) - Modulus	
			<input type="checkbox"/>	Layer 4 (Subgrade) - Modulus	
			<input type="checkbox"/>	Layer 4 (Subgrade) - Rutting Property Alpha	
			<input type="checkbox"/>	Layer 4 (Subgrade) - Rutting Property Mu	
			<input type="checkbox"/>	Traffic - ESALs or AADTT	

Figure 73. TxME Reliability/Performance Criteria Input for Test Section FM 3549.

FM 3549 Performance Prediction Result

Figure 74–Figure 76 show the performance/distress prediction result in terms of rutting, AC, fatigue cracking, thermal cracking, respectively.

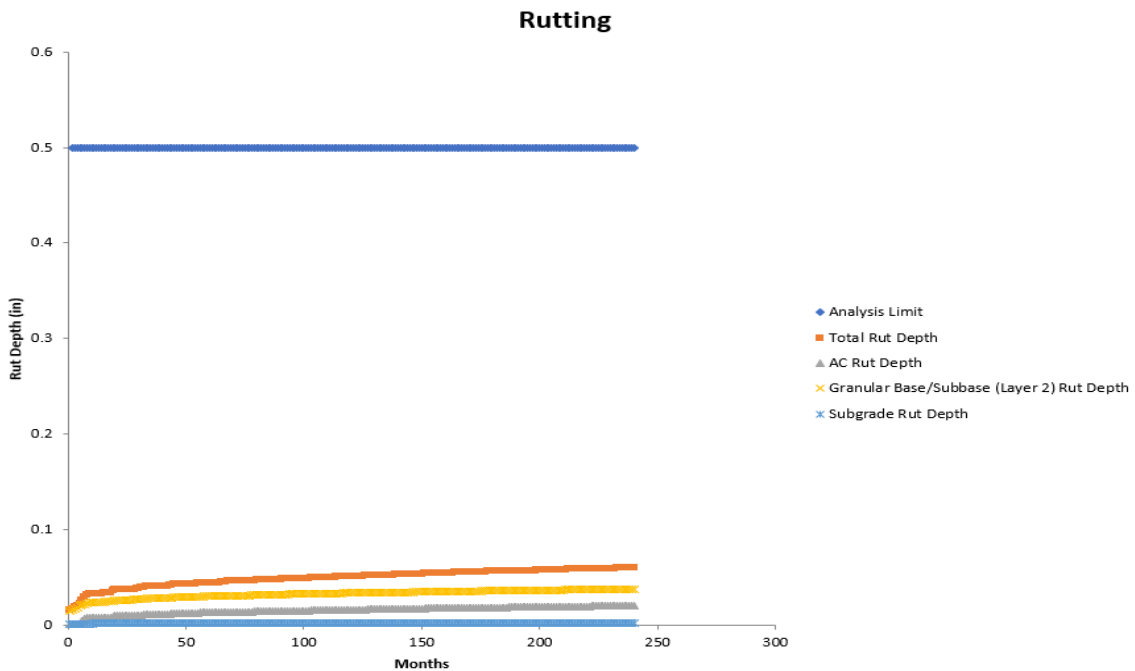


Figure 74. TxME Predicted Rut Depth for Test Section FM 3549.

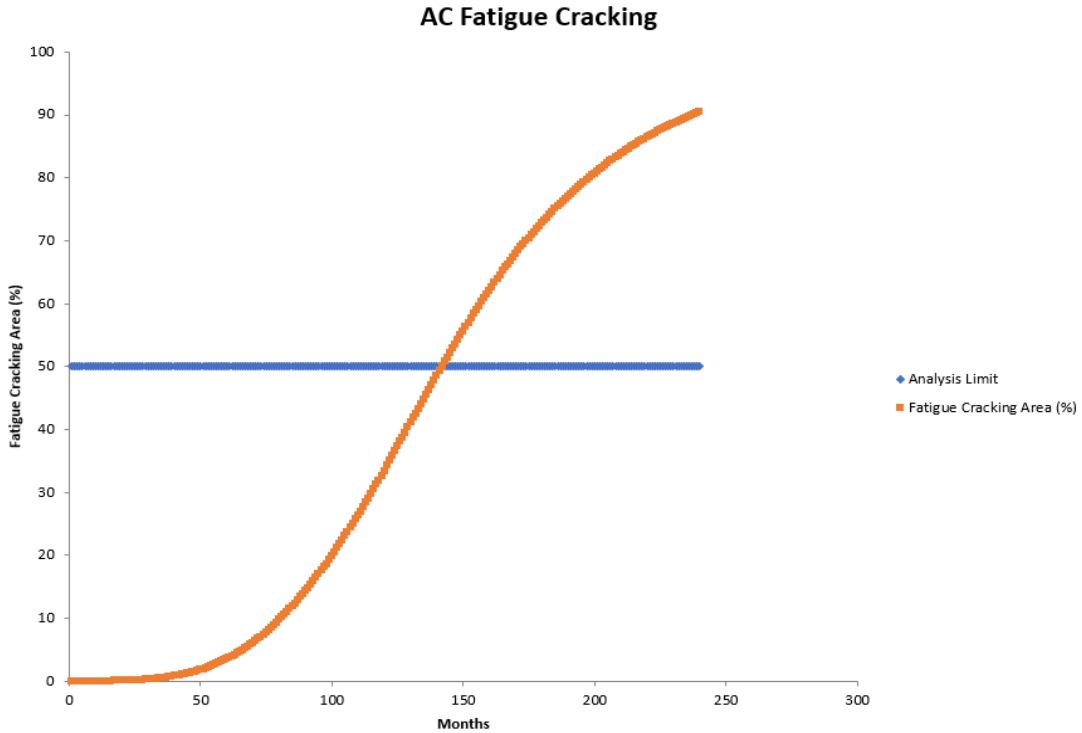


Figure 75. TxME Predicted AC Fatigue Cracking for Test Section FM 3549.

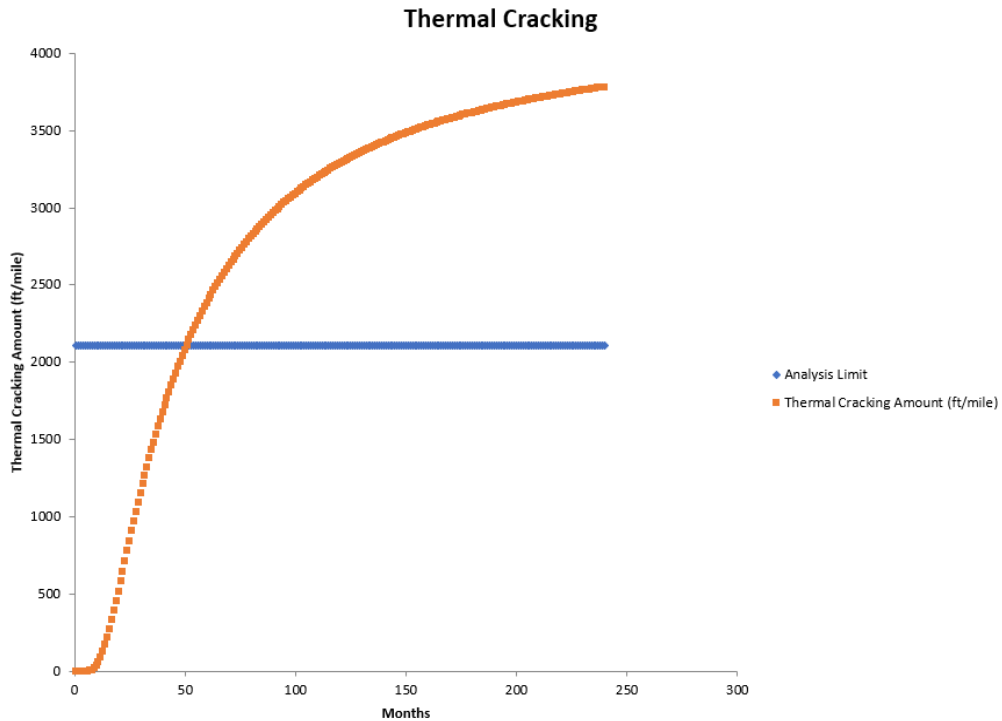


Figure 76. TxME Predicted Thermal Cracking for Test Section FM 3549.

COMPARE TXME PREDICTED PERFORMANCE WITH FIELD SURVEY

The Appendix lists the TxME prediction results for all 11 test sections. According to these prediction results, it was concluded that:

- TxME predicts that SH 6 and SH 7_S1 have significantly more rut depth than other test sections, which matches the field survey result that “Except test section SH 6 and SH 7_S1, no rut was found on other test sections.”
- TxME predicts significant thermal cracking on FM 3549, this matches the survey result “FM 3549 has significant amount of thermal cracking.”
- TxME predicts no thermal cracking for other test sections, which matches the field survey observation too.
- TxME predicts that FM 3549 and SH 7_S1 have fatigue cracking potential. FM 3549 will show some fatigue cracking starting from the 5th year, and SH 7_S1 will show some fatigue cracking starting from the 4th year. This need to be verified by future survey.
- Currently, TxME does not have a model to predict longitudinal cracking, thus researchers could not compare the survey of FM 3549 and FM 1463 _S4 longitudinal cracking with TxME prediction.
- TxME predicts the performance of US 259 two section using embedded default HMA properties. Both these default values and predicted performance need to be validated/verified by future survey or study.

For further comparison, Figure 77 shows the rut depth comparison between TxME prediction and field survey for test section SH 6. Note in this figure, TxME predicts the rut depth based on both level 2 – ESALs input and level 2 – Load Spectra input since portable WIM data are available for this section. Figure 78 shows the TxME predicted versus field survey rut depth for SH 7_S1 test section. The TxME predicted versus field survey thermal cracking of FM 3549 is plotted in Figure 79. These plots verified that TxME has very reasonable predictions comparing with field measured performance. More detailed prediction results can be found in the Appendix.

SH 6 Rut Depth, TxME Predicted vs. Field Survey

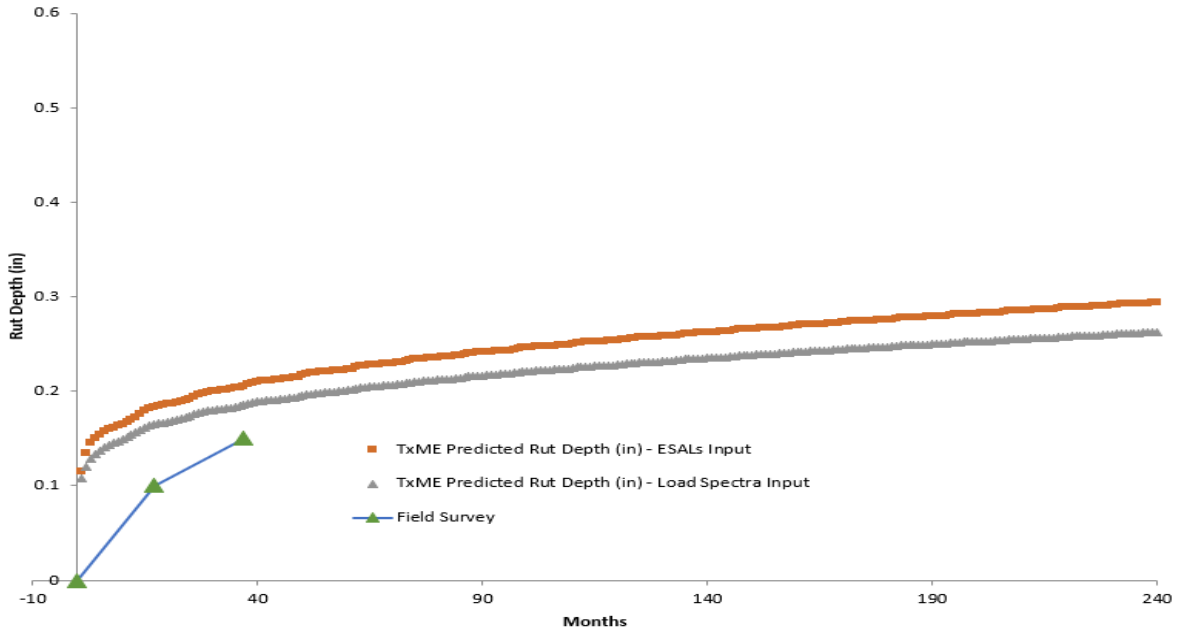


Figure 77. SH 6 Rut Depth Comparison between TxME Prediction and Field Survey.

SH 7_S1 Rut Depth, TxME Predicted vs. Field Survey

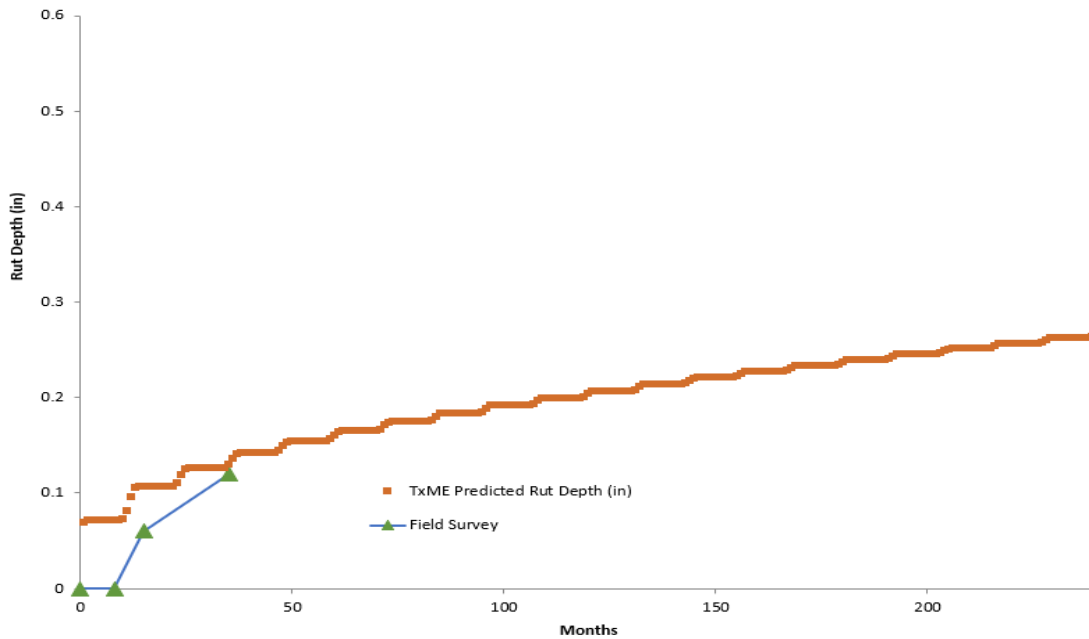


Figure 78. SH 7_S1 Rut Depth Comparison between TxME Prediction and Field Survey.

FM 3549 Thermal Cracking, TxME Predicted vs. Field Survey

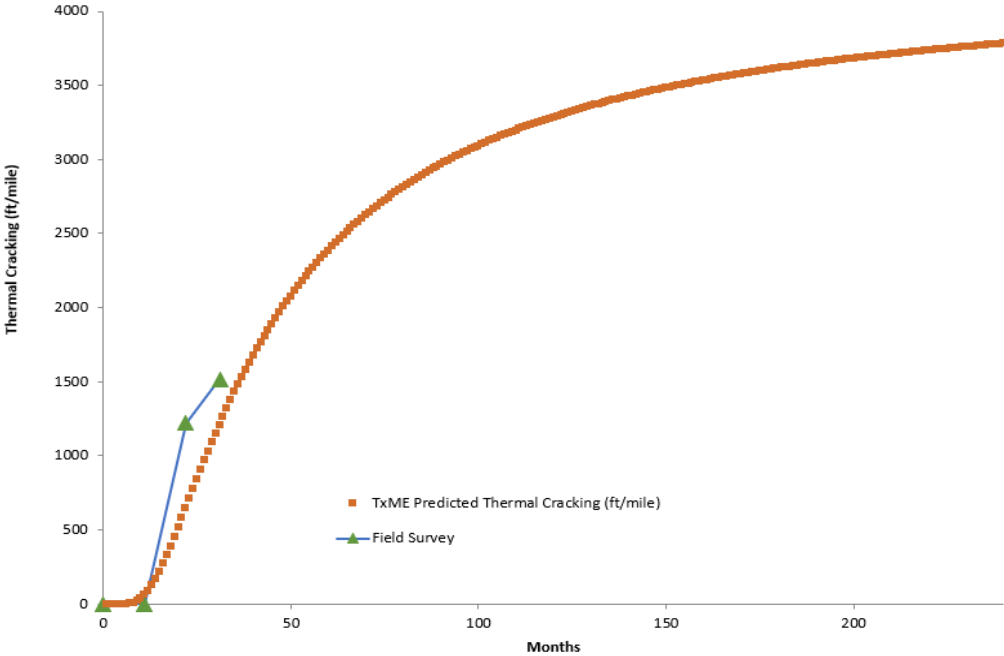


Figure 79. FM 3549 Thermal Cracking Comparison between TxME Prediction and Field Survey.

CHAPTER 8. CONCLUSIONS AND RECOMMENDATIONS

TxME was developed to enable Texas pavement designers to take full advantage of new or premium materials, with a full consideration of the influential factors including pavement structure, traffic volume, and environmental condition. The main features of TxME include:

- Mechanistic-Empirical modeling.
- Performance-based material characterization.
- Hourly climatic data.
- Traffic load spectrum incorporation.
- Design input variability-based reliability methodology.
- Incremental distress prediction.
- Fast running speed.
- User friendly interface.
- Convenient connection with relevant FPS inputs and thickness outputs.

This report mainly focuses on how default values such as default material properties, load spectra, and initial construction cost were developed and incorporated into the TxME. These updates improve system's versatility and help optimize designs for specific TxME applications. The enhanced TxME was then calibrated based on Texas Flexible Pavement Database and verified by the field test sections.

Based on the work presented in the previous chapters, the conclusions and recommendations are provided in the following sections.

SUMMARY AND CONCLUSIONS

The summary and conclusion are listed in the following:

- TxME provides a seamless connection with FPS 21 to conduct the performance check for each FPS 21 recommended design option. The information of each design option is automatically imported into TxME from FPS 21 and the benefits of improved base materials or superior asphalt mixes can then be determined by TxME. In addition, TxME will predict the impact of climate and axle load spectrum on the performance of the structure.
- Five TxME workshops were conducted and more than 85 TxDOT engineers from different districts attended the workshops learning how to use the TxME to analyze pavement performance and conduct pavement designs. According to the discussions during the workshops and the evaluation forms collected after the training workshop, the attendees believed that TxME is a very helpful and useful tool and easy to use. They fully supported to have TxME to become part of Texas pavement design process in the near future.

- According to workshop comments and feedbacks, researchers added the following updates to the TxME system:
 - Default material properties for more Texas mixtures including RAP/RAS mixes.
 - Default load spectra.
 - Initial construction cost defaults and analysis.
 - Help file.
- The default material properties developed in this study include the default dynamic modulus, rutting/cracking property of AC mixtures, and moduli of other layer materials. Especially, the relationships between RAP/RAS contents and the AC material properties were established and incorporated into the TxME. This greatly enhanced the practicality and ease of using TxME when conducting pavement performance prediction.
- Traffic data from more than 27 WIM stations were used to develop the default load spectra. In this study, Texas highways are divided into four categories: energy sector, IH, SH/US, and FM roads. For each type of roads, according to their truck volume (high, medium, low) and weight (heavy, medium, and light) features, the corresponding default/typical load spectra information such as VCD, ALD, MAF, and APT information were recommended and incorporated into the TxME.
- The initial construction costs of pavement layer materials especially the AC mixtures with RAP/RAS were developed and incorporated into the TxME software. This feature enhanced the TxME pavement design when choosing an optimal design option from the cost-beneficial point of view.
- The Texas Flexible Pavement Database was used to calibrate the TxME performance models. The base/subgrade rutting model was calibrated based on the identified surface treatment pavement test sections in the database, and the AC rutting and fatigue cracking model were calibrated based on the identified conventional pavement test sections.
- Eleven test sections were identified in six different districts. Their layer materials were sampled and tested, and their field performances were monitored. The calibrated and enhanced TxME was employed to conduct performance predictions for these identified test sections and was verified by the comparison between the performance predictions and the field survey results.

RECOMMENDATIONS

Overall, the current TxME is practical, user-friendly, and ready for statewide implementation. It offers great promise for accurately predicting distresses for flexible pavements. Its prediction is rational and reasonable. Therefore, it is strongly recommended to:

- Use TxME to perform design checks for FPS 21 solutions for statewide implementation.

- Conduct regional or district based TxME training/demonstration, perform case studies with selected projects, and support districts to develop their own default material properties.
- Continue monitoring the test sections constructed in this study.
- Use TxME to evaluate pavement rehabilitation designs for oil and gas development locations, since considering the influence of overloaded truck is very important to the success of these pavement designs.
- Keep enhancing/updating the TxME program based on feedbacks and comments from actual user experience.

REFERENCES

- AASHTO TP62-03, *Standard Method of Test for Determining Dynamic Modulus of Hot-Mix Asphalt Concrete Mixtures*, 2003.
- Hu, S., F. Zhou, and T. Scullion. *Texas M-E Flexible Pavement Design System: Literature Review and Proposed Framework*, 0-6622-1, Texas Transportation Institute, College Station, TX, USA, <http://tti.tamu.edu/documents/0-6622-1.pdf>, 2012a.
- Hu, S., F. Zhou, T. Scullion, and J. Leidy. “Calibrating and Validating Overlay Tester-Based Fatigue Cracking Model with Data from National Center for Asphalt Technology,” In *Transportation Research Record: Journal of the Transportation Research Board*, No. 2296, pp. 57–68, 2012b.
- Hu, S., X. Hu, F. Zhou, and L. Walubita. “Development, Calibration, and Validation of a New M-E Rutting Model for HMA Overlay Design and Analysis,” *Journal of Materials in Civil Engineering*, Vol. 23, pp. 89–99, 2011.
- Hu, S., F. Zhou, and T. Scullion. *Development of Texas Mechanistic-Empirical Flexible Pavement Design System (TxME)*. Report FHWA/TX-14/0-6622-2. Texas A&M Transportation Institute, College Station, 2014.
- Liu, W. and T. Scullion. *Flexible Pavement Design System FPS 19W: User’s Manual (Reprint)*, TxDOT Research Report 0-1869-1, Texas Transportation Institute, Texas A&M University System, 2006.
- Rosenblueth, E. “Point Estimates for Probability Moments,” In *Proceedings of National Academies of Science*, USA, 72(10): pp. 3812–3814, 1975.
- TxDOT. *Average Low Bid Unit Prices*. Online. No Date. Available at <https://www.txdot.gov/business/letting-bids/average-low-bid-unit-prices.html>. Accessed June 2018.
- Walubita, L. F., G. Das, E. M. Espinoza, J. H. Oh, T. Scullion, S. Nazarian, I. Abdallah. *Texas Flexible Pavements and Overlays: Data Analysis Plans and Reporting Format*. Technical Report 0-6658-P3, Texas A&M Transportation Institute, College Station, Texas, 2012.
- Walubita, L. F., S. Lee, A.N. Faruk, I. Abdallah, S. Ravi, J.L. Garibay. *The Data Storage System (DSS) and Other Data Files*. Technical Report: 0-6658-P2, Texas A&M Transportation Institute, Texas A&M University, College Station, Texas, 2015.
- Witczak, M.W. and A. Solti. *A Recommended Methodology for Developing Dynamic Modulus E* Master Curves from Non-Linear Optimization*, Project Report, NCHRP Project 9-19: Arizona State University, Tempe, AZ, 2004.
- Zhou, F. and T Scullion. *Guidelines for Development Input Parameters of Enhanced VESYS5 Program*. FHWA/TX-05/9-1502-01-P5, Texas Transportation Institute, College Station, Texas, 2004.

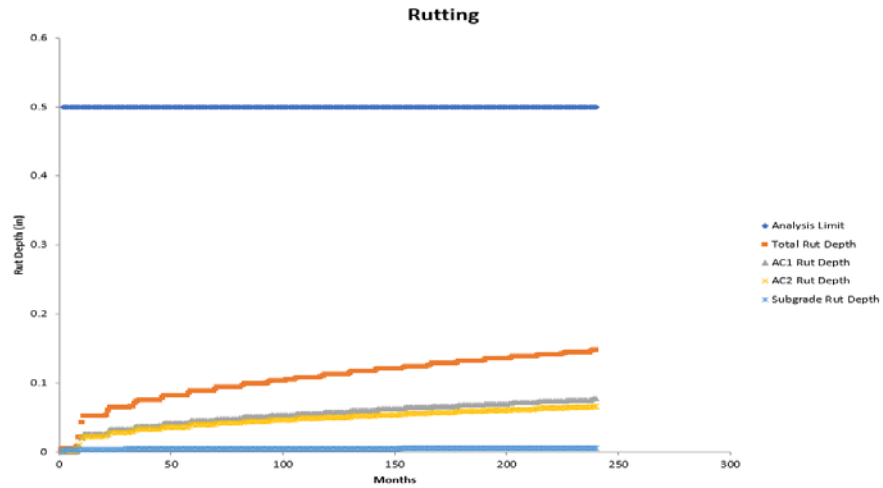
APPENDIX: TXME PREDICTION RESULTS FOR 11 TEST SECTIONS

Table 53 lists the name of each test section and their corresponding distress predicted by TxME.

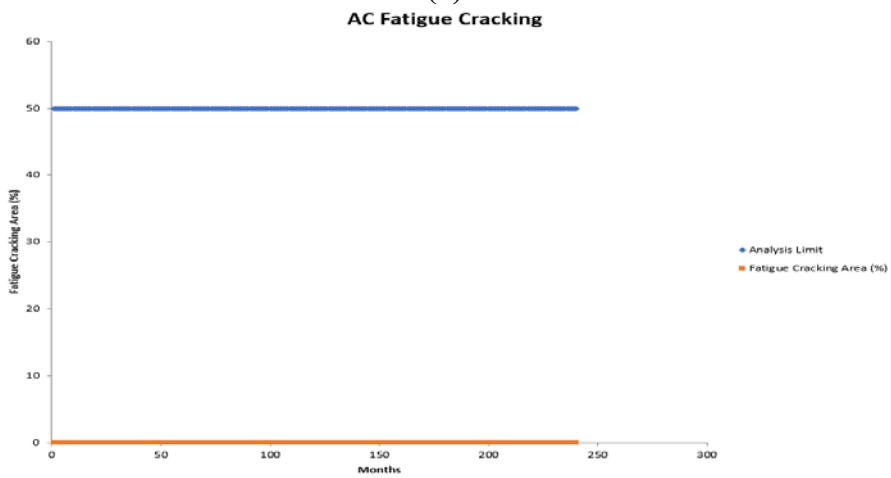
Table 53. TxME Predicted Distress for Each Test Section.

Test Section	Pavement Type	TxME Predicted Distress
US 259_S1	Conventional	Total Rut Depth, AC Fatigue Cracking, Thermal Cracking
US 259_S2	Conventional	Total Rut Depth, AC Fatigue Cracking, Thermal Cracking
SH 6	Surface Treatment	Total Rut Depth
SH 7_S1	Conventional	Total Rut Depth, AC Fatigue Cracking, Thermal Cracking
SH 7_S2	Surface Treatment	Total Rut Depth
FM 3549	Conventional	Total Rut Depth, AC Fatigue Cracking, Thermal Cracking
US 87	Milled and in-Lay	AC Rut Depth, AC Fatigue Cracking, Thermal Cracking
FM 1463_S1	Milled and overlay	AC Rut Depth, AC Fatigue Cracking, Thermal Cracking
FM 1463_S2	Milled and overlay	AC Rut Depth, AC Fatigue Cracking, Thermal Cracking
FM 1463_S3	Milled and overlay	AC Rut Depth, AC Fatigue Cracking, Thermal Cracking
FM 1463_S4	Milled and overlay	AC Rut Depth, AC Fatigue Cracking, Thermal Cracking

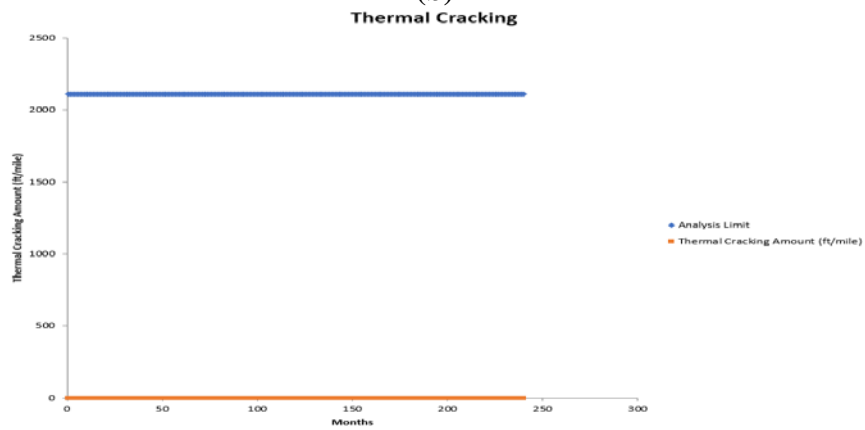
Figure 80–Figure 90 show the TxME predicted distresses for each test section, respectively.



(a)



(b)



(c)

Figure 80. US 259_S1 TxME Prediction of (a) Rut Depth, (b) Fatigue Cracking, and (c) Thermal Cracking.

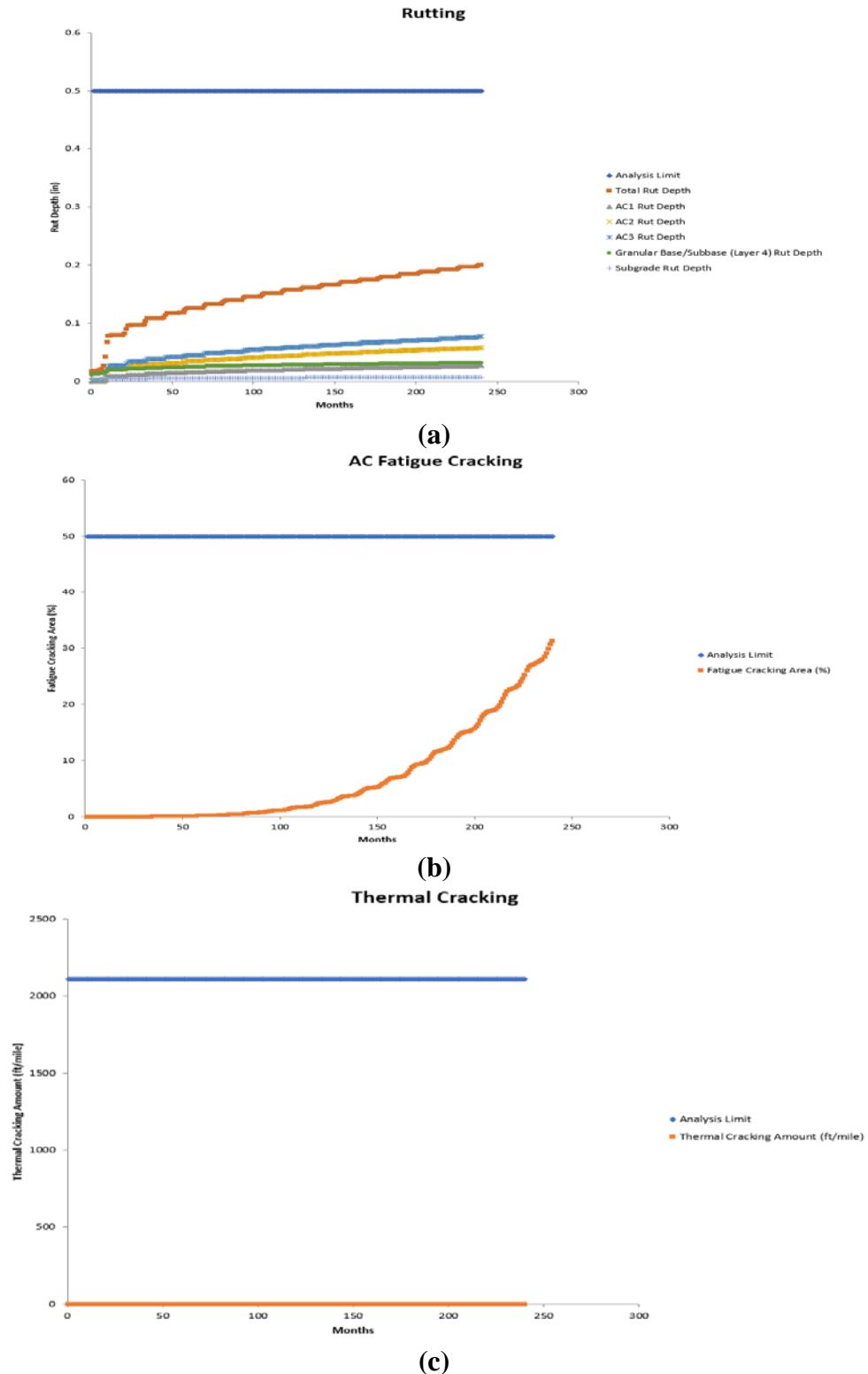
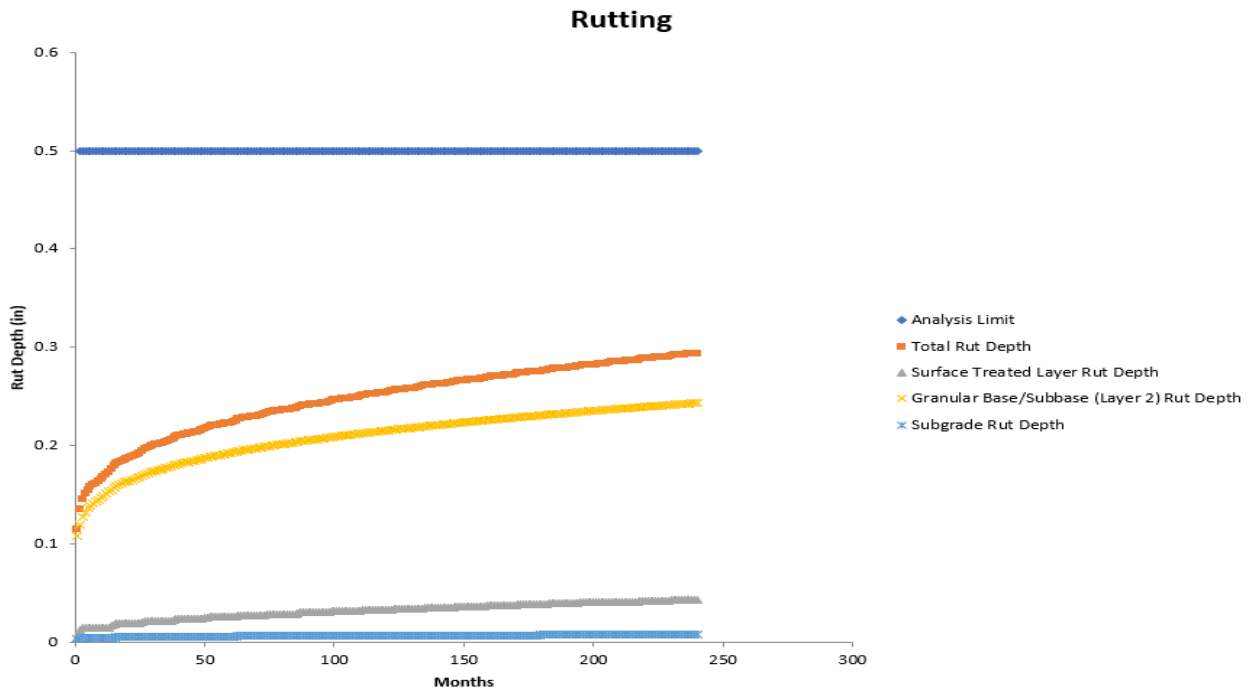
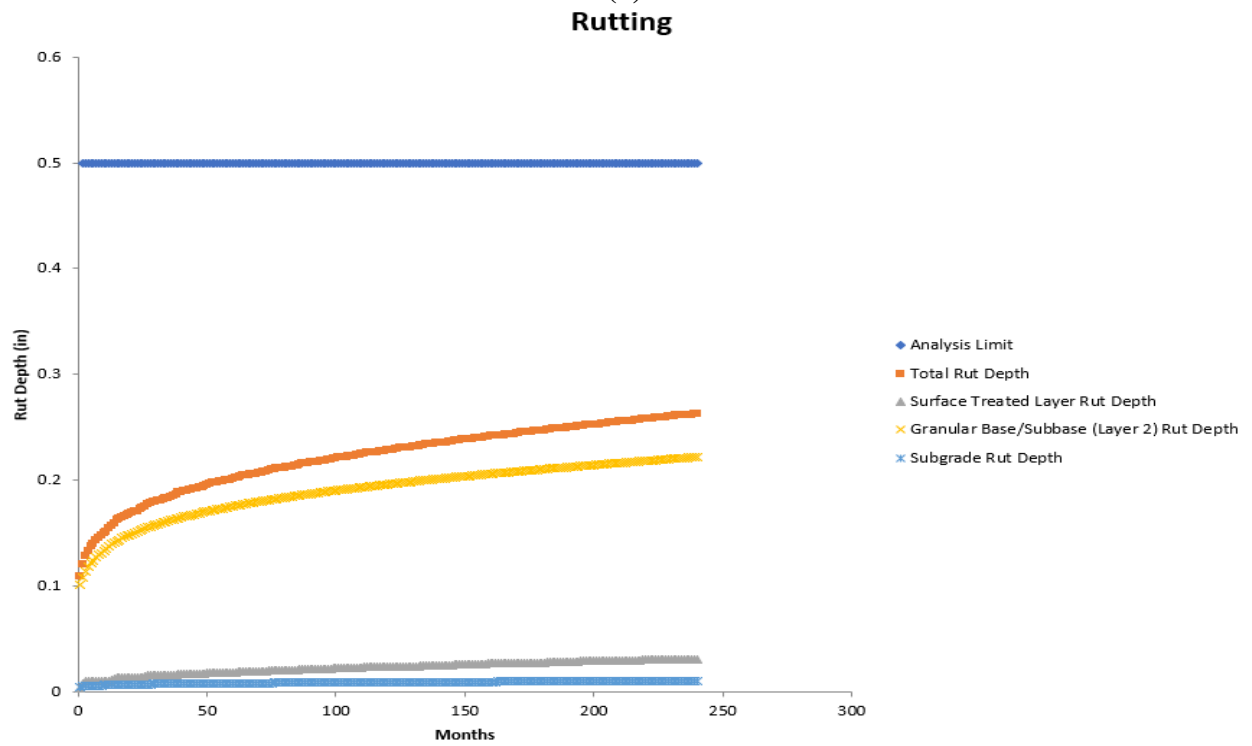


Figure 81. US 259_S1 TxME Prediction of (a) Rut Depth, (b) Fatigue Cracking, and (c) Thermal Cracking.

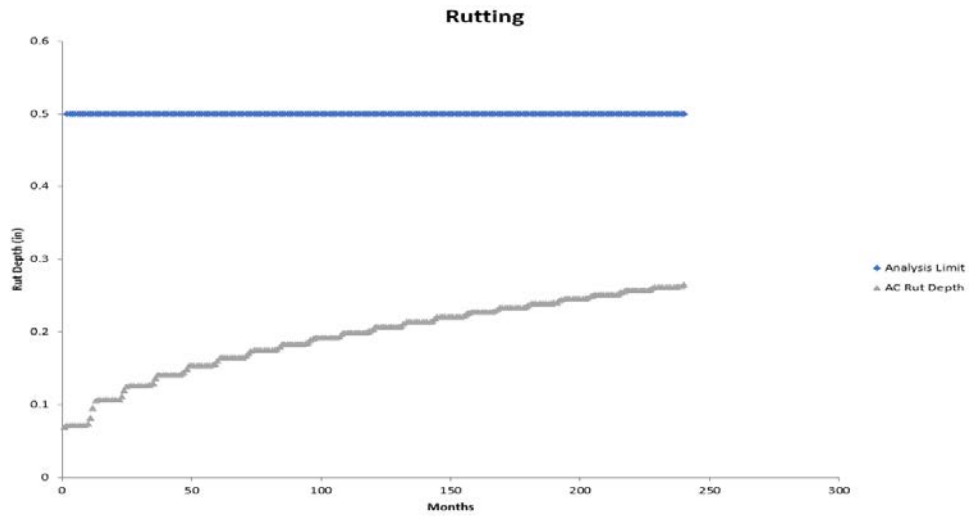


(a)

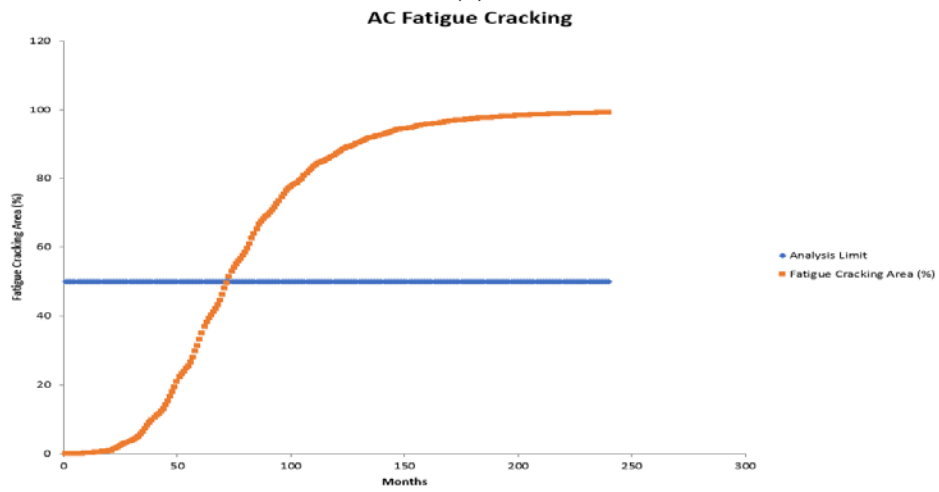


(b)

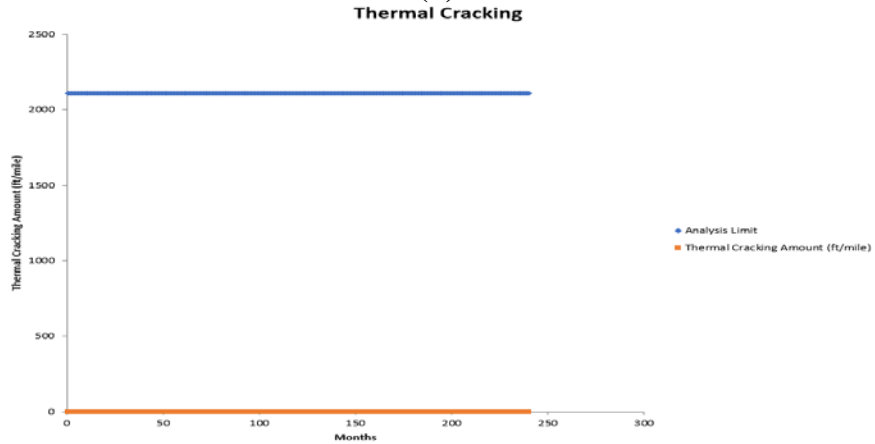
Figure 82. SH 6 TxME Prediction of Total Rut Depth when Traffic Input Is (a) Level 2 – ESALs and (b) Level 1 – Load Spectra.



(a)



(b)



(c)

Figure 83. SH 7_S1 TxME Prediction of (a) AC Rut Depth, (b) Fatigue Cracking, and (c) Thermal Cracking.

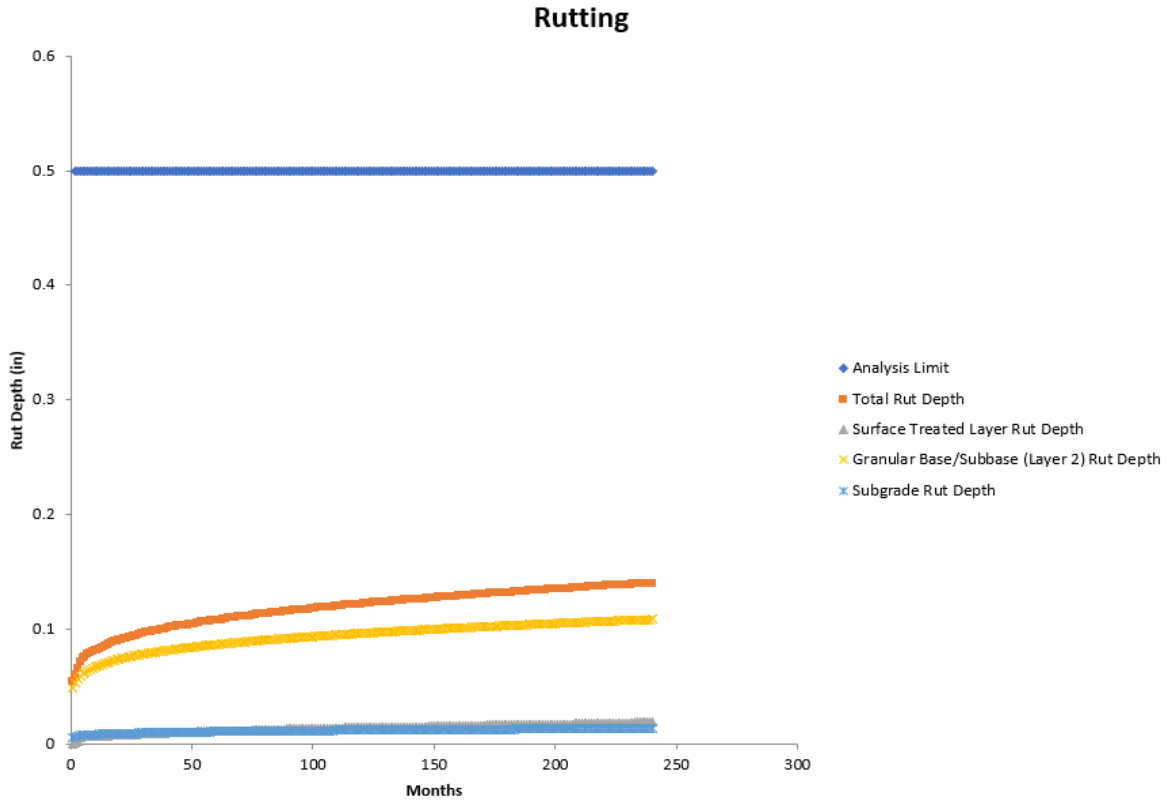
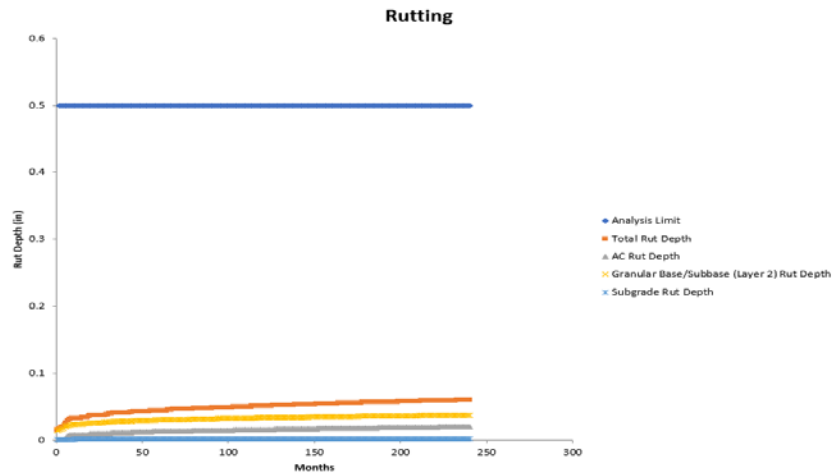
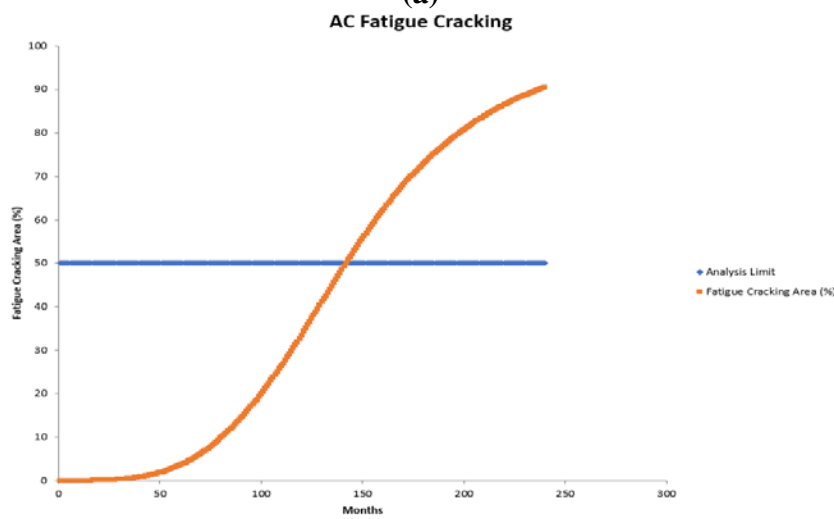


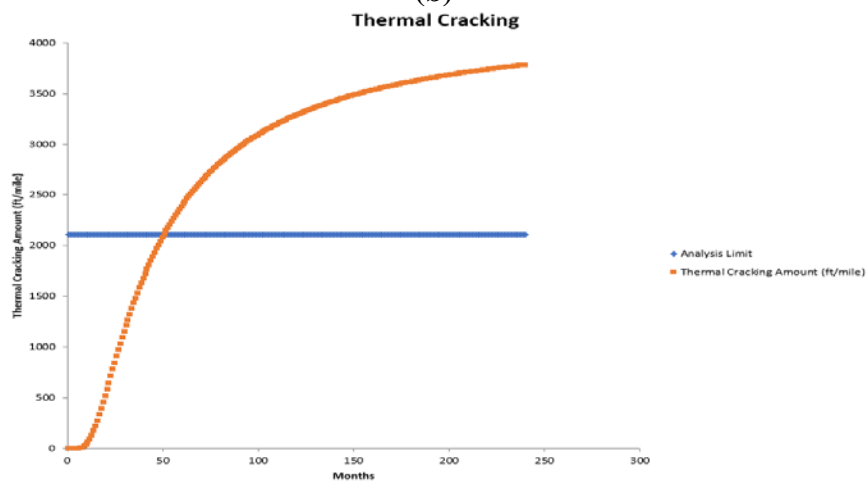
Figure 84. SH 7_S2 TxME Prediction of Total Rut Depth.



(a)

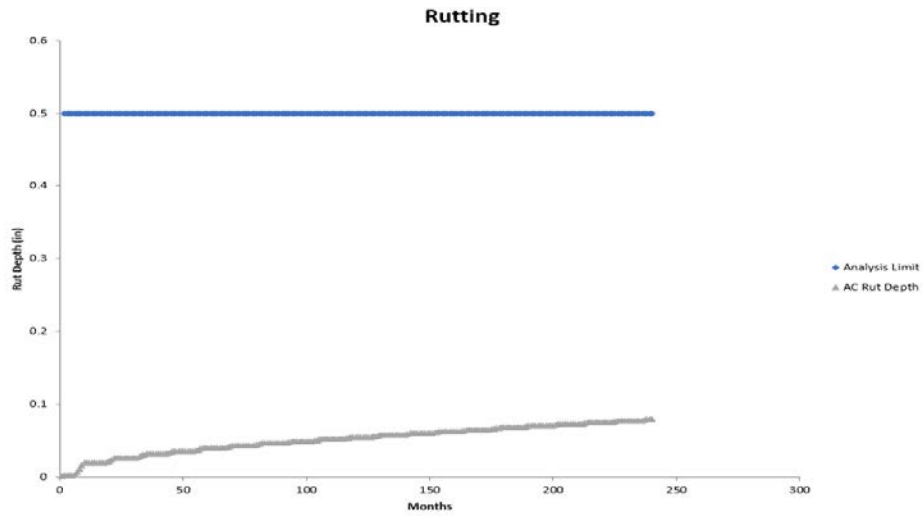


(b)



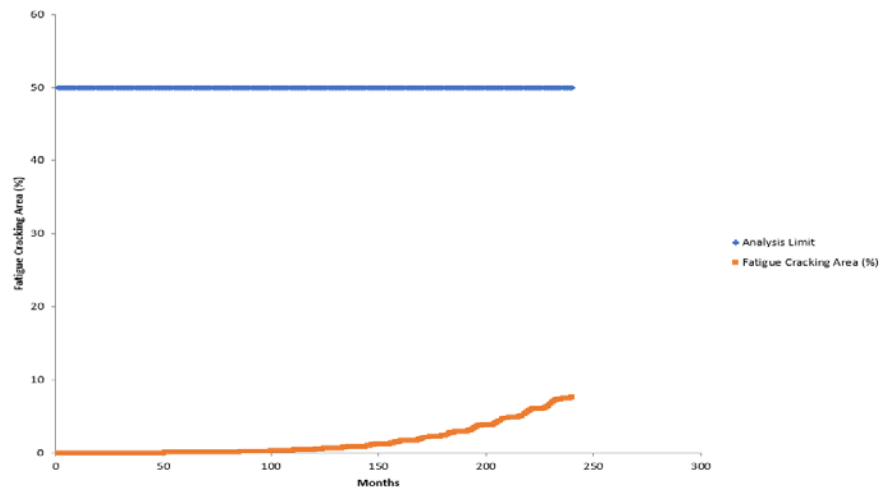
(c)

Figure 85. FM 3549 TxME Prediction of (a) Total Rut Depth, (b) Fatigue Cracking, and (c) Thermal Cracking.



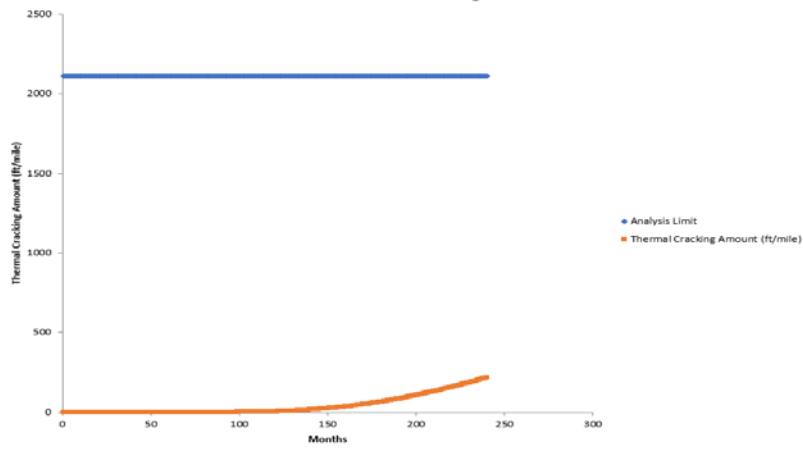
(a)

AC Fatigue Cracking



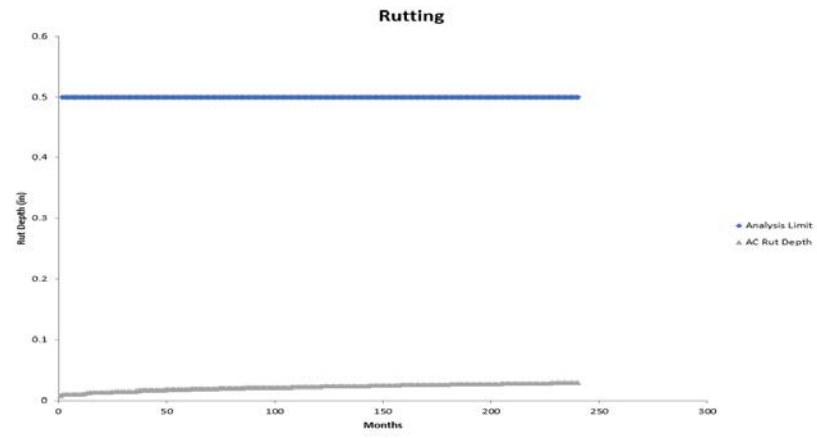
(b)

Thermal Cracking

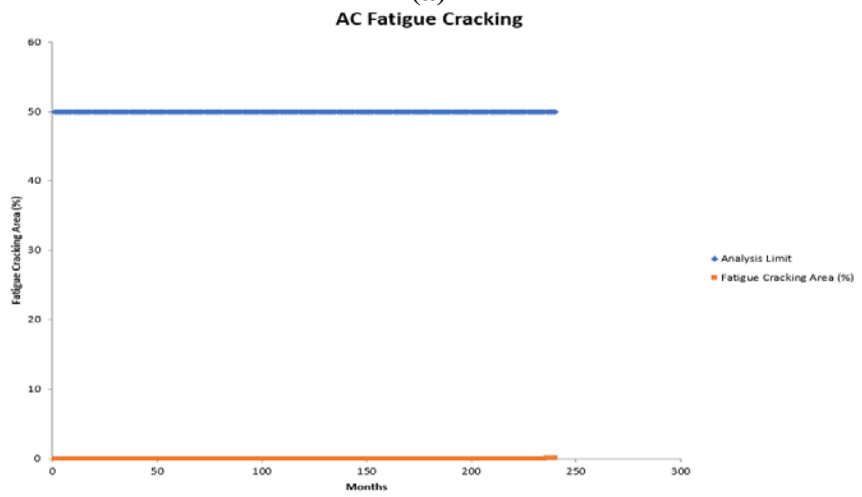


(c)

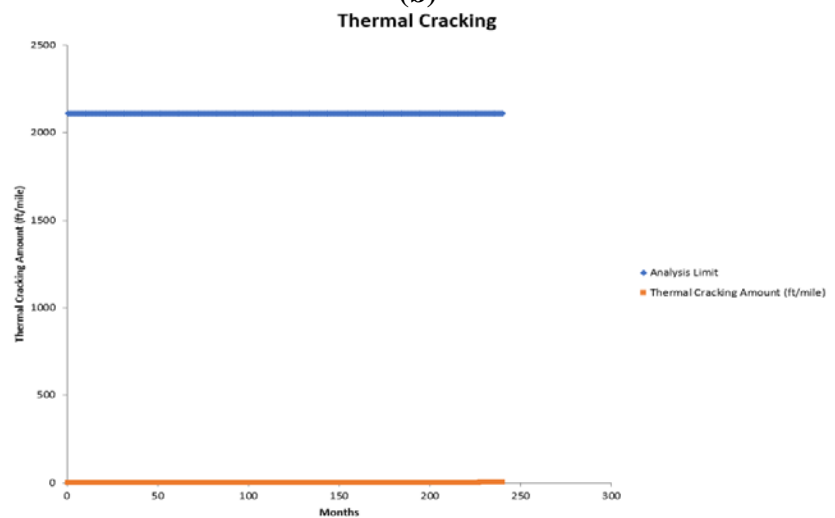
Figure 86. US 87 TxME Prediction of (a) AC Rut Depth, (b) Fatigue Cracking, and (c) Thermal Cracking.



(a)

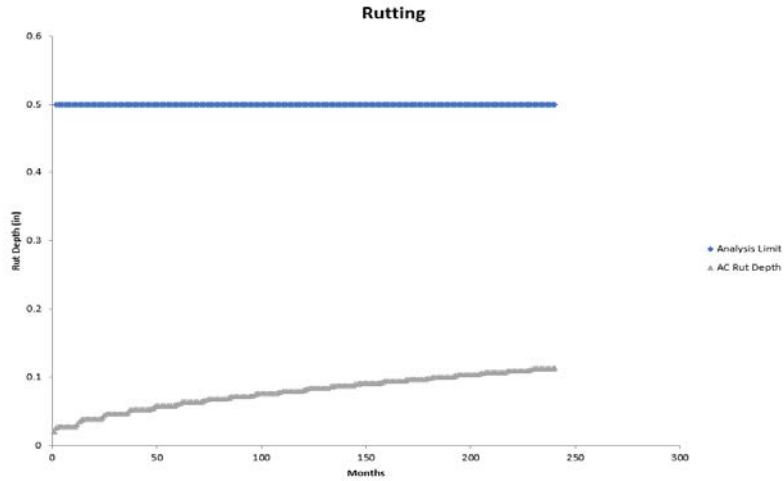


(b)



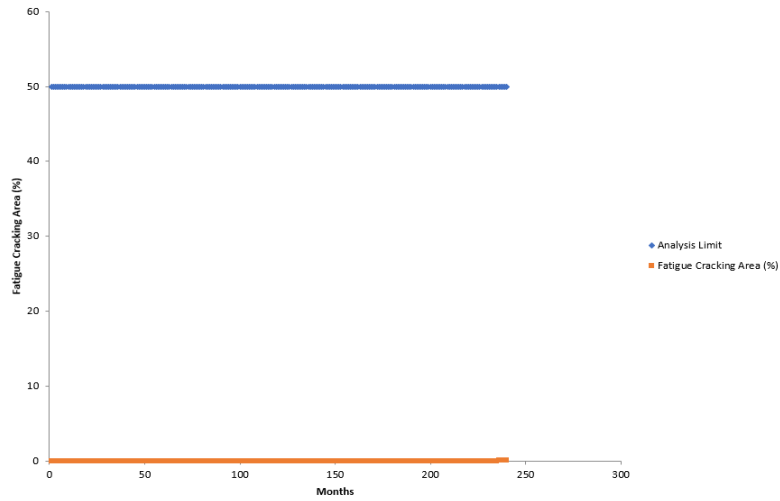
(c)

Figure 87. FM 1463_S1 TxME Prediction of (a) AC Rut Depth, (b) Fatigue Cracking, and (c) Thermal Cracking.



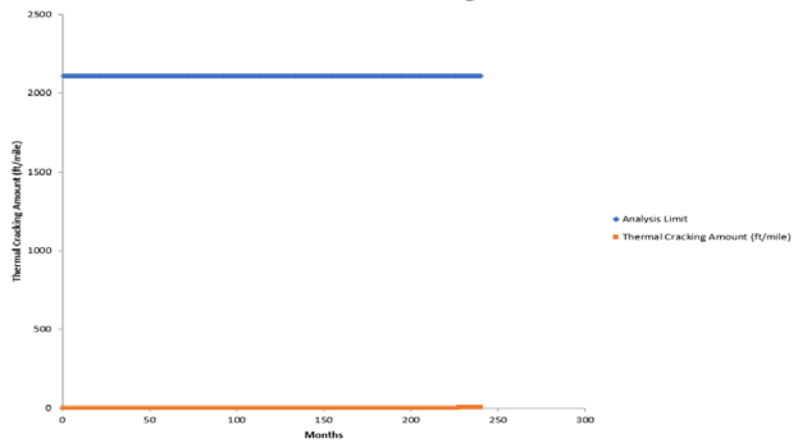
(a)

AC Fatigue Cracking



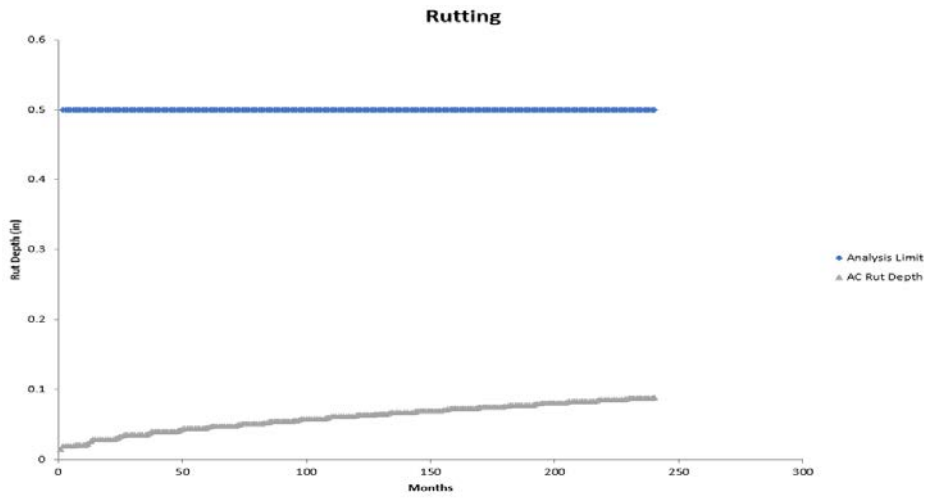
(b)

Thermal Cracking

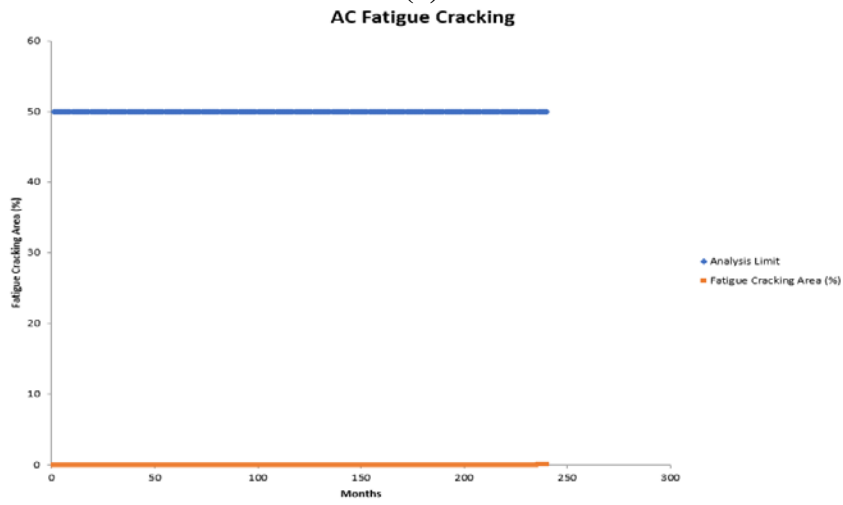


(c)

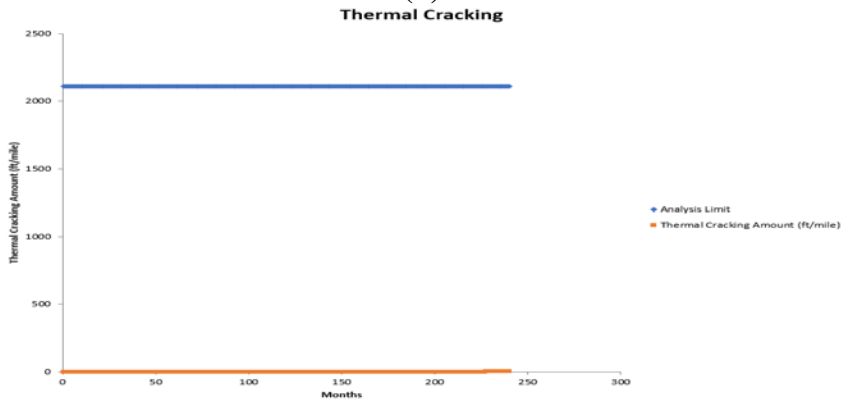
Figure 88. FM 1463_S2 TxME Prediction of (a) AC Rut Depth, (b) Fatigue Cracking, and (c) Thermal Cracking.



(a)

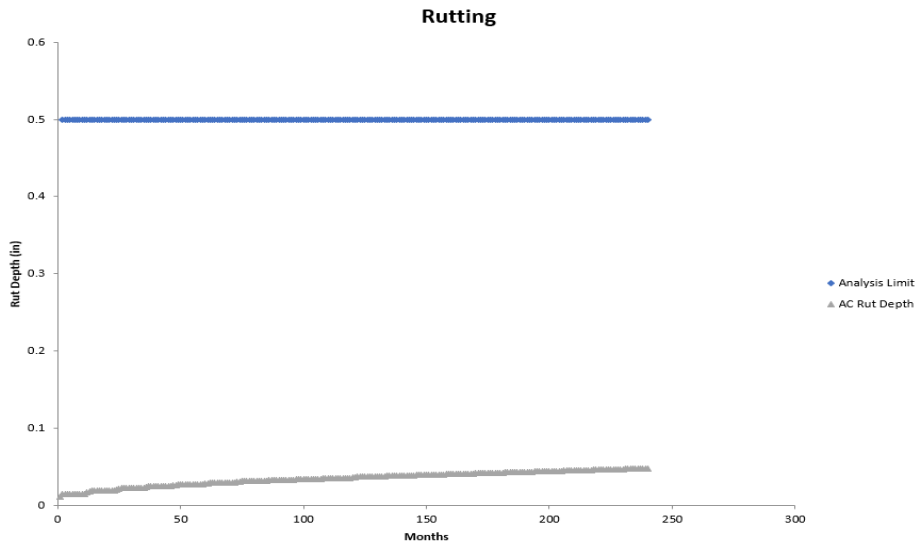


(b)

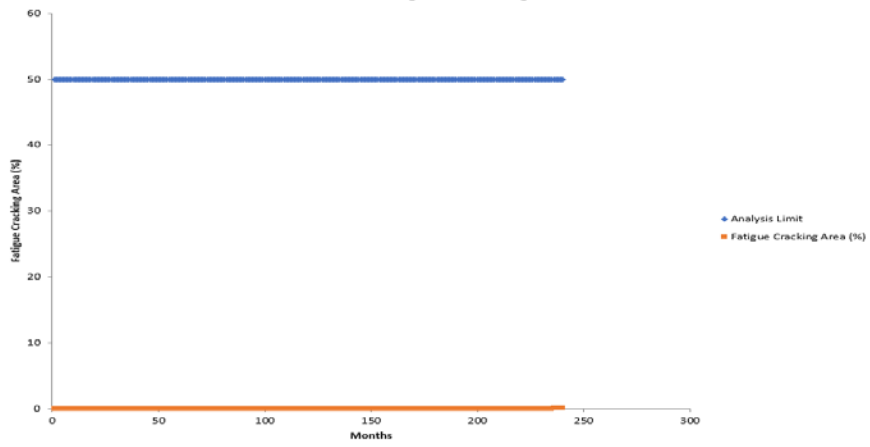


(c)

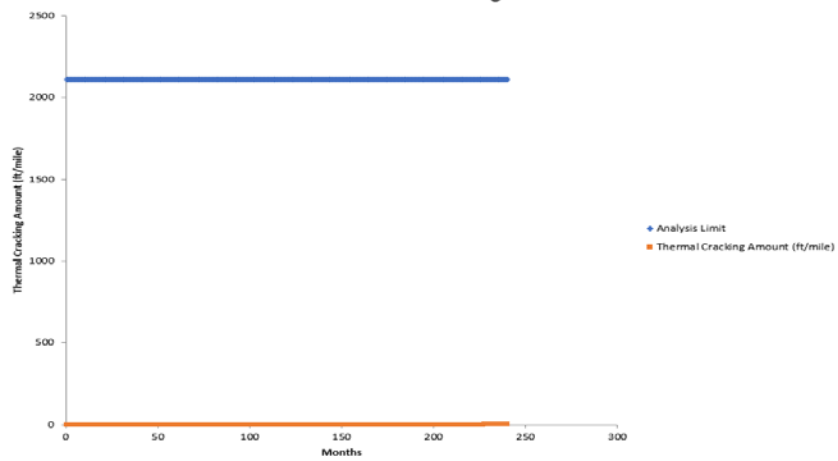
Figure 89. FM 1463_S1 TxME Prediction of (a) AC Rut Depth, (b) Fatigue Cracking, and (c) Thermal Cracking.



(a)
AC Fatigue Cracking



(b)
Thermal Cracking



(c)

Figure 90. FM 1463_S1 TxME Prediction of (a) AC Rut Depth, (b) Fatigue Cracking, and (c) Thermal Cracking.